

**The use of remote sensing for soil moisture estimation using
downscaling and soil water balance modelling in
Malmesbury and the Riebeeek Valley**

Jason John Möller

For a full Master's thesis:

*A thesis submitted in partial fulfilment of the requirements for
the degree of Magister Scientiae in the Department of Earth
Science, University of the Western Cape*

WESTERN CAPE

Supervisor: Prof D. Mazvimavi

Co-supervisor: Prof N. Jovanovic

June 2014

Keywords:

Remote sensing

Soil water balance modelling

Microwave imagery

Soil moisture downscaling

Spatial variability

Soil water flux

Spatial resolution

Semi-arid climate



Abstract

The use of remote sensing for soil moisture estimation using downscaling and soil water balance modelling in Malmesbury and the Riebeeek Valley

J. J. Moller

MSc Thesis, Department of Earth Science,

University of the Western Cape

Date: July 2014

Soil moisture forms an integral part of the hydrological cycle and exerts considerable influence on hydrological processes at or near the earth's surface. Knowledge of soil moisture is important for planning and decision-making in the agricultural sector, land and water conservation and flood warning. Point measurements of soil moisture, although highly accurate, are time consuming, costly and do not provide an accurate indication of the soil moisture variation over time and space as soil moisture has a high degree of spatial and temporal variability. The spatial variability of soil moisture is due to the heterogeneity of soil water holding properties, the influence of plants, and land uses.

The downscaling of satellite microwave soil moisture estimates and soil water balance modelling was investigated at six transects in the semi-arid, Western Cape Province of South Africa, as alternatives to in situ soil measurements. It was found that microwave soil moisture estimates compared well to in situ measurements at the six transects (study sites), with coefficient of determination (r^2) values greater than 0.7 and root mean square error (RMSE) values less than 1.5%. Downscaling using the universal triangle method, performed well at 4 of the 6 transects, with r^2 values great than 0.65 and low to moderate RMSE values (0.5-12%). Soil water balance modelling similarly performed well in comparison with in situ measurements at 4 of the transects with regards to r^2 values (>0.6) but had moderate to high RMSE (4.5-19%). Poor downscaling results were attributed to fine scale (within 1 km) surface heterogeneity while poor model performance was attributed to soil hydrological and rainfall heterogeneity within the study areas.

Declaration

I declare that “*The use of remote sensing for soil moisture estimation using downscaling and soil water balance modelling in Malmesbury and the Riebeeek Valley*” is my own work, that it has not been submitted for any degree or examination in any other university, and that all the sources I have used or quoted have been indicated and acknowledged by complete references.

Full name: Jason Möller

Date: 17 September 2014

Signed:



Acknowledgements

During the course of my research I have received tremendous support from many, without which the completion of my thesis would not have been possible. I would like to thank my wife and son, my parents (mine, my wife's and the stand in parental figures when the biological ones were far away), brothers, family and friends for their wonderful support at home. A great home life makes managing professional responsibilities so much easier.

I would like to thank both of my supervisors, Prof D Mazvimavi and Prof N Jovanovic. Firstly I would like to them for helping me in securing funding during my MSc, this was vital during my research period. I would also like to thank both supervisors for always making time for any assistance needed, no matter how small the issue. This "open door" policy and open lines of communication streamlined the challenging process which is research. Secondly I would also like to thank them for their invaluable insight and recommendations during crucial parts of the research. I sincerely hope that I will be afforded in opportunity to work with them again in the future. A special thanks to Mr Jonker who advised on many issues regarding admin and some of the concepts of research. His support and insights were much appreciated.

I would then like to thank all of the support staff UWC, as their hard work helps so many fulfil the day to day requirements of a research student. I would like to thank my funders, NUFFIC and the CSIR, without their support the research would not have been possible. I would also like to thank our NUFFIC partners in the Netherlands particularly Prof Mannaerts, who gave wonderful support during his visits to South Africa and also via correspondence.

Lastly, I would like to thank all of my colleagues for their support and Mathew for his assistance in the field. A "buzzing" environment at university, where colleagues can exchange ideas and views, is at the very core of research and learning.



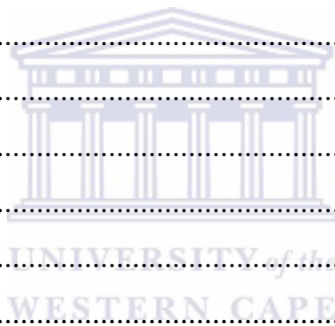
UNIVERSITY *of the*
WESTERN CAPE

Table of Contents

Contents

List of Tables	ix
List of Figures	x
1. Introduction	1
1.1 Problem Statement	2
1.2 Aim of the study	3
1.2.1 Research Questions	3
1.2.2 The objectives of this study were:	3
2. Literature Review	5
2.1 Introduction	5
2.2 The role of soil moisture in the hydrological cycle	5
2.3 The importance of soil moisture information in environmental and water management	6
2.3.1 Drought	6
2.3.2 Irrigation management	8
2.3.3 Flooding	9
2.4 Factors affecting soil moisture and measurement of soil moisture content	9
2.5 In situ measurements	11
2.6 Remote sensing estimation of soil moisture	11
2.6.1 Gamma radiation techniques	12
2.6.2 Reflected solar techniques	12
2.6.3 Thermal techniques	12
2.6.4 Microwave techniques	13
2.7 Downscaling of remote sensing derived soil moisture	14
2.8 Soil Water Balance Modelling	15
3. Methodology	17
3.1 Introduction	17
3.2 Approach to the study	17
3.3 In situ soil moisture measurements	17

3.4 Remote sensing of soil moisture	19
3.5 Downscaling: Brightness temperature linear regression model	20
3.6 Soil moisture modelling	23
3.6.1 Introduction	23
3.6.2 Rainfall	24
3.6.3 Runoff and infiltration	25
3.6.5 Evapotranspiration	25
3.6.4 Recharge	26
3.7 Model evaluation	27
3.7.1 Pearson's correlation coefficient (r) and coefficient of determination (r^2)	28
3.7.1 Root mean square error	28
3.8 Criteria for site selection	29
4. In situ measurements	30
4.1 Introduction	30
4.3 Site description	30
4.3.1 Site 1: Malmesbury	30
4.3.2 Site 2: Riebeeck Valley	30
4.4 Sampling Transects	35
4.5 Data collection	40
4.6 In Situ Soil Moisture Measurement	41
4.7. Soil Moisture Probe Evaluation	41
4.8 Analysis of Soil Moisture at each Transect	43
4.9. Transect physical properties and soil moisture	55
4.10. Summary of Hydroprobe soil moisture estimates	57
5. Remote sensing derived soil moisture and downscaling	58
5.1. Introduction	58
5.2. Coarse resolution soil moisture product processing	58
5.3 Coarse resolution soil moisture analysis	58
5.4 Data preparation- LST and NDVI	67
5.5 LST-NDVI relationship	67
5.6 Summary	75



6. Soil Water Balance Model.....	76
6.1 Introduction	76
6.2 Daily rainfall and evapotranspiration.....	76
6.3 Soil hydraulic properties for the Malmesbury and Riebeek sites.....	78
6.4 Method of model calibration	79
6.5 Simulation results	82
6.6 Sensitivity analysis	88
6.7 Summary	89
7. Remote sensing derived and simulated soil moisture.....	90
7.1 Introduction	90
7.2 In situ soil moisture results	90
7.3 Simulated and remotely sensed soil moisture	102
7.4 Comparison of ASCAT, downscaled and simulated soil moisture to Hydroprobe measurement points.....	109
7.5 Summary	122
8. Discussion and Conclusion.....	125
8.1 Introduction	125
8.2 In situ soil moisture measurements	125
8.3 Microwave derived soil moisture estimates	126
8.4 Downscaled soil moisture estimates.....	127
8.5 Soil water balance model	128
8.6 Summary	129
9. References.....	132
Appendices.....	140
Appendix A: Transect A – Riverlands Nature Reserve	141
Appendix B: Transect B - Rondevlei Farm	142
Appendix C: Transect C- Niewepost	143
Appendix D: Transect D- Goedetrou Farm	144
Appendix E: Transect E- De Gift.....	145
Appendix F: Transect F- De la Gift	146

List of Tables

Table 4.1: Site Transect Information	35
Table 4. 2: Description of Transects A-F.....	37
Table 4.3: Cover Type Information for both study sites.....	38
Table 4.4: Soil analyses results for transects a-f.....	39
Table 4.5: Field data collection schedule.....	40
Table 4.6: Soil moisture probe (Hydroprobe) evaluation results as compared to volumetric soil moisture measurements obtained using the gravimetric method, including the coefficient of determination (r^2), the root mean square error (RMSE) and the linear relationship between the two (Trendline) for each transect.....	41
Table 4. 7: Correlation matrix for transect physical properties and soil moisture averages for both study sites- depicting <i>slope</i> , <i>silt-clay-sand</i> proportions, <i>bulk density</i> , <i>relative elevation (E_R)</i> and <i>soil moisture</i> for all sampling days. Used to compare soil moisture to depict the change in relationship between soil moisture and transect physical properties throughout the study period.	56
Table 5. 1: Calibrated coefficients for brightness temperature linear regression model for Malmesbury and Riebeek study sites.....	69
Table 6.1: Calibrated parameter values for <i>field capacity (F_c)</i> , <i>runoff coefficient (β)</i> , <i>rainfall interception (P_i)</i> and <i>evapotranspiration coefficient</i> for all transects.....	81

List of Figures

Figure 4.1: Daily rainfall measurements for the Malmesbury and Riebeek study sites for the period 1 January to 31 December 2013, from the South African Weather Services (Malmesbury) and the Institute for Soil, Climate and Water Agro-Climatology (Riebeek).	31
Figure 4.2: Daily average air temperature (°C) for the Malmesbury and Riebeek study sites for the period 1 January to 31 December 2013, from the South African Weather Services (Malmesbury) and the Institute for Soil, Climate and Water Agro-Climatology (Riebeek).	32
Figure 4.3: Study site locations of the Malmesbury and Riebeek Valley sites (purple squares) within the coastal region of the Western Cape Province of South Africa with rainfall station WS1 and WS2 (red dots).	33
Figure 4.4: Digital elevation models (DEMs) for Malmesbury and Riebeek study sites corresponding to their relevant ASCAT 12.5 km pixels from NASA’s SRTM30, DEMs accessed on the 30 November 2013.	34
Figure 4.5: Land cover maps of the Malmesbury and Riebeek Valley study sites, depicting the dominant cover types (<i>Natural Vegetation, Urban, Vineyards and Wheat and Pasture</i>) as well as the six sampling transects, from the National Survey General, produced May 2012.	36
Figure 4.6: Hydroprobe measurements plotted against gravimetric method measurements for each transect showing the r^2 and RMSE values for the total measurements, with soil moisture given in percent.	42
Figure 4.7: Variation of Hydroprobe soil water content along Transect A from 26 September 2013- 22 January 2014. The error bars indicate the standard deviation of the three measurements used to obtain the soil moisture estimate at each point.	44
Figure 4.8: Variation of Hydroprobe soil water content along Transect B from 24 July- 16 October 2013. The error bars indicate the standard deviation of the three measurements used to obtain the soil moisture estimate at each point.	45
Figure 4.9: Variation of Hydroprobe soil water content along Transect B from 7 November 2013- 22 January 2014. The error bars indicate the standard deviation of the three measurements used to obtain the soil moisture estimate at each point.	46
Figure 4.10: Variation of Hydroprobe soil water content along Transect C from 24 July- 16 October 2013. The error bars indicate the standard deviation of the three measurements used to obtain the soil moisture estimate at each point.	47
Figure 4.11: Variation of Hydroprobe soil water content along Transect C from 7 November 2013- 22 January 2014. The error bars indicate the standard deviation of the three measurements used to obtain the soil moisture estimate at each point.	48
Figure 4.12: Variation of Hydroprobe soil water content along Transect D from 25 July 2013- 25 September 2013. The error bars indicate the standard deviation of the three measurements used to obtain the soil moisture estimate at each point.	49

Figure 4.13: Variation of Hydroprobe soil water content along Transect D from 16 October 2013- 22 January 2014. The error bars indicate the standard deviation of the three measurements used to obtain the soil moisture estimate at each point.....	50
Figure 4.14: Variation of Hydroprobe soil water content along Transect E from 25 July 2013- 25 September 2013. The error bars indicate the standard deviation of the three measurements used to obtain the soil moisture estimate at each point.	51
Figure 4. 15: Variation of Hydroprobe soil water content along Transect D from 16 October 2013- 22 January 2014. The error bars indicate the standard deviation of the three measurements used to obtain the soil moisture estimate at each point.....	52
Figure 4.16: Variation of Hydroprobe soil water content along Transect E from 8 August 2013- 16 October 2013. The error bars indicate the standard deviation of the three measurements used to obtain the soil moisture estimate at each point.	53
Figure 4.17: Variation of Hydroprobe soil water content along Transect E from 6 November 2013- 22 January 2014. The error bars indicate the standard deviation of the three measurements used to obtain the soil moisture estimate at each point.....	54
Figure 5.1: Comparison of ASCAT 12.5km course resolution soil moisture estimates and rainfall (mm) for the Mablesbury site (above) and Riebeek site (below) for the period of 19 July 2013- 22 January 2014, with soil water content given in percentage.....	60
Figure 5.2: ASCAT 12.5km coarse resolution soil moisture estimates (solid line) and in Hydroprobe moisture estimates (triangles) at Transect A, B and C for the Malmesbury site for the period 19 July 2013 to 27 January 2014, with soil water content (SWC) given in percentage.....	62
Figure 5.3: ASCAT 12.5km coarse resolution soil moisture estimates and Hydroprobe soil moisture estimates at Transect A, B, C and averages for the Malmesbury site for the period 19 July 2013- 27 January 2014, with soil water content given in percentage.....	63
Figure 5.4: ASCAT 12.5km coarse resolution soil moisture estimates (solid line) and Hydroprobe soil moisture estimates (triangles) at Transect D, E and F for the Riebeek site for the period 19 July 2013 to 27 January 2014, with soil water content (SWC) given in percent.....	65
Figure 5.5: ASCAT 12.5km coarse resolution soil moisture estimates and Hydroprobe soil moisture estimates at transect D, E, F and averages for the Riebeek site for the period 19 July 2013 to 27 January 2014, with soil water content given in percent.....	66
Figure 5.6: Universal triangle depicting soil moisture relationship with Normalized Difference Vegetation Index (NDVI) and Land Surface Temperature (LST) ($^{\circ}$ C) at Malmesbury (above) and Riebeek (below).....	68
Figure 5.7: Downscaled 1km fine resolution soil moisture estimates (solid line) and Hydroprobe soil moisture estimates (squares) for Transects A, B and C at the Malmesbury site for the period 19 July 2013 to 27 January 2014, with soil water content (SWC) given in percent.....	71
Figure 5.8: Downscaled 1km soil moisture estimates (solid line) and in Hydroprobe soil moisture estimates (square) for Transects D, E and F at the Riebeek site for the period 19 July	

2013 to 27 January 2014. Soil water content (SWC) is given in percent.....	73
Figure 5.9: Downscaled 1km soil moisture estimates and Hydroprobe soil moisture estimates for Transect D, E and F at the Riebeek site for the period 19 July 2013 to 27 January 2014, with soil water content given in percentage.....	74
Figure 6.1: Daily rainfall for the Malmesbury (dotted line) and Riebeek (solid line) sites from 17 July 2013 to 27 January 2014.....	76
Figure 6.2: Reference evapotranspiration in mm calculated using the Hargreaves and Samani (1985) method at the Malmesbury and Riebeek sites for the period 19 July 2013 to 27 January 2014.....	77
Figure 6.3: Hydraulic conductivity (mm/d)-soil water content ($m^3 m^{-3}$) relationships for Malmesbury and Riebeek fitted with an exponential trend line (equations displayed on graphs).....	78
Figure 6.4: Soil water balance model simulation variations as observed with changes in field capacity, runoff coefficient, rainfall interception and evapotranspiration coefficient for the period of 19 July 2013 to 27 January 2014, with soil water content (SWC) given in percent.....	81
Figure 6.5: Simulated soil moisture estimates (dotted line) and Hydroprobe soil moisture estimates (squares) for Transects A, B and C at the Malmesbury study site for the period 19 July 2013 to 22 January 2014, with soil water content (SWC) given in percent.....	83
Figure 6.6: Simulated soil moisture estimates and Hydroprobe soil moisture estimates for Transect A, B, C and overall at the Malmesbury site for the period 19 July 2013 to 27 January 2014, with soil water content is given in percent.....	84
Figure 6.7: Simulated soil moisture estimates (dotted line) and Hydroprobe soil moisture (squares) for Transects D, E and F fat the Riebeek study site for the period 19 July 2013 to 22 January 2014, with soil water content (SWC) given in percent.....	86
Figure 6. 8: Simulated soil moisture estimates and Hydroprobe soil moisture estimates at Transect D, E, F and overall for the Riebeek site for the period 19 July 2013 to 27 January 2014, with soil water content given in percent.....	87
Figure 6.9: Sensitivity analysis of soil water balance model to <i>field capacity</i> , <i>runoff coefficient</i> , <i>rainfall interception</i> and <i>evapotranspiration coefficient</i> . The root mean square error (RMSE) is given in soil water content (%).....	88
Figure 7. 1: Hydroprobe (solid line and square), ASCAT 12.5km (dashed and dotted line), Downscaled 1km (dotted line) and Simulated (dashed line) soil moisture estimates at Transect A from 26 September 2013 to 22 January 2014 with soil water content (SWC) given in percentage.....	91
Figure 7.2: Hydroprobe (solid line and square), ASCAT 12.5km (dashed and dotted line), Downscaled 1km (dotted line) and Simulated (dashed line) soil moisture estimates at Transect B from 24 July 2013 to 16 October 2013 with soil water content (SWC) given in percentage.....	93
Figure 7.3: Hydroprobe (solid line and square), ASCAT 12.5km (dashed and dotted line), Downscaled 1km (dotted line) and Simulated (dashed line) soil moisture estimates at Transect B from 7 November 2013 to 22 January 2014 with soil water content (SWC) given in	

percentage.....	94
Figure 7.4: Hydroprobe (solid line and square), ASCAT 12.5km (dashed and dotted line), Downscaled 1km (dotted line) and Simulated (dashed line) soil moisture estimates at Transect C from 24 July 2013 to 16 October 2013 with soil water content (SWC) given in percentage.....	95
Figure 7.5: Hydroprobe (solid line and square), ASCAT 12.5km (dashed and dotted line), Downscaled 1km (dotted line) and Simulated (dashed line) soil moisture estimates at Transect C from 7 November 2013 to 22 January 2014 with soil water content (SWC) given in percentage.....	96
Figure 7.6: Hydroprobe (solid line and square), ASCAT 12.5km (dashed and dotted line), Downscaled 1km (dotted line) and Simulated (dashed line) soil moisture estimates at Transect D from 25 July 2013 to 25 September 2013 with soil water content (SWC) given in percentage...	97
Figure 7.7: Hydroprobe (solid line and square), ASCAT 12.5km (dashed and dotted line), Downscaled 1km (dotted line) and Simulated (dashed line) soil moisture estimates at Transect D from 16 October 2013 to 22 January 2013 with soil water content (SWC) given in percentage.	98
Figure 7.8 Hydroprobe (solid line and square), ASCAT 12.5km (dashed and dotted line), Downscaled 1km (dotted line) and Simulated (dashed line) soil moisture estimates at Transect E from 25 July 2013 to 25 September 2013 with soil water content (SWC) given in percentage...	99
Figure 7.9 Hydroprobe (solid line and square), ASCAT 12.5km (dashed and dotted line), Downscaled 1km (dotted line) and Simulated (dashed line) soil moisture estimates at Transect E from 16 October 2013 to 22 January 2013 with soil water content (SWC) given in percentage.....	100
Figure 7.10: Hydroprobe (solid line and square), ASCAT 12.5km (dashed and dotted line), Downscaled 1km (dotted line) and Simulated (dashed line) soil moisture estimates at Transect F from 14 August 2013 to 16 October 2013 with soil water content (SWC) given in percentage.	101
Figure 7.11: : Hydroprobe (solid line and square), ASCAT 12.5km (dashed and dotted line), Downscaled 1km (dotted line) and Simulated (dashed line) soil moisture estimates at Transect F from 6 November 2013 to 22 January 2014 with soil water content (SWC) given in percentage.....	102
Figure 7.12: Soil water balance model simulated soil moisture estimates and ASCAT 12.5km soil moisture estimates for Transect A, B and C at the Malmesbury study site for the period 19 July 2013 to 22 January 2014 with soil water content (SWC) given in percentage.....	104
Figure 7.13: Soil water balance model simulated soil moisture estimates and downscaled 1km soil moisture estimates for Transect A, B and C at the Malmesbury study site for the period 19 July 2013 to 22 January 2014 with soil water content (SWC) given in percentage.....	105
Figure 7.14: Soil water balance model simulated soil moisture estimates and ASCAT 12.km soil moisture estimates for Transect D, E and F at the Riebeek study site for the period 19 July 2013 to 22 January 2014 with soil water content (SWC) in percent.....	107
Figure 7.15: Soil water balance model simulated soil moisture estimates and downscaled 1km soil moisture estimates for Transect D, E and F at the Riebeek study site for the period 19 July 2013 to 22 January 2014 with soil water content (SWC) given in percent.....	108



UNIVERSITY *of the*
WESTERN CAPE

1. Introduction

Soil moisture forms an integral part of the hydrological cycle and exerts considerable influence on hydrological and pedogenic processes (Martinez et al., 2008). It has been noted that soil moisture flux is a key variable in understanding land-atmosphere interactions, as the transfer of water from the soil to the atmosphere via evapotranspiration (ET) influences wet and dry anomalies over continental regions (Bosch et al., 2006). Soil water is also a dominant factor in shaping an ecosystem's response to the physical environment (Wei, 1995).

Soil moisture influences growth of rangeland plants and cultivated crops, and the susceptibility of soils to degradation processes (Tansey et al., 1999) and flooding (Brocca et al., 2011, Brocca et al., 2010, Koster et al., 2010). For these reasons, soil moisture has been recently introduced as one of the “Essential Climate Variables” (ECV), which along with others are needed to properly characterise the earth's climate (Global Climate Observing System (GCOS), Summit, 2010). Thus, soil moisture information is regarded as crucial for several applications in water resource management and planning.

Careful consideration must be made when deciding on the most appropriate method for gathering soil moisture information as there are many factors which influence the distribution of soil moisture in time and space. The temporal and spatial dynamics of soil moisture are influenced by topography, soil properties, vegetation cover, depth to the water table and meteorological conditions (Gómez-Plaza et al., 2001). Thus, soil moisture usually exhibits high spatial heterogeneity near the surface.

There are three approaches for estimating soil moisture, namely in situ measurement, estimation based on remote sensing, and estimation based on simulation modelling (Martinez et al., 2007). In situ measurements of soil moisture is considered as the most accurate approach for soil moisture assessment, yielding errors of less than 2% (vol/vol) (Brocca et al., 2012).

Direct measurements of soil water fluxes in many cases are not feasible due to the high degree of spatial and temporal variability of soil characteristics of an area, combined with the relatively small volumes investigated (Lacava et al., 2010), which is only a few square meters or less

(Brocca et al., 2007, Penna et al., 2009). There are few established soil moisture monitoring ground networks. Soil moisture information is crucial for management of water resources, especially in water stressed areas. Most of the western regions of South Africa are arid and semi-arid, in which the dominant land use is agriculture, which greatly depends on improved management of water resources within these water stressed regions.

For these reasons, remote sensing and soil water balance modelling offer feasible alternatives to ground measurements of soil moisture as they are able to estimate average values for larger areas and are potentially much more cost effective and efficient than collecting in situ data. However, remote sensing products for soil moisture estimation with reasonably short revisit times are generally characterised by coarse spatial resolution ($>10 \text{ km}^2$ for remote sensing platforms) (Brocca et al., 2011). Fine scale resolution for remote sensing platforms will thus refer to scales $\sim 1 \text{ km}^2$ in this study. Coarse spatial resolution of remote sensing information is too coarse for certain water management applications at meso-scale (which in this study depicts scales of $1\text{-}100 \text{ km}^2$ for hydrological applications). This scale is derived from Schultz (1994), who also advocates the use of remote sensing for hydrological applications at meso-scales. In addition, remote sensing derived soil moisture products have not been extensively validated in semi-arid regions for extended periods of time, to fully investigate the accuracy levels of satellite estimation over wet and dry seasons.

1.1 Problem Statement

In situ monitoring of soil moisture may not always be feasible due to the small spatial volume investigated, high cost, as well as the considerable time required for data collection.

Remote sensing provides an alternative means to derive soil moisture information which addresses all these concerns. There are however two major concerns which arise from deriving soil moisture information from satellite sensors within semi-arid region for such aforementioned scales:

1. The coarse spatial resolution of high temporal resolution products
2. The relatively short duration of validation studies for such products (<1 month)

Soil moisture investigations in semi-arid regions show that these areas display high spatial variability at different time scales (Cantón et al., 2004). Most satellite soil moisture validation

studies in semi-arid regions however, focus either on investigating soil moisture at a meso-scale through downscaling (e.g. Mekonnen, 2009), or focus on coarse resolution soil moisture product validation over an extended period of time (Cosh et al., 2008, Cosh et al., 2006).

Thus for water management at meso-scale within semi-arid regions, there exists a need to investigate the downscaling of coarse spatial resolution satellite soil moisture estimates, over an extended period of time (during wet and dry periods). This is partly owing to the fact that dramatic variations in temporal and spatial dynamics of soil moisture in semi-arid regions make quantification of soil moisture difficult over short periods difficult (Cosh et al., 2008). This in turn makes validation of the downscaled satellite soil moisture products difficult during short field validation studies.

1.2 Aim of the study

The aim of this study was to determine whether satellite derived soil moisture are realistic at spatial and temporal scales, which are appropriate for meso-scale water resource management, within semi-arid regions.

1.2.1 Research Questions

1. Are soil moisture products derived from remote sensing realistic estimates of actual soil moisture content in the semi-arid regions?
2. Can remote sensing products be used to estimate acceptable soil moisture estimates at meso-scales?
3. Can readily available meteorological data and knowledge of soil physical properties be used to predict temporal variations in soil moisture content?

1.2.2 The objectives of this study were:

1. To determine whether soil moisture products derived from remote sensing provide realistic estimates of actual soil moisture content in semi-arid regions.
2. To determine whether remote sensing products can be used to estimate soil moisture at meso-scales.

3. To determine whether readily available meteorological data and knowledge of soil physical properties can be used to predict temporal variation in soil moisture.



2. Literature Review

2.1 Introduction

In this chapter the role of soil moisture in the hydrological cycle is discussed, after which a few examples on the importance of information about soil moisture to various stakeholders is examined. Once some needs for soil moisture information are highlighted, the factors affecting the derivation of such information are discussed. Lastly, the specific approaches to collecting soil moisture information are discussed.

2.2 The role of soil moisture in the hydrological cycle

Assessment of the various elements of the hydrological cycle is important for the development and sustenance of society and ecosystems (Richter et al., 2003). Even though the concept of the hydrological cycle is relatively simple, the phenomenon is enormously intricate as it is not one cycle but many interwoven cycles occurring at continental, regional and local scales, among which the total volumes of water are continuously changing (Chow et al., 1988, Ward and Tribble, 2003).

Fresh water occurs in the atmosphere as water vapour, and as a liquid or solid on both the surface, and subsurface of the. The three main physical processes which redistribute water between the atmosphere, the earth's surface and the subsurface, are precipitation, surface and subsurface runoff and evapotranspiration (ET). Soil moisture is a key variable in helping to understand these relationships within the hydrological cycle, because soil exists at the interface between the atmosphere, lithosphere, biosphere and hydrosphere (White, 2006). The rate at which, and amount of rainfall that infiltrates the soil surface is controlled by the soil moisture conditions at the time of a storm event (Bronsert and Plate, 1997). Thus soil affects the partitioning of water into runoff and subsurface storage. The reflection and absorption of downward solar radiation on the earth's surface is controlled by the soil moisture content (Carlson, 2007). The available net radiation influences meteorological conditions through additions of water vapour into the lower regions of the atmosphere.

Measurement of soil moisture fluxes with an acceptable accuracy level remains a challenge. This is due to various factors, such as the high variability in time and space of processes such as rainfall (Kidd, 2001). Accurate soil moisture information has important applications, in understanding relationships and interactions between land and atmosphere (Bosch et al., 2006). Soil moisture information is thus important in quantifying many other processes which have major implications for water management for various stakeholders.

2.3 The importance of soil moisture information in environmental and water management

Soil moisture information is regarded as crucial for a number of applications in hydrology and related science and management disciplines. Timely and adequate information on various components of the hydrological cycle for managers and authorities are important. This is partly due to the increased competition for water resources, and partly both the magnitude and frequency of floods and droughts are influenced by soil moisture (Pahl-Wostl, 2007). Droughts are regarded as some of the world's costliest disasters, and due to the lack of ground measurements of soil moisture, it is often difficult to quantify the spatial and temporal variations of these events (Dai et al., 2004, Robock et al., 2000). Soil moisture also influences growth of rangeland plants and cultivated crops (Tansey et al., 1999) and flooding (Brocca et al., 2011, Brocca et al., 2010, Koster et al., 2010).

2.3.1 Drought

Drought is a phenomenon which is generally characterised by prolonged and abnormal soil water deficiency. This is mainly caused by the natural climatic variability (Dalezios et al., 2000, Dalezios et al., 1991, Palmer, 1965). Droughts are classified into meteorological, hydrological and agricultural droughts, and each category has a unique signature (Rouault and Richard, 2003). Agricultural droughts generally last between 3 and 6 months, and usually result in crop damages (Harsch, 1992). Studies of normalised difference vegetation index show that the impacts of agricultural droughts on vegetation are particularly strong where annual rainfall varies between 300 and 500 mm a⁻¹ (Richard and Pocard, 1998). Hydrological droughts generally last between 12 months and 2 years and affect the surface and subsurface water at different time scales (Meigh et al., 1999).

South Africa has experienced frequent and long droughts during the past 30 years (Hassan and Backeberg, 2010). Between 1982 and 1993, 7 of the 11 years were characterised by below

average rainfall in South Africa, with the 1992/93 agricultural droughts causing 70% crop failure nationally, reducing agricultural exports by \$250 million, which constituted a 2.4% drop in the country's gross domestic product (Hassan and Backeberg, 2010). One of the major problems in Africa is the lack of soil moisture data at scales at which drought effects have to be managed (Hassan and Backeberg, 2010).

Current approaches for drought assessment use meteorological indices, process based indices, and satellite based indices. Meteorological indices, such as the standardized precipitation index (SPI) and Palmer Drought Severity Index (PDSI), are derived by analysing precipitation data over an extended period of time (Narasimhan and Srinivasan, 2005). Problems are likely to arise using this approach where precipitation patterns display high degrees of spatial heterogeneity as this approach might aggregate affected and unaffected areas, lowering the accuracy of prediction. This approach is also likely to fail in the assessment of short term droughts (Hayes et al., 1999). This is potentially the case in South Africa, which has high spatial rainfall heterogeneity (SA Weather South African Weather Bureau, 1972). Due to this complexity of the rainfall regime in South Africa, it is difficult to monitor droughts using meteorological based indices, which is likely to hinder relief efforts by government and various organisations as they rely on information for decision making purposes (Rouault and Richard, 2003).

Process based drought indexes are derived by simulating or estimating hydrological processes, such as in the Soil Moisture Deficit Index (SMDI) and Evapotranspiration Deficit Index (ETDI) (Narasimhan and Srinivasan, 2005). These approaches were found to capture spatial variability of droughts over shorter periods (Narasimhan and Srinivasan, 2005). Satellite based indicators for drought are NDVI, vegetation condition index (VCI), temperature condition index (TCI) and soil moisture index (SMI). They offer the advantage of monitoring spatial and temporal variations of droughts at regional and continental scales due to their large spatial and frequent temporal coverage (Su et al., 2003). Satellite derived soil moisture products in particular have good potential for drought monitoring, as they represent a direct measurement of the land surface moisture conditions. This can reduce possible errors that can be introduced through data interpretation of other satellite products, such an analysis of NDVI for drought, which is dependent on vegetation species and climate zones (Wang et al., 2007). Satellite soil moisture products also provide a means of improving drought models as is shown by Bolten et al. (2010).

2.3.2 Irrigation management

Even though only 17% of the world's cropland is irrigated, this land produces more than a third of the world's food and fibre (Willel, 2000). The consequence of growing competition for freshwater resources between municipal, industrial and agricultural sectors has resulted in a decrease in the available freshwater for allocation to agriculture (Tilman et al., 2002). Intensive vegetable production systems are commonly located in warm climatic regions, such as South Africa, because growing conditions are favourable for numerous vegetable species. Due to limited available water resources, there is growing pressure on farmers to optimise their use of irrigation water, which requires knowledge about the soil moisture content (Thompson et al., 2007).

Many farmers base irrigation scheduling on experience (Feres et al., 2003) which frequently results in over-irrigation to ensure that water does not limit production (Thompson et al., 2007). Information about soil moisture content is needed to determine the irrigation water requirements of crops (Thompson et al., 2007). Soil moisture sensors can be used with automated irrigation systems, so that soil moisture content does not reach a threshold limit- so as not to subject crops to water stress. Unfortunately, due to the spatial and logistical constraints of point measurements of soil moisture, ground based techniques do not offer spatially distributed information for irrigation water management. Remotely sensed soil moisture products provide a feasible alternative to overcome this potential shortcoming. Satellite derived soil moisture products also have the potential for deriving performance based indicators in irrigated agriculture through (Bastiaanssen and Bos, 1999):

1. Monitoring irrigation events at scales > 500 ha in a regular fashion and
2. revealing the overall water resources utilization

Thus there is a potential for using remote sensing to derive soil moisture information required for irrigation water management. There is however still a need for standardization of irrigation performance indicators, so as to provide a better platform for such work to be undertaken (Bastiaanssen and Bos, 1999).

2.3.3 Flooding

There are many causes of floods but all floods are characterised by the overflowing of water that submerges land which is usually dry (Kobiyama and Goerl, 2007). Floods have the potential to cause widespread damage and devastation through economic losses and loss of human lives. In South Africa alone between the years 1980 and 2010 there have been flood related deaths totalling 1068 persons. There are also records of great economic losses due to widespread flooding in South Africa between the period December 2010 and February 2011, of which the estimated damages were \$1.1 billion (Africa, 2011).

There are numerous mechanisms which influence the occurrence of floods of various magnitudes, which vary spatially and temporally (O'Connor and Costa, 2004). One of the key areas of interest for reducing flood damages is early warning/forecasting systems. Even though much uncertainties may be present in, forecasting information provided before flood events may provide enough lead time so that mitigation measures can be undertaken (Norbiato et al., 2008).

The formation of floods depends on specific catchment conditions, such as slopes gradient, surface permeability, soil saturation or anthropogenic factors (e.g. alterations to natural drainage). Soil moisture conditions are among the most important of these hydrological properties (Norbiato et al., 2008). The consideration of initial soil moisture conditions in flood vulnerability assessment is a critical step in predicting the locations within the catchment that will be affected by the flood (Norbiato et al., 2008). Satellite-derived soil moisture products provide soil moisture information at spatial and temporal scales which can be used in early flood warning systems.

Flood forecasting in ungauged basins poses a problem due to lack of data. Soil moisture data, derived from remote sensing, can provide flood forecast models with temporal and spatial variation of soil moisture. Even in cases where accuracy of soil moisture data is not high, such critical information still provides better results than no information of soil moisture conditions (Norbiato et al., 2008).

2.4 Factors affecting soil moisture and measurement of soil moisture content

Soil moisture distribution is affected by topography, soil properties, vegetation cover, depth to water table and evapotranspiration (Gómez-Plaza et al., 2001). The influence of these factors vary spatially and temporally (Famiglietti et al., 1998). An example of this is that topographic

and soil characteristics vary in the downslope direction. For such reasons, differentiating the relative magnitudes of influence of contributing factors affecting the distribution of soil moisture is complex.

Soil moisture dynamics are affected by both external and internal factors. Soil physical and chemical attributes affect the spatial and temporal distribution of soil moisture content. Soil texture and particle arrangement are noted as stable properties and are useful indices for several other properties such as field capacity and hydraulic conductivity (White, 2006).

In addition to the aforementioned soil properties which may affect the distribution and movement of water in soils, one must also understand the forces acting on water, which affect its potential energy in soils. The energy status of soil water thus also influences its availability to plants (White, 2006). Due to the complexity of processes occurring at plot scale, which affect soil moisture, an alternative is to consider spatial patterns and controls on a larger scale ($>100 \text{ km}^2$), depending on the intended application of a soil moisture distribution conceptual model.

Grayson et al. (1997) proposed two main states of spatial soil moisture patterns: the first state occurring during periods when precipitation exceeds ET, making topography upslope of a given point the dominant control (nonlocal control), and the second state occurring during periods when ET exceeds precipitation, in which case soil moisture spatial patterns reflect soil and vegetation differences (local control). Local terrain usually only influences the spatial distribution patterns of soil moisture in areas where high local convergence may cause a temporary increase in the soil water content following rainfall events. Few studies though, have analyzed soil moisture variability over large areas ($> 100 \text{ km}^2$) and for extended periods of time ($> 1 \text{ year}$) (Entin et al., 2000, Fernandez and Ceballos, 2005, Vinnikov et al., 1996). Two important findings in scientific literature which help us understand soil moisture variability in time and space are:

1. Soil moisture spatial patterns can be represented by a small-scale component dominated by soil type, topography and vegetation, while a large-scale component is dominated by atmospheric quantities such as precipitation and ET (Entin et al., 2000)
2. Soil moisture spatial patterns display temporal or rank stability (Chen, 2006) for a range of scales.

Due to the many aforementioned factors which affect the distribution of moisture in the soil, careful consideration must be made when measuring and analysing this information. The measurement of soil moisture may be broadly categorised into in situ measurement, remote sensing estimation and modelling.

2.5 In situ measurements

The standard method for measuring soil moisture content is known as the thermogravimetric method. This method involves oven-drying a soil sample (at 105°C) of a known volume and weight at and then determining the weight loss thereafter. It is an indispensable method for calibration and evaluation of soil moisture probes (Walker et al., 2004). This method is time consuming and damages the soil sample and therefore cannot be used for repetitive measurements.

There are however a host of commonly used automated soil moisture measurement methods which include neutron scattering, gamma ray attenuation, soil electrical conductivity, tensiometry, hygrometry and soil dielectric constant (Walker et al., 2004). Generally speaking, these automated methods make use of the contrasting physical and chemical properties between soil that is saturated and soil samples which are dry. Advantages and disadvantages are discussed in more detail by Wilson (1971), Schmugge et al. (1980), Zeglin (1996) and Topp (2003). Automated soil moisture content measurement methods should always be verified by thermogravimetric measurements.

Ground based techniques yield accurate soil moisture measurements (errors of less than 2% vol/vol) (Brocca et al., 2012). Even so, such measurements may only be representative of less than a few square metres of soil moisture conditions and thus they may not be appropriate in areas which are regarded as heterogeneous, with regards to soil properties, typography, weather and land use/land cover (LU/LC).

2.6 Remote sensing estimation of soil moisture

Remote sensing techniques for retrieval of soil moisture information have been widely investigated for the past 40 years as they potentially offer a means of retrieving soil moisture information for wider spatial scales than the conventional ground based methods. Soil moisture

estimation using remote sensing may be broadly grouped into gamma radiation, reflected solar, thermal and microwave techniques (Mekonnen, 2009).

2.6.1 Gamma radiation techniques

This method is based on detecting the difference in the natural terrestrial gamma radiation flux between wet and dry soils. This is made possible because of the ability of water in soils to attenuate gamma radiation (Mekonnen, 2009). Gamma radiation measurements are typically made by a low flying aircraft at an altitude between 100m and 200m, over a flight length of about 15-20km, with a swath width of 300m (Caroll, 1981). This would produce soil moisture estimates of about 4.5-6km² per flight line. An investigation by Loijens (1980) in Canada determined measurements of the top 10cm of the soil column to have an error margin of 3% (vol/vol), while measurements of the top 25cm of the soil column yielded an error of 2.5% (vol/vol). This method however does require calibration using ground measurements for flight lines (Caroll, 1981, Mekonnen, 2009).

2.6.2 Reflected solar techniques

Soil moisture influences reflection of shortwave radiation from soil surfaces in the very near infra-red (VNIR) (400-1100 nm) and short wave infra-red SWIR (1100-2500nm) parts of the electromagnetic spectrum (Lobell and Asner, 2002). Deriving soil moisture information from reflectance measurements of these portions of the electromagnetic spectrum remains difficult, as organic matter and texture of soil, surface roughness and vegetation cover are regarded as noise and thus complicate interpretation of the sensor measurements (Asner, 1998, Ben-Dor et al., 1999). There are also few studies that have investigated these approaches at intermediate soil moisture levels (Lobell and Asner, 2002).

2.6.3 Thermal techniques

Volumetric soil moisture content for the top 4cm of soil has been linearly related to the amplitude of diurnal soil temperature for certain soil types (Idso et al., 1975, Mekonnen, 2009). Surface temperature is primarily dependent on the thermal inertia of the soil, which in turn is dependent on the thermal conductivity and heat capacity of the soil. Thermal conductivity and heat capacity of the soil increases with increasing soil moisture content (Mekonnen, 2009). Thus, a relationship can be established between surface temperature and soil moisture content by

measuring the diurnal temperature change. This relationship however, depends on the soil type and is largely limited to bare soil conditions.

The presence of vegetation and clouds largely limit the applicability of the thermal technique, especially when there are thin cirrus clouds in the atmosphere, as thermal relationships with moisture are affected (Mekonnen, 2009). In addition to this, surface radiant temperature is very insensitive to soil water content in the root zone, except in extreme water deficit conditions (Arrett and Clark, 1994). This is due to a daytime decoupling effect, where the upper few centimetres of soil are more representative of near surface air temperature (Jackson, 1980).

2.6.4 Microwave techniques

Microwave techniques for estimating soil moisture content include active and passive microwave techniques. These approaches have been investigated since the 1970's and are capable of measuring only the top 5cm of the soil (for electromagnetic wavelengths of ~ 21 cm). These techniques are largely based on the contrast in dielectric properties between water and dry soil, when subjected to an electromagnetic field. As soil moisture increases, the dielectric constant increases to a value of 20 (dimensionless) or more (Albergal et al., 2009, Schmutge, 1983).

Passive microwave techniques make use of radiometers, which measure the intensity of the emissions from the soil surface, referred to as the microwave brightness temperature. Microwave brightness temperature is proportional to the product of surface temperature and surface emissivity (Mekonnen, 2009). These approaches are characterised by low spatial resolution (≥ 12.5 km), but high temporal resolution (≥ 1 day) (Brocca et al., 2011).

Active microwave techniques make use of radar backscatter from soil and vegetation layers to determine soil moisture content. These approaches are generally characterised by a better spatial resolution than passive microwave sensors (in the order of tens of meters) (Walker et al., 2003), but consequently have generally lower temporal resolution (up to 36 days- due to satellite orbit revisit times).

Microwave techniques can be used for all weather conditions, provide a direct measure of soil moisture content and are capable of penetrating vegetation cover. At fine resolutions, satellite active microwave soil moisture sensors are more sensitive to surface roughness, topographic features and vegetation cover than passive sensors (Walker et al., 2003). Because of the potential

high temporal frequency of microwave derived soil moisture sensors and the fact that data availability is not dependent on weather conditions, passive microwave soil moisture sensors would be able to capture temporal soil moisture variations. The spatial resolution however is better suited for larger scale application and management ($\geq 1000\text{km}^2$). Another key issue is the validation of coarse scale remote sensing products because of the large disparity between them and ground measurements (Jackson et al., 2010). There are however studies that indicate that point scale measurements can be representative of larger areas (Brocca et al., 2011, Brocca et al., 2010, Fernandez and Ceballos, 2005).

2.7 Downscaling of remote sensing derived soil moisture

Remote sensing derived soil moisture products potentially have a short revisit time (1-2 days) and provide soil moisture estimates at catchment scale and are thus advocated by many researchers (e.g. Gruhier et al., 2010, Wagner et al., 2007). Unfortunately, most of these soil moisture products are characterised by coarse spatial resolution (tens of km), which may not always be representative of the scales at which hydrological processes take place (1km or less) (Merlin et al., 2006), or suitable for meso-scale hydrological management. For this reason much recent work has gone into the downscaling of soil moisture estimates derived from remote sensing from coarse scale (tens of km) to finer scale ($\sim 1\text{km}$) (Chauhan et al., 2003, Das et al., 2011, Kim and Barros, 2002, Merlin et al., 2008). The extent of the finer scale is generally determined by the scale at which regularly (1-2 days) and freely available auxiliary input remotely sensed data is available, such as that of the Moderate Resolution Imaging Spectroradiometer (MODIS).

Downscaling of soil moisture can broadly be grouped into two classes; stochastic and deterministic approaches. In the stochastic approaches, statistical probabilities are inferred for fine scale compositions of which coarse scale pixels are made up of, often using binomial probabilities (Boucher, 2007). One of the major shortcomings of this approach however is that downscaled products are often not derived from physically based inputs and therefore can have several possible solutions (Kim and Barros, 2002). This can give rise to error propagation as there is no physically based data or information which determines the solution. Deterministic approaches on the other hand make use of measurements or estimates of land surface attributes

for downscaling and thus rely on data which has physical meaning to perform such downscaling operations.

Recent methods for soil moisture downscaling include the use of fractal interpolation methods with fine-scale surface information (Kim and Barros, 2002), interpolation of passive microwave data with fine-scale active microwave data (Bindlish and Barros, 2002, Das et al., 2011), distributed hydrological modelling with local information on topography (Pellenq et al., 2003), brightness temperature linear regression (Chauhan et al., 2003) and downscaling using soil evaporative efficiency (Merlin et al., 2008). For the purpose of this study, it would be beneficial to downscale coarse resolution microwave soil moisture products, using a deterministic approach, with data that is routinely available.

2.8 Soil Water Balance Modelling

Hydrological models are classified as lumped, distributed or semi-distributed models. Lumped models have spatially averaged parameters that cannot easily be related to physical basin properties. Such models estimate parameters and parametric relationships based on calibration. Thus, lumped models require less understanding of area and vertical variability of hydrological processes (Bergström, 1991). Lumped models rely on calibrated parameters which are usually used to represent aggregated processes and as such may often outperform distributed models, but a good model performance does not always mean hydrological processes are accurately represented.

Distributed models are supposed to have model parameters directly related to the physical characteristics of the catchment and capture the spatial variability of both physical characteristics and meteorological conditions (Refsgaard, 1997). These types of models are usually more feasible at smaller scales, where there is lower variability of physical parameters (Bergström, 1991). Even though distributed models are capable of incorporating heterogeneity of model parameters and physical processes, their data requirements are usually higher as well as their relative level of complexity. This however does allow parameters to be derived directly from field measurements. This in turn raises another concern for this type of model, in that their performance has a limit which is restricted by the accuracy and representativeness of input data. Thus, heterogeneity of hydrological processes responses and unknown scale dependant parameters may also limit the performance of such model (Bevan, 1989).

Semi-distributed models are a combination of the aforementioned model types and seek to incorporate the benefit of each. Models usually make use of a predefined set of input parameters and then based on their structure, simulate a specific set of outputs, such as soil moisture content. Such processes or simulations are described by differential equations based on simplified physical laws or empirical algebraic equations (Arnold et al., 1998). Based on the relative simplicity of lumped models and their applicability for a wide range of conditions which may be adjusted based on parametric calibration, this model type was selected for this study.

The type of model selected and its structure is usually based on its intended usage or desired output(s), which in the case of this study is to simulate soil moisture in the top few centimetres of the soil. Owing to the relatively small areas for which the model is intended for (1 km²), in order to compare to in situ measurements and downscaled remote sensing soil moisture estimates, a conceptual-lumped hydrological model was selected.

A soil water balance approach was selected for this as water balance approaches have been shown to work well for modelling soil water content in the top layer of the soil column in previous studies (Eilers et al., 2007, Panigrahi and Panda, 2003, Soares and Almeida, 2001). This is achieved through the systematic evaluation of the losses and gains to the soil profile, which has a bucket structure. This approach is also referred to as a volume based model and is often preferred to dynamic models as they are usually simpler and require fewer parameters (Panigrahi and Panda, 2003)

3. Methodology

3.1 Introduction

This chapter describes the methodology followed during the course of the research project. This includes the general approach to the study. This is followed by the methods selected for in situ soil moisture measurement, satellite derived soil moisture data, the downscaling method used and the structure of the soil moisture model. A description of all data sources is presented thereafter with criteria for model evaluation and the criteria for selection of the study area are discussed.

3.2 Approach to the study

This study was conducted by comparing soil moisture obtained from in situ soil moisture measurements, remote sensing data and hydrological modelling. This was done as a comparative analysis, where two different areas were investigated. The reason for this was to determine if differences in topography and soil properties affected the accuracy of the methods used or if these approaches are widely applicable in semi-arid conditions such as those found in the Western Cape of South Africa. Soil moisture information from the aforementioned sources was collected from 19 July 2013 till 27 January 2014 which included the wet and dry seasons, so as to assess the applicability of the selected methods under different hydrological conditions.

3.3 In situ soil moisture measurements

There are several methods which exist for in situ measurements of soil water content, as discussed in Chapter 2.5. Due to the relatively large volume of soil moisture measurements required to characterise the soil moisture variability at meso-scale, an automated soil moisture probe (one which could provide instant soil moisture readings in the field) was selected for its ability to perform repeated measurements without damaging or disrupting the soil column. This was accompanied by gravimetric measurements of selected points during wet, intermediate and dry periods, to infer the soil moisture probe's accuracy in the selected study areas. These gravimetric measurements were then used to test and correct the calibration of the soil moisture probe provided by the manufacturer for general use in a wide range of soil types.

The Hydrosense 2 soil moisture probe by Campbell Scientific (Hydroprobe) (Figure 3.1) was selected for in situ measurements, because it is a handheld sensor which is easy to carry around in the field and has the ability to store soil moisture measurements. This probe functions on the Time Domain Reflectometry (TDR) principle and makes use of electromagnetic waves to measure soil moisture.



Figure 3. 1: The Hydrosense 2 soil moisture probe (Hydroprobe) by Campbell Scientific

The ability of electromagnetic waves to determine properties in porous media has been extensively investigated and recognised for most of the past century, but identifying frequencies which yield the most accurate results when measuring such properties as soil water content, is relatively more recent (Rinaldi and Francisca, 1999). Among the most popular methods for this are TDR and capacitance measurements due to their simplicity and data logging capabilities.

TDR is widely used for the measurement of soil water content and electrical conductivity. TDR application for the measurement of soil moisture was first reported by Topp et al. (1980) and is often favoured over other methods, because of its minimal calibration requirements and relatively high accuracy (1-2% volumetric water content) Jones et al. (2002). The principle on which TDR works is that the measurement of the bulk electrical permittivity (ϵ_b) of the soil surrounding the probe can be determined as a function of electromagnetic wave velocity and the length of the electromagnetic length of the probe. Thus volumetric water content (θ_v) of soil is calculated using its relationship with (ϵ_b), as proposed by Topp et al. (1980), for a variety of soil

types and conditions. This was achieved by using a third order polynomial to describe this relationship as is given by:

$$\theta_v = -5.3 \times 10^{-2} + 2.92 \times 10^{-2} \varepsilon_b - 5.5 \times 10^{-4} \varepsilon_b^2 + 4.3 \times 10^{-6} \varepsilon_b^3 \quad (3.1)$$

This relationship however, is only valid for water content ranges $<0.5 \text{ m}^3\text{m}^{-3}$ and shows decreased accuracy for soils high in organic and/or clay content (Jones et al., 2002).

3.4 Remote sensing of soil moisture

Based on the literature reviewed, microwave techniques would be most suitable for remote sensing of soil moisture, as they offer daily coverage over the study area and are capable of retrieving estimates in all weather conditions. Albergal et al. (2009), argues that L-band (frequency of 1-2GHz) is the optimal microwave wavelength for sensors to detect changes in soil moisture in the top layer of soil. There are currently several satellite sensors operating at or near that frequency, such as the Soil Moisture and Ocean Salinity (SMOS), the Advanced Microwave Scanning Radiometer for the Earth Observing System (AMSR-E) on board the Aqua satellite, and the Advanced Scatterometer (ASCAT) on board the Meteorological Operational (METOP) satellite. Of these, ASCAT offers the best combination of spatial (12.5km) and temporal (1-2 days) resolution. This product was found to compare very well to ground measurements in several validation studies (Albergal et al., 2009, Brocca et al., 2011). For these reasons, ASCAT was selected as the satellite platform from which to obtain soil moisture estimates in this study. There have however not been studies comparing ASCAT soil moisture estimates to ground measurements in semi-arid areas.

ASCAT has been operating on board the METOP satellite since 2006. This is a C-band scatterometer (5.255 GHz, VV polarised) with a radiometric accuracy of better than about 0.3 dB (Verspeek et al., 2010). C-band scatterometers are used for soil moisture retrieval by making use of the Vienna University of Technology (TUWIEN) change detection algorithm proposed by Wagner et al. (1999) and improved by Naeimi et al. (2009). Processing for soil moisture retrieval using ASCAT is set at 12.5km spatial resolution.

ASCAT is a real-aperture radar instrument, which measures radar backscatter. Measurements occur on either side of the satellite tract of the METOP, generating two 550km wide swaths of

data (Albergal et al., 2009). Thus, on both sides of the METOP, a triplet of backscattering coefficients (σ^o), using three separate antenna beams, is produced by ASCAT. This backscattering coefficient measurement is the result of averaging several radar echoes. Measurements are made at 45° , 90° and 135° azimuth angles relative to the satellite track.

Due to this registry of backscatter at multiple incident angles (45° , 90° and 135°), it is made possible to determine the yearly cycle of the backscatter incident relationship, which is an essential prerequisite for correcting seasonal vegetation effects (Bartalis et al., 2007, Gelsthorpe et al., 2000). For the actual retrieval of soil moisture, Wagner et al. (1999) proposed to scale the backscattering coefficient extrapolated to a reference angle at 40° ($\sigma^o(40)$), using the lowest and highest values of $\sigma^o(40)$ over an extended period of time- essentially, wet and dry limiting cases. ASCAT derived soil moisture content (θ_A), is given by:

$$\theta_A(t) = \frac{\sigma^o(40, t) - \sigma^o_{dry}(40, t)}{\sigma^o_{wet} - \sigma^o_{dry}(40, t)} \quad (3.2.)$$

where wet and dry limiting cases are denoted by $\sigma^o_{dry}(40, t)$ for backscatter at dry limiting cases and $\sigma^o_{wet}(40, t)$ for backscatter at wet limiting cases respectively, where t is time.

This equation can only be applied if the ground is not frozen and is only representative of the top few centimetres of soil (Schmugge, 1983). Soil moisture is given as the degree of saturation in percentages from 0% (dry) to 100% (saturated). ASCAT measurements or overpass times generally occur twice daily, in the morning and early evening. Jackson (1980), recommends the use of morning soil moisture estimates, when soil is most likely in equilibrium, in order to avoid the daytime decoupling effect between the topmost layer of soil (0-2cm) and the layer beneath it.

3.5 Downscaling: Brightness temperature linear regression model

Of the various downscaling methods discussed in Section 2.8, it was determined that the method selected should be able to provide downscaled soil moisture estimates at a moderately high temporal resolution (1-2 days), so as to compare this estimate to the measured and simulated soil moisture content. A physically based model was determined as the most suitable approach for this study. For this, the combination of active and passive microwave remote sensing was the most suitable method, but because of limited data access to synthetic aperture radar (SAR) for

the time period during which the study took place, this method was not used. Thus, the brightness temperature linear regression model was selected. This method is referred to as a stochastic model (Merlin et al., 2008), but still makes use of physical measurement and thus represents a combination of the physical and stochastic approach.

Studies have determined that spatial variations of radiant surface temperature strongly depend on surface soil water content (Merlin et al., 2006). Vegetation still plays an important role in this relationship, as there is no universal relationship between soil moisture and land surface temperature in the presence of vegetation (Chauhan et al., 2003). It was however concluded that there exists unique relationships between soil moisture availability and land surface temperature relative to the corresponding normalised difference vegetation index (NDVI) over specific climatic conditions and land surface types (Carlson et al., 1994, Chauhan et al., 2003). This is evident in Carlson et al. (1994) and (Gillies et al., 1997), where regression relationships among soil moisture and surface temperature for NDVI values were generated; as confirmed by results obtained using the Soil Vegetation Atmosphere Transfer (SVAT) model through an energy budget approach (Carlson et al., 1995).

Soil moisture estimation from optic/infrared (IR) remote sensing techniques pose some difficulties, as discussed in Section 2.7. A method is proposed by Chauhan et al. (2003), to overcome these limitations by combining coarse resolution microwave soil moisture retrievals with that of the finer resolution optic/IR remote sensing parameters. This is achieved through determining regression relationships between surface soil moisture and surface temperature for specific vegetation types and densities, which in conjunction with the coarse resolution microwave soil moisture estimates (~12.5 km) are regressed to obtain soil moisture at a higher spatial resolution (~1km).

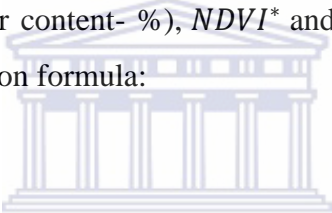
The spatial correlation between land surface temperature (LST) and near surface soil moisture is explained by the capacity of the soil to counter the increase of its physical temperature by evaporating the soil water content at the surface (Merlin et al., 2006). As there are other factors that affect surface skin temperature, other than soil moisture content, NDVI is used to empirically calibrate the correlation between surface skin temperature and soil moisture content for various vegetation covers. These relationships are, sometimes referred to as the ‘universal

triangle'. The regression relations between temperature, NDVI and soil moisture are determined from Equations (3.3) to (3.5) as given below:

$$T^* = \frac{T - T_0}{T_s - T_0} \quad (3.3)$$

$$NDVI^* = \frac{NDVI - NDVI_0}{NDVI_s - NDVI_0} \quad (3.4)$$

where T is land surface temperature (LST) ($^{\circ}\text{C}$) and $NDVI$ is normalised difference vegetation index (dimensionless), the subscripts s and 0 depict maximum and minimum values, and the superscript $*$ depicts prime (dimensionless). Carlson et al. (1994), proposed that the relationship between soil moisture θ (soil water content- %), $NDVI^*$ and T^* (NDVI and temperature index) can be expressed through a regression formula:



$$\theta(t) = \sum_{i=0}^{i=n} \sum_{j=0}^{j=n} \alpha_{ij} NDVI^{*(i)} T^{*j} \quad (3.5)$$

where i and j indicate the order of the polynomial.

Expanding equation (3.5) gives the following second order polynomial:

$$\begin{aligned} \theta(t) = & \alpha_{00} + \alpha_{10}NDVI^* + \alpha_{20}NDVI^{*2} + \alpha_{01}T^* + \alpha_{02}T^{*2} + \alpha_{11}NDVI^*T^* + \alpha_{21}NDVI^{*2}T^* \\ & + \alpha_{12}NDVI^*T^{*2} + \alpha_{22}NDVI^{*2}T^{*2} \end{aligned} \quad (3.6)$$

Third order terms were ignored owing to their relative insignificance (Chauhan et al., 2003). For the calibration of the coefficients α_{00} - α_{22} , coarse resolution soil moisture (θ_c) is substituted into the left hand side of Equation 3.6, while LST and NDVI values for the same resolution are substituted on the right side. Once the coefficients are calibrated, fine resolution LST and NDVI

values are substituted on the right side of the equation, which then yields soil water content at fine resolution (θ_F).

This approach is however limited by the fact that the optic/IR data can only be used on cloudless days. The method also assumes that these regression relationships are constant for the entire microwave soil moisture pixel, which may not hold true, especially in areas with high surface and surface-meteorological heterogeneity. The calibrated coefficients a_{00} - a_{22} are representative of LST-NDVI soil moisture relationships at fine scale. For this reason, homogeneously agricultural areas will be examined, to minimise effects of heterogeneous land cover within a coarse resolution satellite soil moisture pixel.

3.6 Soil moisture modelling

3.6.1 Introduction

The model consists of five basic processes, namely interception (P_i), runoff (Q) and infiltration (I), recharge (R) and evapotranspiration (ET) - all of which are modelled on a daily time step (so that soil moisture output values could be compared to in situ soil moisture probe estimates as well as remote sensing outputs). The soil profile being modelled is divided into two layers in this model, because the surface moisture is more sensitive to precipitation and evapotranspiration, while deeper soil moisture may vary less with time. It is assumed that the soil profile is physically homogenous at fine scale ($\sim 1\text{km}^2$).

All available water which exceeds field capacity moves to the underlying soil layer at the beginning of the time step (e.g. Riha et al., 1994). This however may still introduce errors in arid and semi-arid regions, as redistribution of water in the soil column through infiltration may persist for many days after a precipitation event (Hillel, 1989, Kendy et al., 2003). For this reason, infiltration curves were generated using soil hydraulic model simulations in the Hydrous 1D version 4.17 software package (Šimůnek et al., 1998) to determine hydraulic conductivity (K). Soil hydraulic conductivity is generally high in areas with sandy soils, which are very common in the Western Cape (Hardie and Botha, 2010), and hydraulic conductivity decreases exponentially with decreasing soil moisture (Brutsaert, 2005). For these reasons, infiltration in the unsaturated zone was modelled at a 30min time step which would allow the model to reevaluate this relationship more regularly. At this short time step, water movement out of the soil

reservoir, namely recharge (R), was more realistically represented. Thus, R comprises of the daily total of 30 min recharge amounts.

There is no analytical solution for the calculation of simultaneous infiltration and evapotranspiration (Kendy et al., 2003), and for this reason infiltration and evapotranspiration were treated as two separate and sequential processes as successfully implemented in other modelling efforts (e.g. Kendy et al., 2003, Kuo et al., 1999, Zollweg et al., 1996).

Infiltration of precipitation (with the addition of irrigation where necessary), was determined using a runoff coefficient (β), so as to model infiltration of water into the soil profile without having rainfall intensity information (Brutsaert, 2005). Values for β were adopted from relevant literature through knowledge of soil physical properties. This was done because high temporal resolution precipitation data is not available and thus, it was assumed that the total daily rainfall is lumped together and added as input at the beginning of the day.

For this model, it was assumed that the lateral flow of water in the vadoze zone is negligible, because of the high hydraulic conductivities found in sandy soils. It is also assumed that there are no additions of water into the soil column from groundwater sources as groundwater is generally deep and there is no capillary rise (Bugan et al. (2012)). The total depth of the soil column being modelled is 1m, which would then also be deep enough to make provision for root depth of various agricultural crops (mostly wheat in the Western Cape) and indigenous vegetation (fynbos) while shallow enough to minimise the possibility of the groundwater table intruding into it. Research indicated that the root depths of wheat maturing during spring reached up to 1.1m (Thorup-Kristensen et al., 2009), while majority of the fynbos root systems along the western coastal region of the Western Cape Province average ~1m (Jongens-Roberts and Mitchell, 1986). Other assumptions are that, slope and hydraulic conductivity are sufficiently large so that no water remains ponded on the surface and also additions of water from upslope areas through surface runoff are negligible.

3.6.2 Rainfall

Rainfall in this model is regarded as all precipitation and irrigation gains to the soil profile for the entire time step and is added to the top layer of the soil profile at beginning of the modelled time step. Effective rainfall is the total amount of rainfall which reaches the ground after

interception losses and may be derived from literature for various cover types, as adapted from interception losses to shortgrass and midgrass areas (Thurow et al., 1987). This is given by:

$$P_e(t) = P(t) - P_i(t) \quad (3.7)$$

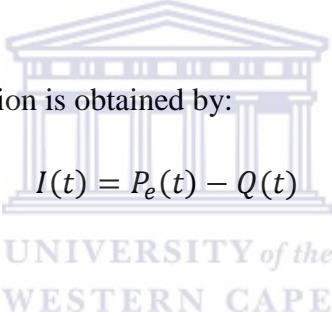
where P_e is effective rainfall (mm), P is total rainfall (mm), P_i is rainfall interception (mm).

3.6.3 Runoff and infiltration

Runoff and infiltration are grouped together, as infiltration is a residual value obtained by calculating the runoff which occurs when rainfall occurs. This is given by:

$$Q(t) = P_e(t)\beta \quad (3.8)$$

where Q is runoff such that infiltration is obtained by:



$$I(t) = P_e(t) - Q(t) \quad (3.9)$$

Infiltration is applied to the uppermost layer until it is filled to saturation, after which all excess infiltration is allowed to fill the second layer till saturation through recharge (R). Once the second layer is filled to field capacity, all excess water is lost to groundwater through deep recharge (R_d) for that time step. This relationship is maintained under the assumption that all areas investigated have relatively high hydraulic conductivities and gentle to moderate slopes, so as not to affect the infiltration rate in a significant manner.

3.6.5 Evapotranspiration

Reference evapotranspiration (ET_o) is calculated using the Hargreaves and Samani (1985) method, which is given by:

$$ET_o(t) = 0.0023 \cdot R_a(t) \times \left(\frac{T_{\max}(t) + T_{\min}(t)}{2} + 17.8 \right) \times (T_{\max}(t) - T_{\min}(t))^{0.5} \quad (3.10)$$

where T_{max} ($^{\circ}\text{C}$) is maximum air temperature, T_{min} ($^{\circ}\text{C}$) is minimum air temperature and R_a is extraterrestrial radiation. Thus, once ET_o is determined ET_a can be determined by using a evaporative coefficient (α) derived from literature and determining the relative amount of ET_a as constrained by the available soil moisture through:

$$ET_a(t) = ET_o(t) \times ET_c \left(\frac{\theta_1(t) + I(t) - W_p}{F_c - W_p} \right) \quad (3.11)$$

where ET_c denotes the evaporative coefficient of the cover type, W_p is wilting point and F_c is the field capacity of the soil reservoir. As the biggest proportion of plant roots are located in the top 20cm of the soil column in shrubland (Silva and Rego, 2003) and deeper soil layers account for negligible amounts of water to evaporation losses, reference evapotranspiration in the top layer will account for 70% of the total reference evapotranspiration.

Before recharge can occur an intermediate soil moisture value (SWC) is determined through:

$$SWC(t) = \theta_1 + I(t) - ET_a(t) \quad (3.12)$$

3.6.4 Recharge

This movement of water in the soil column is assumed to only occur in a downward direction, which is shown to be a reasonable assumption (Kendy et al., 2003, Steenhuis et al., 1985). Also, it is assumed that gravitational forces dominated over matric forces and thus lateral movement of water is ignored in the subsurface. Recharge out of the reservoir is calculated by making use of the hydraulic conductivity (K) (mm/d) which is a function of the soil moisture after infiltration. This is calculated each 30min (t_{30}) for each day (t) by:

$$SWC_R(t_{30}) = \theta(t_{30} + 1) \times K \quad (3.13)$$

where SWC_R (mm) is the soil moisture content of the soil layer at the given 30 min interval as determined by:

$$SWC_R(t30) = SWC_R(t30) - SWC_R(t30 - 1) \quad (3.14)$$

Thus recharge (R) is determined by the sum of all SWC_R for each day, which is then the sum of all recharge values obtained at every 30 min interval for one day.

The soil water content ($\theta 1$) (%) for the top layer (20cm) is thus calculated using the equation:

$$\theta 1(t) = (\theta 1(t - 1) + I(t) - R(t) - ET_a)/f \times 100 \quad (3.15)$$

where I is infiltration (mm), ET_a is actual evapotranspiration (mm), R is recharge (mm), f is the thickness of the layer (m) and t denotes time (1 day). Soil water storage in the second layer ($\theta 2$)(mm), is calculated by using a similar water balance equation, but modified to include gains from the first layer through R and losses out of the layer through deep recharge (Rd) (mm), by:

$$\theta 2(t) = \theta 2(t - 1) + R(t) - Rd(t)/f \times 100 \quad (3.16)$$

3.7 Model evaluation

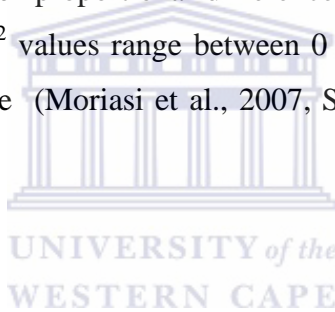
Model performance assessment of hydrological models requires assessment of the accuracy of the simulated behaviour of the model to observations (Krause et al., 2005). A model may be assessed in terms of systematic and/or dynamic behaviour as well as general efficiency. The most fundamental approach to assessing model performance is the subjective approach, through visual inspection of simulated and observed graphs. This type of approach is generally related to the systematic and dynamic behaviour of a model (Krause et al., 2005). More objective assessments generally require the use of statistical criteria to estimate of the error or accuracy between observed and simulated outputs or variables.

Mathematical measures of how well a model simulation fits the related observations are defined as efficiency criteria (Bevan, 2001). Different efficiency criteria usually place emphasis on different systematic and/or dynamic behavioural errors. Usually errors associated with high

values tend to be larger than those associated with lower values, thus calibration attempts aimed at minimizing these types of criteria often result in fitting the higher portions of the resulting graphs at the expense of the lower portions (Krause et al., 2005). For these reasons it is important to define the intended purpose(s) of the model before selecting the efficiency criteria (Janssen and Heuberger, 1995). For sound model calibration and validation, the inclusion of absolute or relative volume error with the relevant efficiency criteria is recommended (Krause et al., 2005).

3.7.1 Pearson's correlation coefficient (r) and coefficient of determination (r^2)

Correlation coefficient (r) which ranges from -1 to 1, is an index of the degree of linearity which exists between observed and estimated values, with 0 describing no linearity and 1 or -1 describing perfect linearity. This criterion however is overly sensitive to high values and may thus be insensitive to low values or proportional differences (Legates and McCabe Jr., 1999). The coefficient of determination r^2 values range between 0 and 1, and typically values greater than 0.5 are found to be acceptable (Moriasi et al., 2007, Santhi et al., 2001, Van Liew et al., 2003).



3.7.1 Root mean square error

The root mean square error (RMSE) evaluates the error of the total volume over the time series being simulated, which is seen as a necessary model evaluation and can be obtained by:

$$RMSE = \sqrt{\frac{\sum_{i=1}^n (a_i - b_i)^2}{n}} \quad (3.17)$$

where a and b are datasets one and two and n is the number of samples. Typically a would be the observed values (which in the case of this study will be the soil moisture probe estimates) and b would be the modelled or simulated value.

3.8 Criteria for site selection

The selection of the two study sites were guided by methodological considerations, as discussed in the remote sensing section of the methodology. The number of transects selected per site was constrained by logistical in situ data collection reasons to three transects per site, as any more would have required additional time or field assistance. Ideally, in situ data would have been collected for at least 10% of the study area. The main contributing factors to site selection were slope and LU/LC. A difference in topography between the study sites was preferred so as to assess the accuracy of microwave soil moisture estimates, which were found to be affected by land surface heterogeneity (as discussed in Chapter 2). Thus two sites were selected with differences mean slope: one with moderate slopes and one with more pronounced slopes. This was so as to determine if there were significant differences in the accuracy of the microwave remote sensing soil moisture estimates between the two sites.

LU/LC was the second major determining factor in site selection, as the downscaling requires that the area should have a homogenous LU/LC. For this reason areas with predominantly agricultural practices were selected. The specific agricultural practice which is dominant in many areas within the Western Cape Province was identified as wheat farming, with a pastureland crop rotation. Wheat farming in this region is mainly in winter and rain fed, and combined with pastureland during fallow periods/years for sheep farming. The other and lesser consideration was selecting areas which were accessible by vehicle and foot for data collection, and where farm owners/managers would allow, so that soil sampling transects were not constricted by boundaries between neighbouring farms. Soil physical properties were also an important consideration in the selection of study sites, as the assessment of remote sensing derived soil moisture estimates and simulated soil moisture estimates for different soil types was preferred to determine these properties effects on estimation accuracy.

Two such areas were identified as study areas for this study. The farming area surrounding the town of Malmesbury and the farming area located in the Riebeek Valley were selected.

4. In situ measurements

4.1 Introduction

In this chapter all in situ measured soil data are discussed. This includes description of the study area. The accuracy of the soil moisture probe is also assessed, after which the in situ soil moisture probe estimates are presented for the entire study.

4.3 Site description

4.3.1 Site 1: Malmesbury

Malmesbury is situated in the western coastal region of the Western Cape Province, in the Groen River catchment (Figure: 4.3). This region is characterised by deep well-leached, generally acidic and coarse sandy soils of marine and aeolian origin as can be seen in Table: 4.4.

This site receives mean annual rainfall of 444 mm a^{-1} , with the northern and southern areas experience annual rainfall means of 290 mm a^{-1} and 660 mm a^{-1} respectively. The coefficient of variation of annual rainfall is about 28% (Rebelo et al., 2006). Most rainfall occurs during the winter season, generally between May and August. Mean daily temperatures vary from about 7°C in July to about 27.9°C in February. The mean annual A-pan evaporation rate is estimated around 2150 mm a^{-1} and the daily rate exceeds rainfall for about 70% of the time.

The land cover in this region is dominated by cultivated lands and natural vegetation. Farming activities include wheat cultivation mixed with cattle farming and vineyards. The natural vegetation is dominated by Atlantis Sand Plain Fynbos, most of which is about 1-1.5m tall emergent shrubs with a dense mid-story of other shrubs and a ground layer of recumbent shrubs, herbaceous species, geophytes and grasses with occasional succulents (Rebelo et al., 2006).

4.3.2 Site 2: Riebeek Valley

The Riebeek Valley is situated in the Western Cape Province of South Africa, approximately 80km northeast of Cape Town (Figure: 4.3). The topography of this valley is relatively flat with a gently undulating land surface. Relatively shallow, brownish sandy loam soils are developed on Malmesbury shales, which are prone to cracking after heavy rains. The topsoil varies in thickness between 0.5 and 1m and is red and yellow in colour. The Riebeek Valley is situated in

a region which experiences warm dry summers and cool wet winters. Rainfall events are usually cyclonic, extending over a few days with significant periods of clear weather in between. The rainy season usually extends from April till October and yields an average annual precipitation of 460mm a^{-1} (DWAF, 2003). The land cover is dominated by cultivated lands and pastures with very little naturally occurring vegetation.

Daily rainfall and maximum temperature are presented for the Malmesbury and Riebeeck study sites for the calendar year of 2013 (Figure 4.1 and 4.2) as measured at the respective rainfall stations, WS1 and WS2 (Figure 4.3). These measurements give an indication of the seasonal trend and typical magnitude of these values throughout the year.

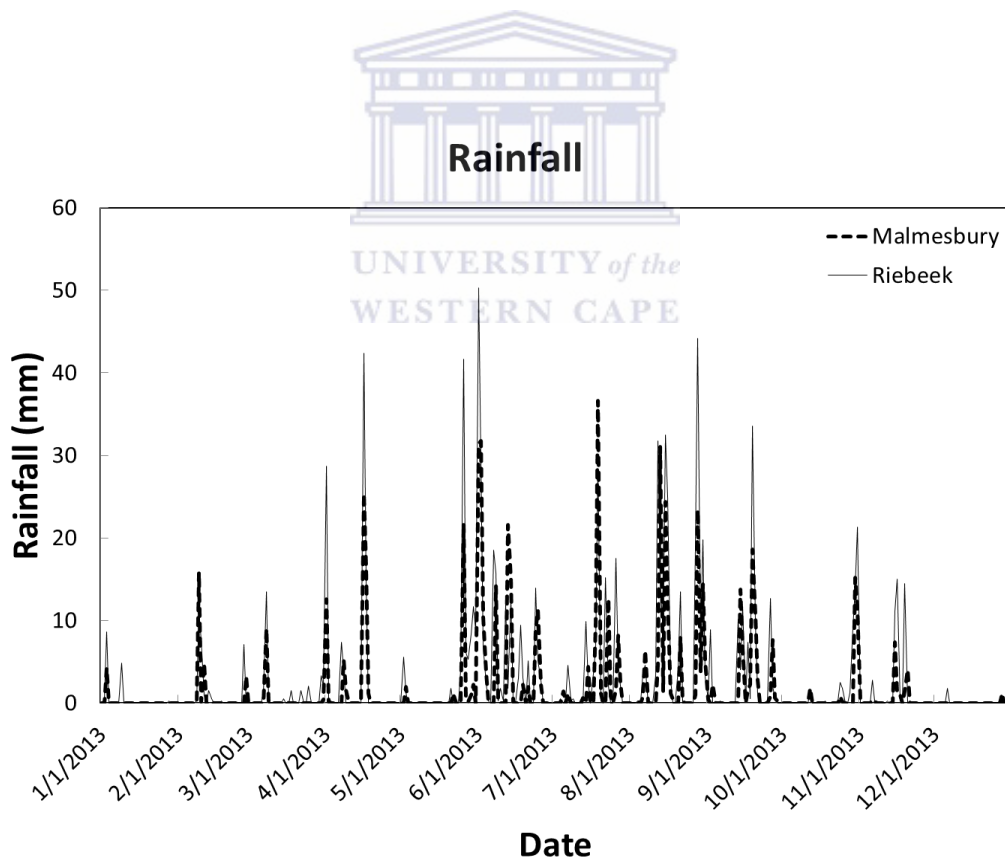


Figure 4.1: Daily rainfall measurements for the Malmesbury and Riebeeck study sites for the period 1 January to 31 December 2013, from the South African Weather Services (Malmesbury) and the Institute for Soil, Climate and Water Agro-Climatology (Riebeeck).

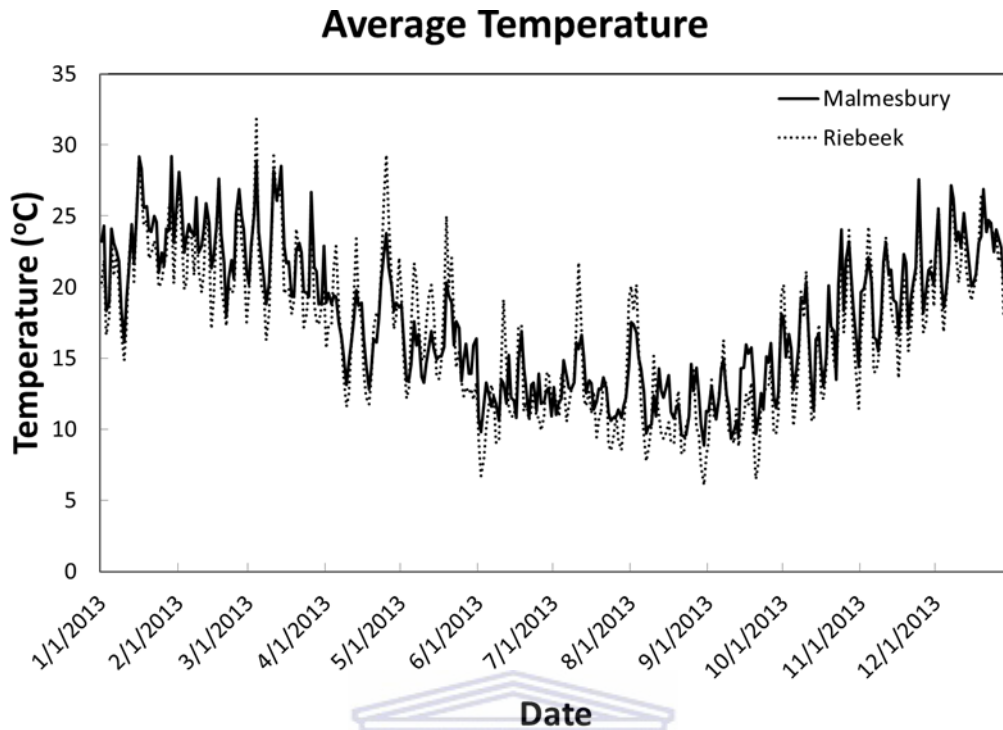


Figure 4.2: Daily average air temperature ($^{\circ}\text{C}$) for the Malmesbury and Riebeek study sites for the period 1 January to 31 December 2013, from the South African Weather Services (Malmesbury) and the Institute for Soil, Climate and Water Agro-Climatology (Riebeek).

These two study sites have very similar seasonality of rainfall and temperature, with Riebeek experiencing higher maximum rainfall while Malmesbury experienced high average temperature. All rainfall and temperature measurements were made at weather station WS1 and WS2 for Malmesbury and Riebeek respectively. WS1, which is located at -33.4720°S and 18.7180°E , was obtained from the South African Weather Services. WS2, which is located at $-33.35115^{\circ}\text{S}$ and 18.83849°E was obtained from the Institute for Soil, Climate and Water Agro-Climatology (ARC). Digital elevation models, which are products of the Shuttle Radar Topography Mission (SRTM), were obtained from the National Aeronautics and Space Administration (NASA) with a spatial resolution of 30 m (SRTM30). This data is freely available (National Aeronautics and Space Administration (NASA), 2014), accessed on 30 November 2013. The study site location (also displaying weather station locations) and digital elevation models for the study sites are presented in Figure 4.3 and 4.4.

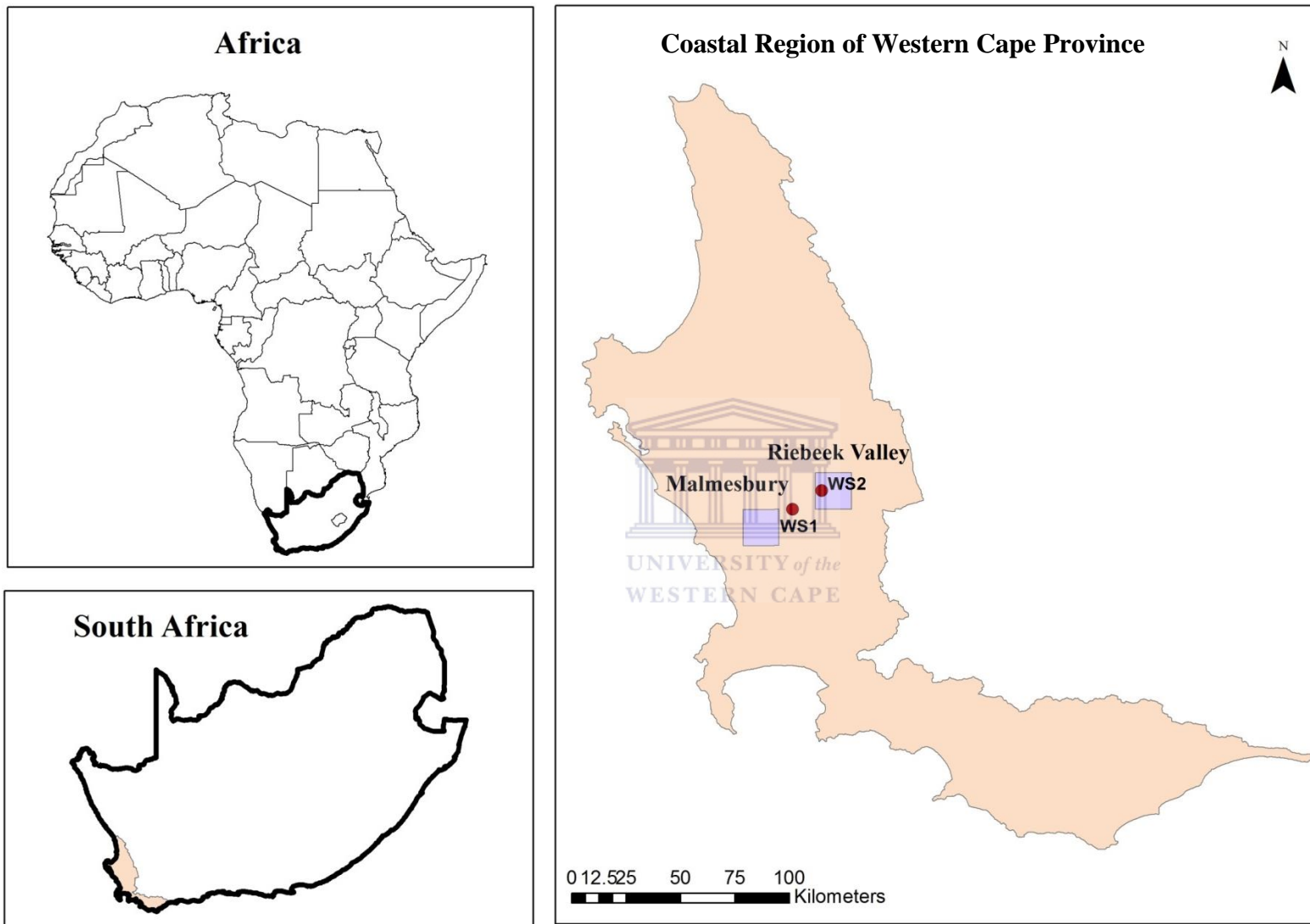


Figure 4.3: Study site locations of the Malmesbury and Riebeeck Valley sites (purple squares) within the coastal region of the Western Cape Province of South Africa with rainfall station WS1 and WS2 (red dots).

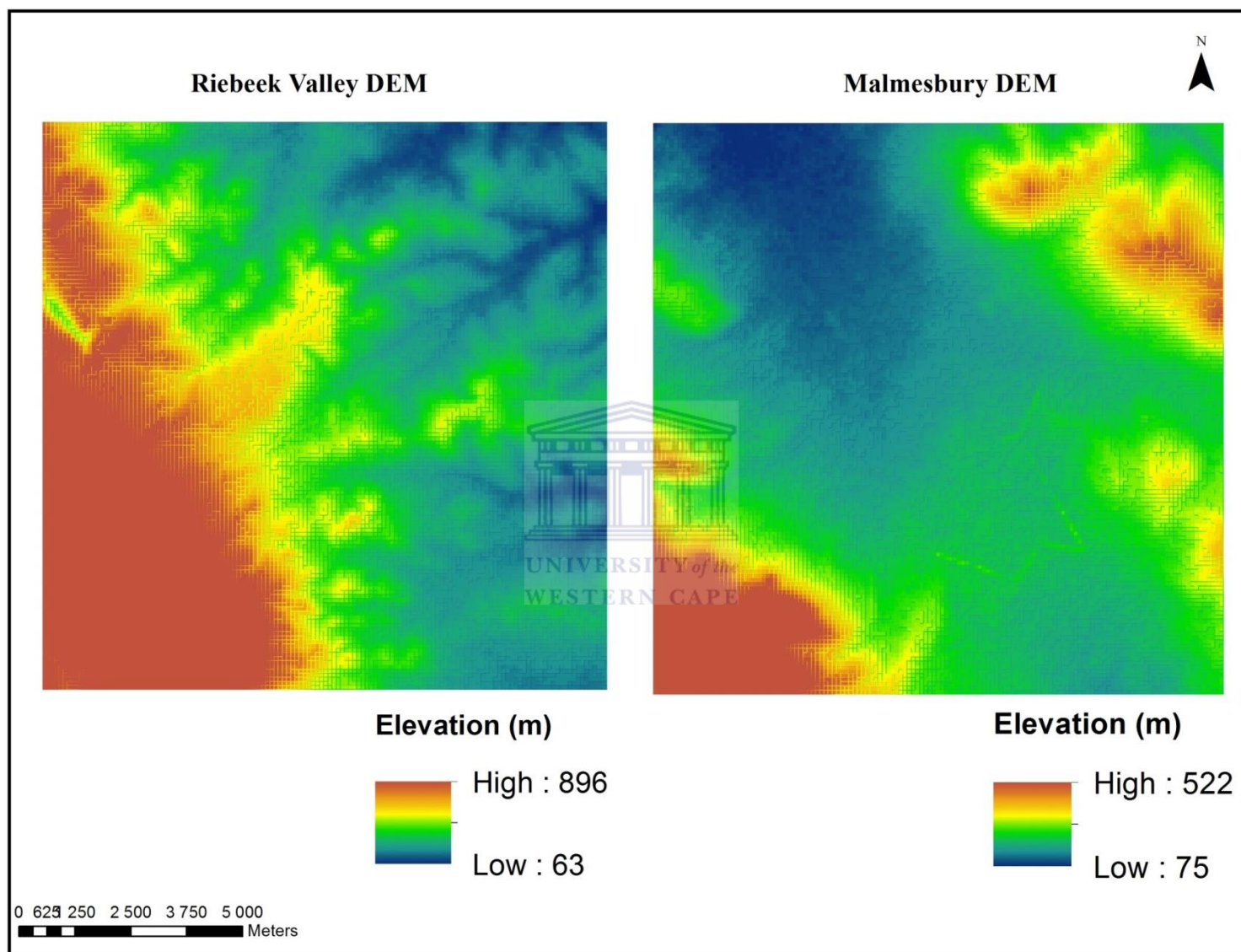


Figure 4.4: Digital elevation models (DEMs) for Malmesbury and Riebeek study sites corresponding to their relevant ASCAT 12.5 km pixels from NASA's SRTM30, DEMs accessed on the 30 November 2013.

4.4 Sampling Transects

Land cover information was generated by digitizing the various land cover classes in the open source GIS software package ILWIS, using cadastral maps of the area obtained from the National Survey General of South Africa (produced May, 2012). Cadastral maps were used for this purpose as it was the most accurate LU/LC information available in these areas. The total area covered by each of the defined land cover classes was then used to determine the percentages of each of the cover types as is described by Table 4.3, with a graphic depiction of land cover and the sampling transects in Figure 4.4.

Six sampling transects were analysed for slope, by using the length and elevation. Land cover analyses were carried out to determine the total area of each land cover type at both study sites. The length was measured using a tape measure and the elevation was measured using a Garmin handheld GPS device. The accuracy of the handheld GPS system is approximately 15m (distance and elevation) (GARMIN, 2014). Transects A-C were selected at the Malmesbury site (corresponding to an ASCAT pixel which will be referred to hereafter as the Malmesbury pixel) and transects D-F were selected at the Riebeeek Valley site (corresponding to an ASCAT pixel which will be referred to hereafter as the Riebeeek pixel), Table 4.1. and Figure 4.5.

Table 4.1: Site Transect Information

Site	Transect	Location	Cover Type	Length (m)	Change in Elevation (m)	Slope (%)
Malmesbury	A	Riverlands	Natural Vegetation	380	10	3.8
	B	Rondevlei	Pasture lands/ Wheat	650	41	6.31
	C	Nieuwepost	Pasture lands/ Wheat	780	12	1.54
Riebeeek	D	Goedetrou	Pasture lands/ Wheat	820	22	2.68
	E	De Gift	Vineyard	560	24	4.29
	F	De la Gift	Natural vegetation	360	6	1.67

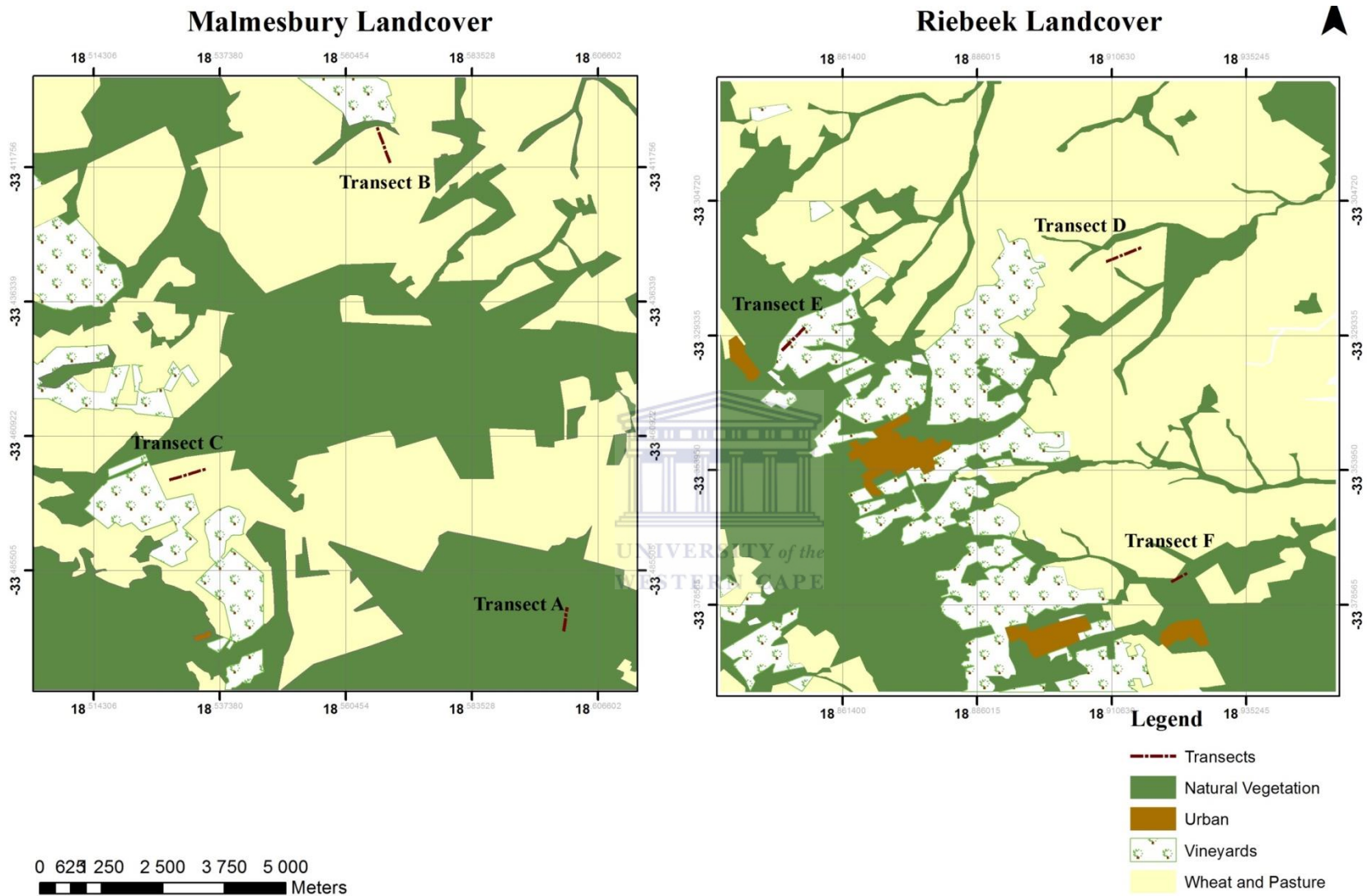


Figure 4.5: Land cover maps of the Malmesbury and Riebeek Valley study sites, depicting the dominant cover types (*Natural Vegetation, Urban, Vineyards and Wheat and Pasture*) as well as the six sampling transects, from the National Survey General, produced May 2012.

Descriptions of Transects A-F are presented in Table 4.2. Photographs of each transect are given in Appendix A-F.

Table 4. 2: Description of Transects A-F

Site	Transect	Description
Malmesbury	A	Characterised by indigenous fynbos, which covers a relatively vast area at the fine scale and is not closely bordered by any other land cover classes. The transect is located on a gradual slope with several surface depressions occurring along it.
	B	Starts at the top of a steeply dipping hill, which gradually flattens to the north. Contours occur perpendicular to the transect line at ~25m intervals which serves to drain excess precipitation. During the study period this transect was left fallow and the short grasses were used for grazing. This area is bordered to the north by vineyards (>1km away)
	C	Occurs 1km northeast of a steeply dipping hill (~520m in elevation) and is relatively flat. The transect tracks northeast and runs parallel to farming contours (5m wide). bordered by vineyards to the west and natural vegetation (dense invasive woods) to the norths (both >1km away)
Riebeeck	D	Is located in gently rolling hills dominated by wheat and pastureland. The transect moved generally northeast from the top of a smaller hill, on which contours are parallel to the transect. There is a small gravel road occurring in the middle of the transect, after which contours are perpendicular to the transect occurring every ~20m. This transect was left fallow during the study and is used for grazing. There are no nearby land cover changes.
	E	Is situated in vineyards, starting at the top of a relatively steep hill and moving downslope in a south-westerly direction. Between vineyard rows, the ground was tilled once during the study because of high compaction at the surface. The slope remains generally constant throughout the transect with the exception of a small access road towards the middle of the transect. This transect is bordered by nearby (>1km) natural vegetation to the north and the west which consists mostly of small bushes and shrubs.
	F	Is characterised by a mix of naturally occurring vegetation types including smaller invasive trees and indigenous bushes, shrubs and grasses. This transect starts next to a road and moved gently downhill in an easterly direction and ends next to a small ephemeral stream. This area is used for cattle grazing throughout the year because of the vegetation close to the stream and is bordered to the north and east by pasturelands (>1km)

Both study areas have similar land cover percentages of wheat/pasture, while the Malmesbury site has a higher cover percentage of natural vegetation and a lower percentage of vineyard cover (Table 4.3).

Table 4.3: Cover Type Information for both study sites

Site	Cover type	Percentage Cover
Malmesbury Pixel	Wheat/Pasture	48.78
	Vineyard	7.32
	Natural Vegetation	43.9
Riebeek Pixel	Wheat/Pasture	48.78
	Vineyard	13.82
	Natural Vegetation	35.77
	Urban	1.63

Soil textural analysis was done using the settling or sedimentation method, which then allowed for the identification of soil class based on the USDS soil textural classification system. The amount of organic matter in the soil was determined by using the loss on ignition method. Soil analyses were done using composite samples at each transect, made of a combination of soil samples collected at the first 4 and last 4 soil sampling points in the transect to depict the upslope and downslope areas. This was feasible as there were not much appreciable differences in soil samples taken at the top and bottom of each of the slopes, determined through visual analysis of soil samples (loosely based on texture and colour). The bulk densities were also determined for each of the samples, which were later averages for the upslope and downslope areas, all of which are given in Table 4.4.

The soil classes at the Malmesbury transects are mostly sandy with the exception of the upslope areas at Rondevlei and Niewepost farms which are loamier, owing to their increased amounts of silt. At the Riebeek transects one can see that the predominant soil classes are loamy sand and sandy loam, showing higher silt and clay amounts than transects at Malmesbury.

Table 4.4: Soil analyses results for transects a-f

Transect	Particle Size	Percentage	Soil Class	Bulk Density (Mg. m⁻³)
Riverlands upslope	Silt	2.94	Sandy	1.38
	Clay	2.35		
	Sand	94.71		
Riverlands downslope	Silt	3.71	Sandy	1.46
	Clay	3.71		
	Sand	92.59		
Rondevlei upslope	Silt	6.54	Loamy Sand	1.52
	Clay	4.62		
	Sand	88.84		
Rondevlei downslope	Silt	3.84	Sandy	1.52
	Clay	4.42		
	Sand	91.75		
Niewepost upslope	Silt	6.07	Loamy Sand	1.92
	Clay	5.69		
	Sand	88.25		
Niewepost downslope	Silt	3.47	Sandy	1.98
	Clay	5.01		
	Sand	91.53		
Goedetrou upslope	Silt	22.39	Sandy Loam	1.45
	Clay	9.90		
	Sand	65.72		
Goedetrou downslope	Silt	32.10	Loam	1.58
	Clay	18.59		
	Sand	49.31		
De gift upslope	Silt	22.42	Sandy Loam	1.56
	Clay	17.60		
	Sand	59.99		
De gift downslope	Silt	12.14	Loamy Sand	1.66
	Clay	6.70		
	Sand	81.16		
De la Gift upslope	Silt	21.35	Loamy Sand	1.46
	Clay	3.42		
	Sand	75.24		
De la Gift downslope	Silt	51.26	Silty Loam	1.5
	Clay	0		
	Sand	48.74		

4.5 Data collection

Data collection and analysis of soil moisture was conducted at each site during the period from 19 July 2013 till 27 January 2014, to investigate soil moisture dynamics during wet and dry periods. Ideally, both sites would have been investigated on one day to save time, but due to unfavourable conditions on certain days and the need to collect soil samples, sampling occurred over two consecutive days for most of the study period as seen in Table 4.5.

Table 4.5: Field data collection schedule

Date	Site 1: Soil moisture measurements	Site 2: Soil moisture measurements	Site 1: Soil sample collection	Site 2: Soil sample collection
24/07/2013	X		X	
25/07/2013		X		
14/08/2013		X		X
11/09/2013		X		X
12/09/2013	X			
25/09/2013		X		
26/09/2013	X			
16/10/2013	X	X		
7/11/2013	X	X	X	
4/12/2013	X	X	X	X
22/01/2014	X	X		

Along each sampling transect, three measurements were taken for each sampling point, which were later averaged to one measurement for that sampling point, also accompanied by the standard deviation value for the point using the three measurements. The distance between each sampling point is 20-25m intervals and was determined using a tape measure. This distance was selected so as to be able to capture soil moisture variations during wet, drying and dry periods. Measurements were taken at the exact same points during each of the data collection trips at each site, with the exception of two specific days when the soil surface was too hard to penetrate with the soil moisture probe at site D and E. All other data sets were obtained from their various sources for these sites for the period during which the study was undertaken.

4.6 In Situ Soil Moisture Measurement

The accuracy of the soil moisture probe was determined by comparing the soil moisture probe measurements to gravimetric soil moisture measurements, by determining the coefficient of determination between the two for all transects. This was done during the wet, drying and dry period for each study site. These results were then used to correct soil moisture probe measurements for the entire study period, using their relationships as derived from a best-fit linear trend line, which was automatically fitted.

4.7. Soil Moisture Probe Evaluation

The evaluation results of the soil moisture probe (Hydroprobe) for each transect is presented in Table 4.6, with all the results plotted in a scatter plot in Figure 4.6, which includes the coefficient of determination (r^2) and root mean square error (RMSE) values for the combined measurements.

Table 4.6: Soil moisture probe (Hydroprobe) evaluation results as compared to volumetric soil moisture measurements obtained using the gravimetric method, including the coefficient of determination (r^2), the root mean square error (RMSE) and the linear relationship between the two (Trendline) for each transect.

Transect	Period	R^2	RMSE	Trendline
A	Dry	0.628	34.515	$y = 0.6396x - 1.0442$
B	Drying	0.983	23.911	$y = 0.8308x - 2.4218$
C	Wet	0.855	35.781	$y = 2.3032x - 8.0972$
D	Drying	0.562	5.88	$y = 0.5613x + 3.0387$
E	Wet	0.983	46.829	$y = 0.5008x + 0.5718$
F	Dry	0.855	25.112	$y = 0.825x - 3.1738$

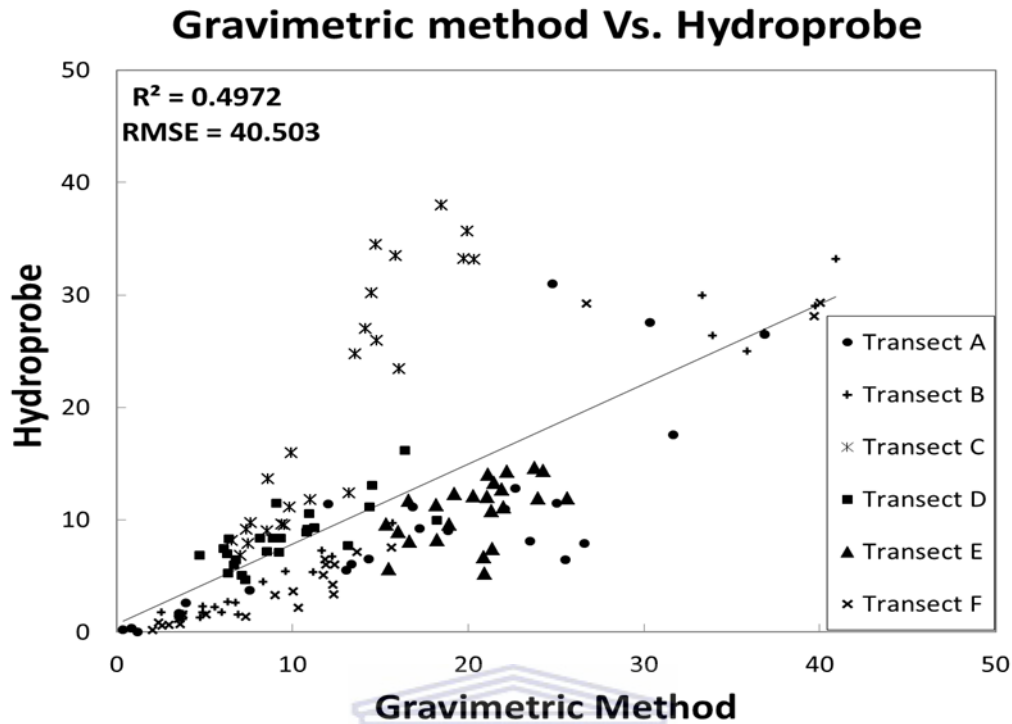


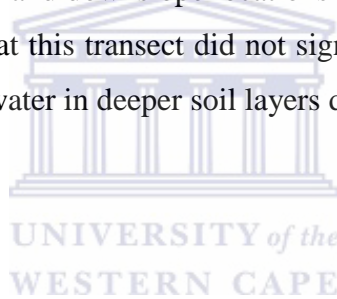
Figure 4.6: Hydroprobe measurements plotted against gravimetric method measurements for each transect showing the r^2 and RMSE values for the total measurements, with soil moisture given in percent.

The Hydroprobe showed good correlation at most sites when compared to the gravimetric method's soil moisture values (Table 4.6). At transects with sandier soils the soil moisture probe has higher r^2 values, but also had generally high RMSE values. Hydroprobe measurements at transects with more loamy soil had lower r^2 values compared to gravimetric method values, but also had generally lower RMSE values. The lowest r^2 values were observed at Transect D, which also had the lowest RMSE. Even so, Hydroprobe measurements at Transect F, which had high silt content, showed high soil r^2 compared to gravimetric method values. Probe measurements at Transect F had high correlation to gravimetric method measurements, but had a different trend to the rest and thus served to lower the collective correlation coefficient of the combined transects. Transect A, B, D and E clustered well together (Figure 4.6).

4.8 Analysis of Soil Moisture at each Transect

Soil moisture graphs were generated for each sampling day for all transects. The soil water content estimated from Hydroprobe measurement was plotted against distance along each transect (Figure 4.7 to 4.17). The variation in elevation along each transect is also shown on the same graphs. This served as a graphic depiction of the variation in soil water content at each transect on a specific sampling date as well as the comparison of soil water content at each transect over the entire sampling period.

Soil moisture values at Transect A generally increased downslope. This was due to localized water ponding at the surface of portions of the transect. Values remained generally high up until November, with a slight decrease in December. In January there was a negligible difference in soil water content between upslope and downslope locations along Transect A (Figure: 4.7). The fynbos and short grass vegetation at this transect did not significantly decrease during the study period, indicating the presence of water in deeper soil layers during the dry period.



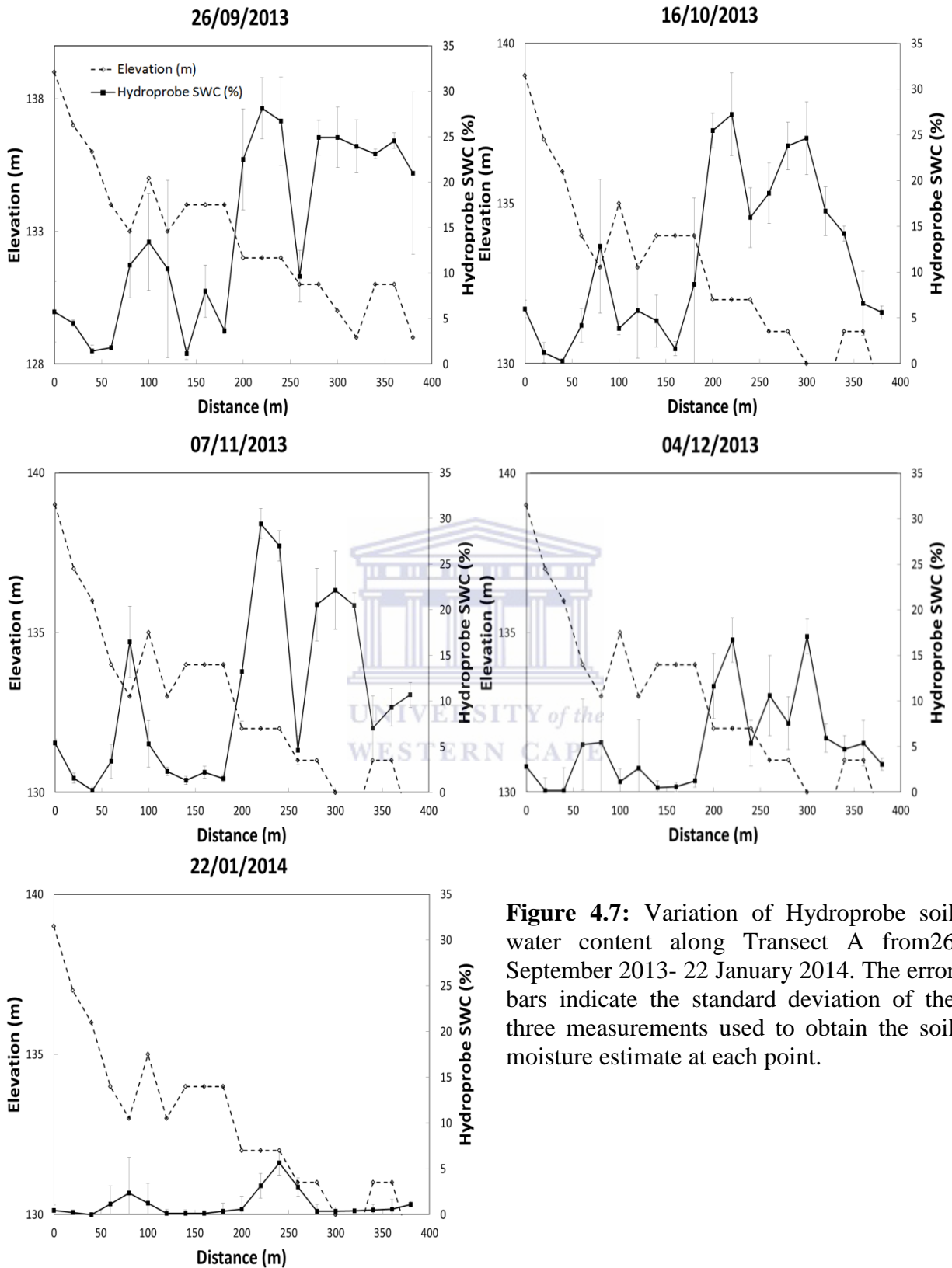


Figure 4.7: Variation of Hydroprobe soil water content along Transect A from 26 September 2013- 22 January 2014. The error bars indicate the standard deviation of the three measurements used to obtain the soil moisture estimate at each point.

At transect B soil moisture increased from July till September 2013, where values remained high until October 2013 (Figure 4.8). The soil was almost dry from December 2013 (Figure 4.9). Soil water content peaks were observed where water ponded next to contour bunds around the middle and end of the transect. Grasses found at this transect were longest following the wet period but thinned out in December 2013. This can be attributed to dry top soil conditions in from December 2013 as well as grazing that occurred at this transect.

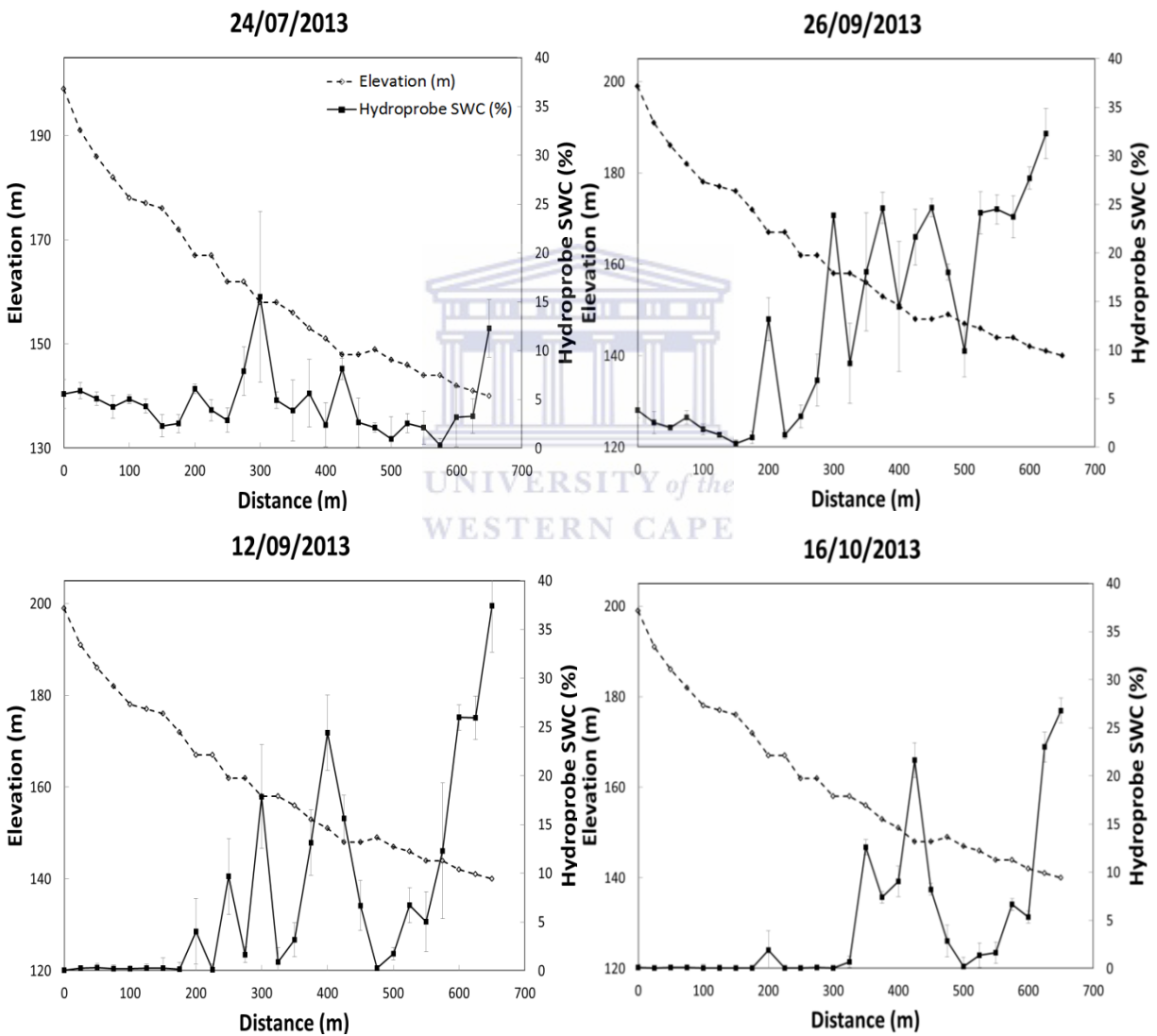


Figure 4.8: Variation of Hydroprobe soil water content along Transect B from 24 July- 16 October 2013. The error bars indicate the standard deviation of the three measurements used to obtain the soil moisture estimate at each point.

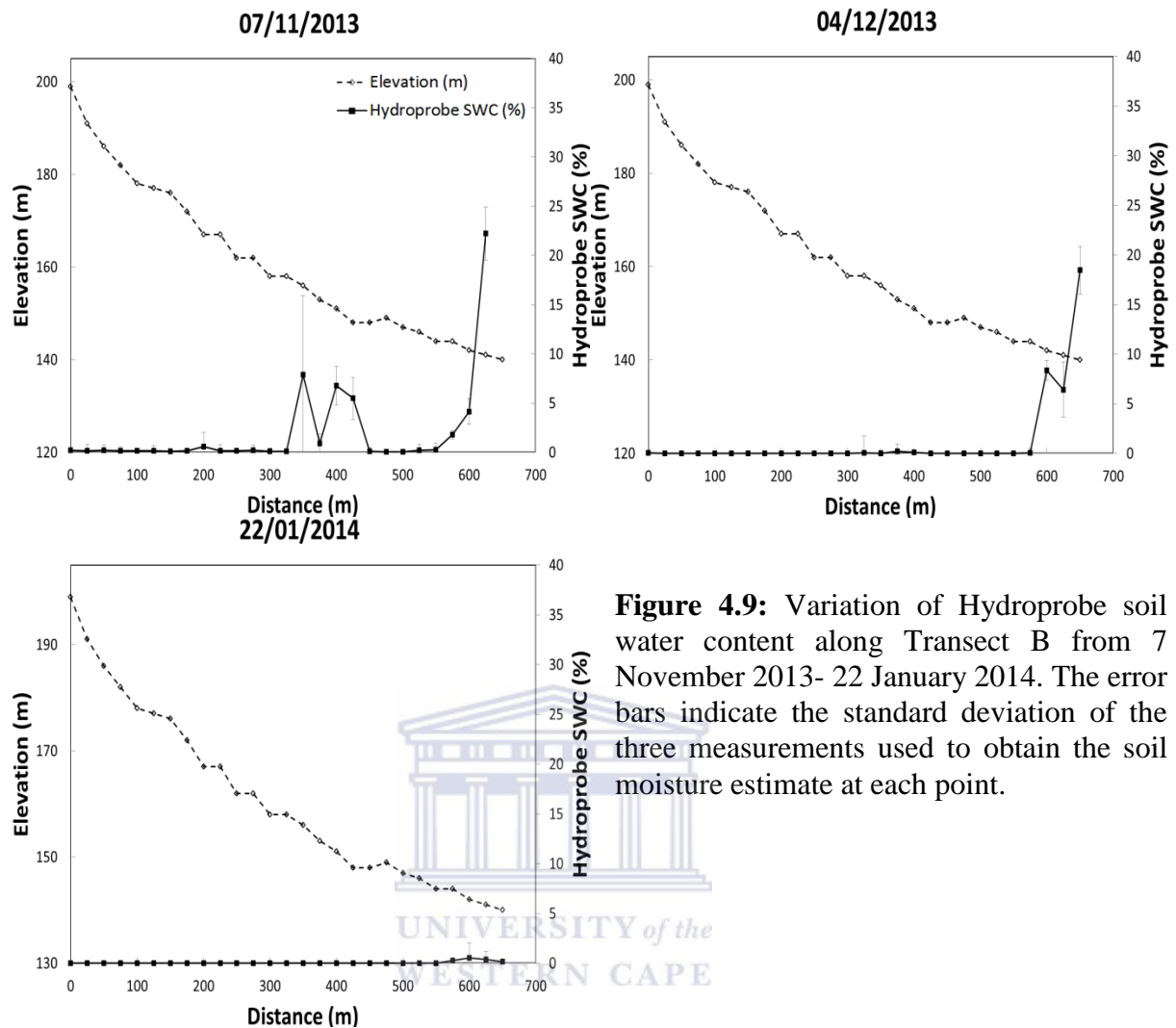


Figure 4.9: Variation of Hydroprobe soil water content along Transect B from 7 November 2013- 22 January 2014. The error bars indicate the standard deviation of the three measurements used to obtain the soil moisture estimate at each point.

Soil moisture at Transect C decreased gradually from July till December 2013 (Figure 4.10 and 4.11). There was not much variation between points in the transect, but there was however high deviation of soil moisture at individual points, owing to the fact that measurements were taken at the top, slope and foot of contours. These deviations however decreased towards the dry period. There was also a slight increase in soil moisture from the top till the bottom of the transect from July till October 2013. It was found that due to the gentle slope, water ponded between contour bunds during the wet period. Transect C had very sparse grasses and shrubs which were all eaten during grazing, leaving the transect completely bare from December 2013.

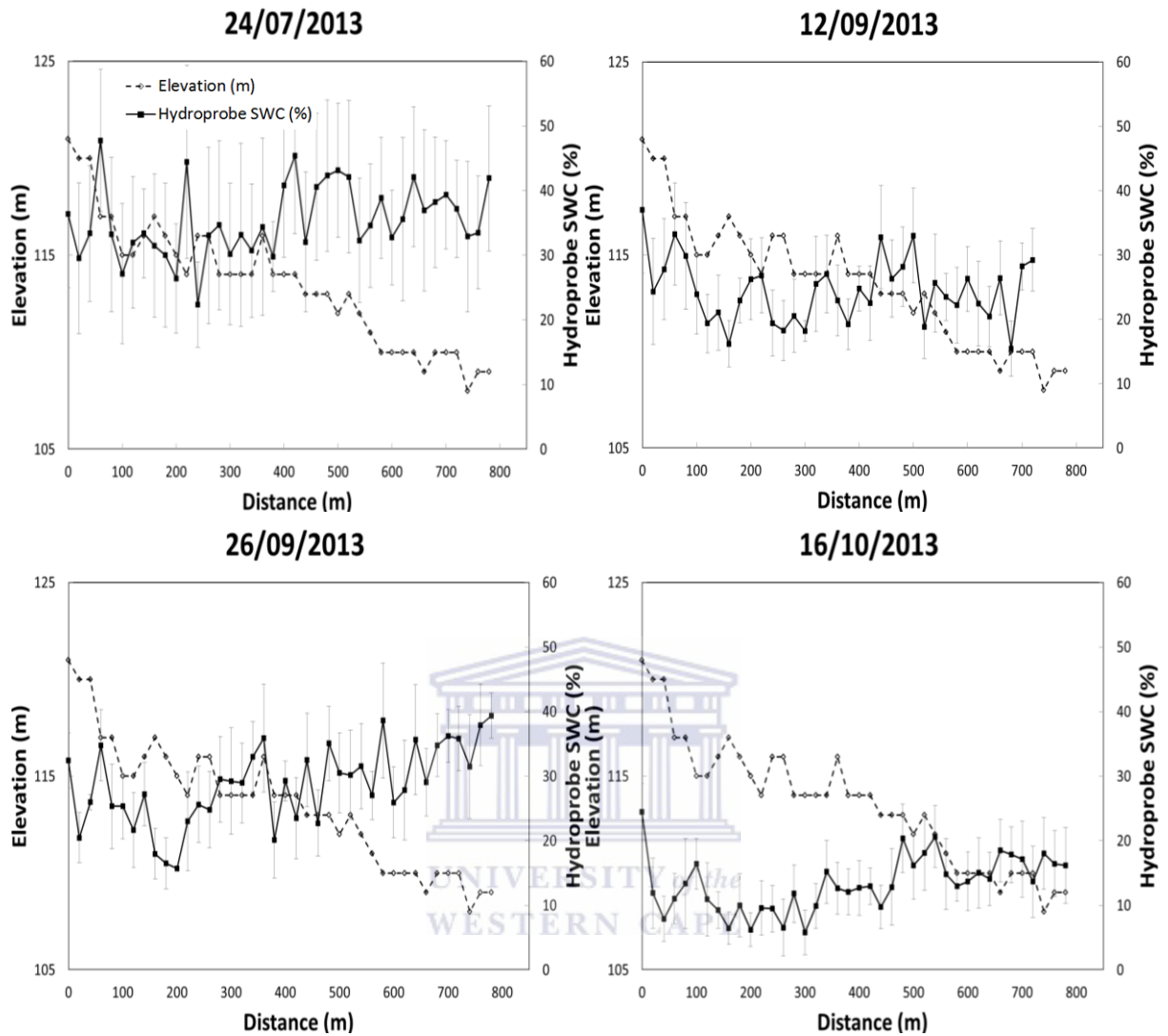


Figure 4.10: Variation of Hydroprobe soil water content along Transect C from 24 July- 16 October 2013. The error bars indicate the standard deviation of the three measurements used to obtain the soil moisture estimate at each point.

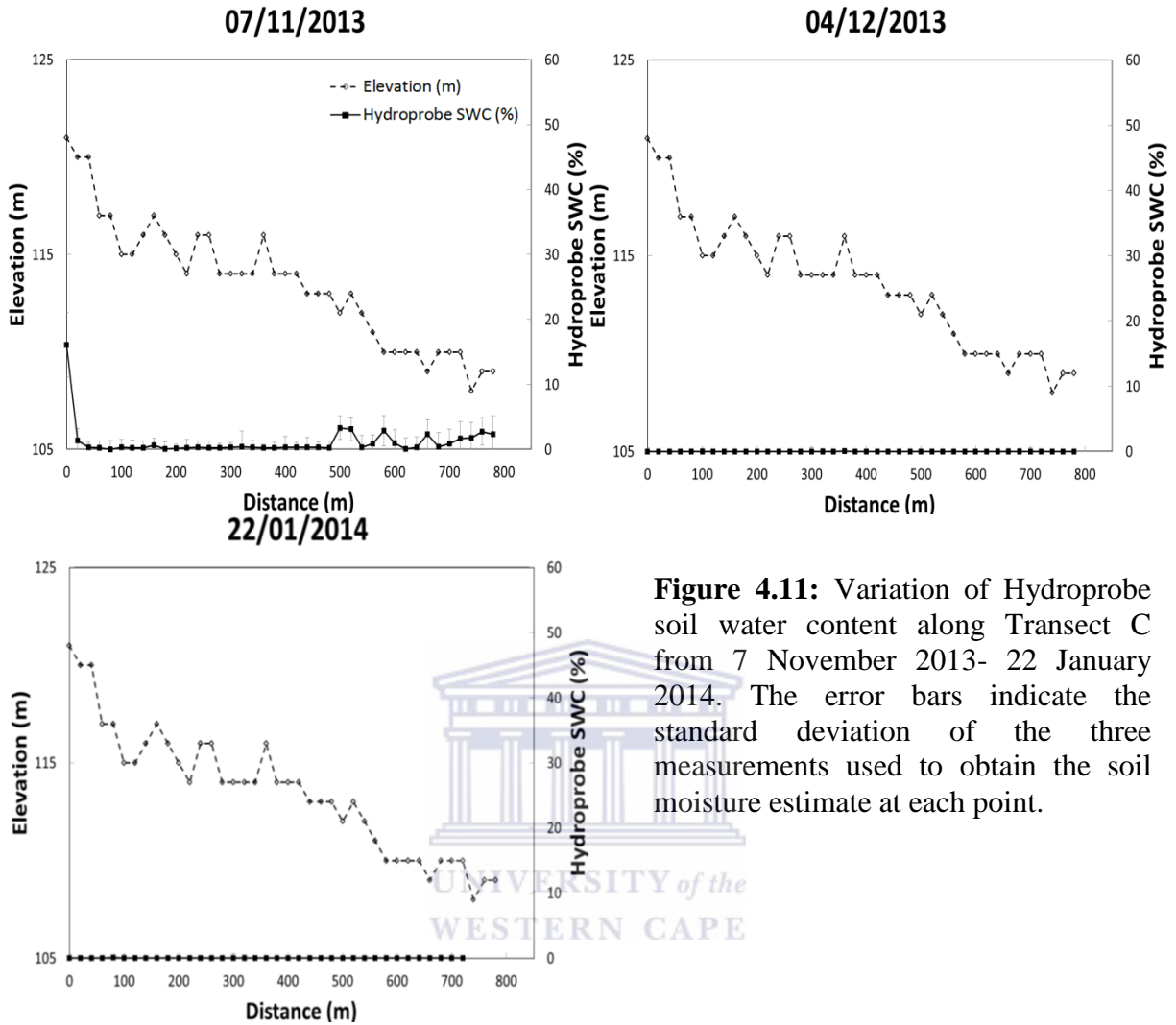


Figure 4.11: Variation of Hydroprobe soil water content along Transect C from 7 November 2013- 22 January 2014. The error bars indicate the standard deviation of the three measurements used to obtain the soil moisture estimate at each point.

Soil water content was generally uniform at transect D on all sampling days (Figure 7.12 and 7.13). Soil moisture gradually increased towards the middle of the transect and then decreased towards the end of the transect during the wet period (July to September 2013). Due to an elevation anomaly, variability of measurements at each sampling point and between points also decreased from the wetter period in July to the drier period in January 2014. Small amounts of water was ponded between contour bunds during the wet period at this transect. The land cover was dominated by short grass, used for grazing which dried and withered during the dry period.

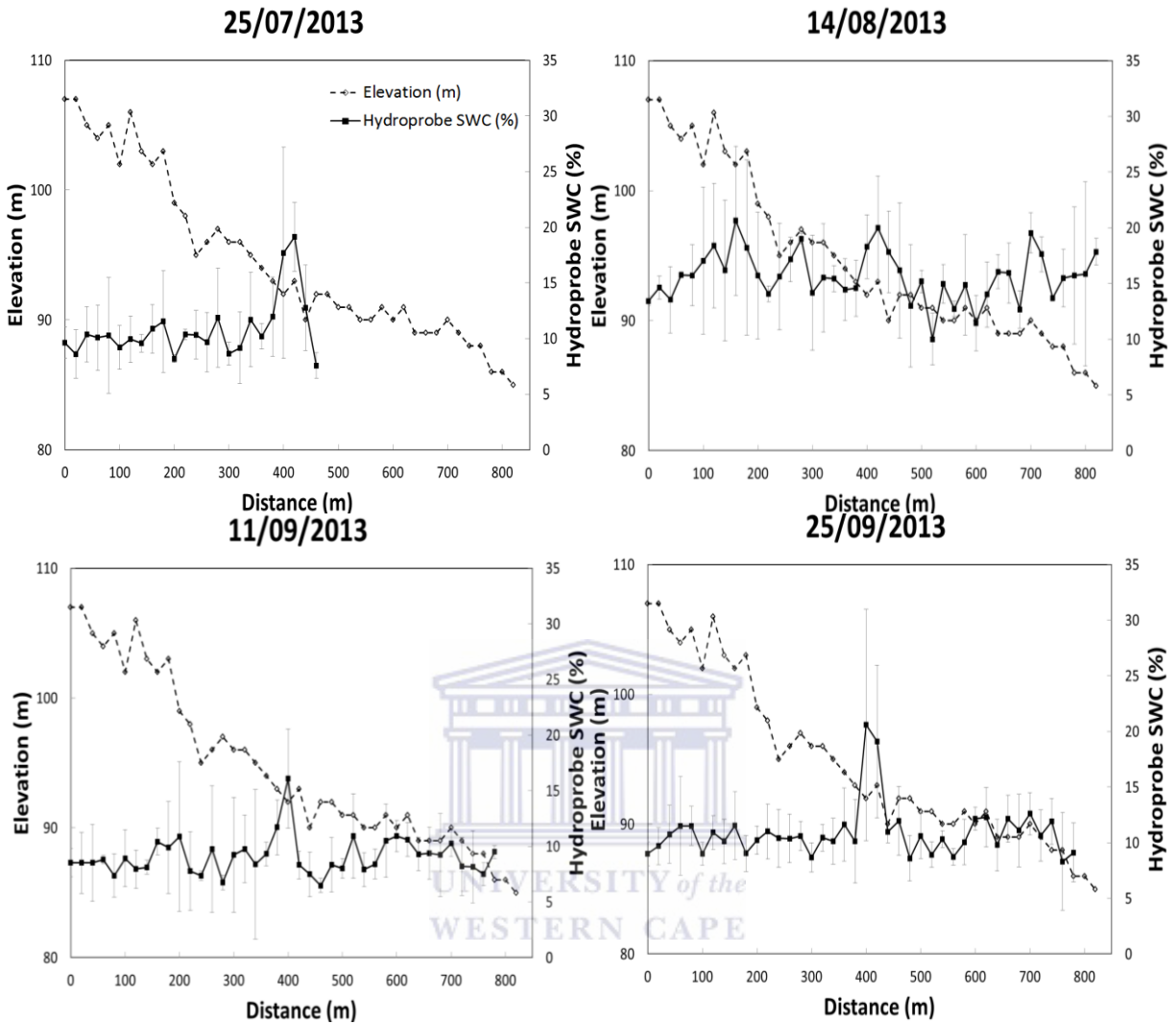


Figure 4.12: Variation of Hydroprobe soil water content along Transect D from 25 July 2013- 25 September 2013. The error bars indicate the standard deviation of the three measurements used to obtain the soil moisture estimate at each point.

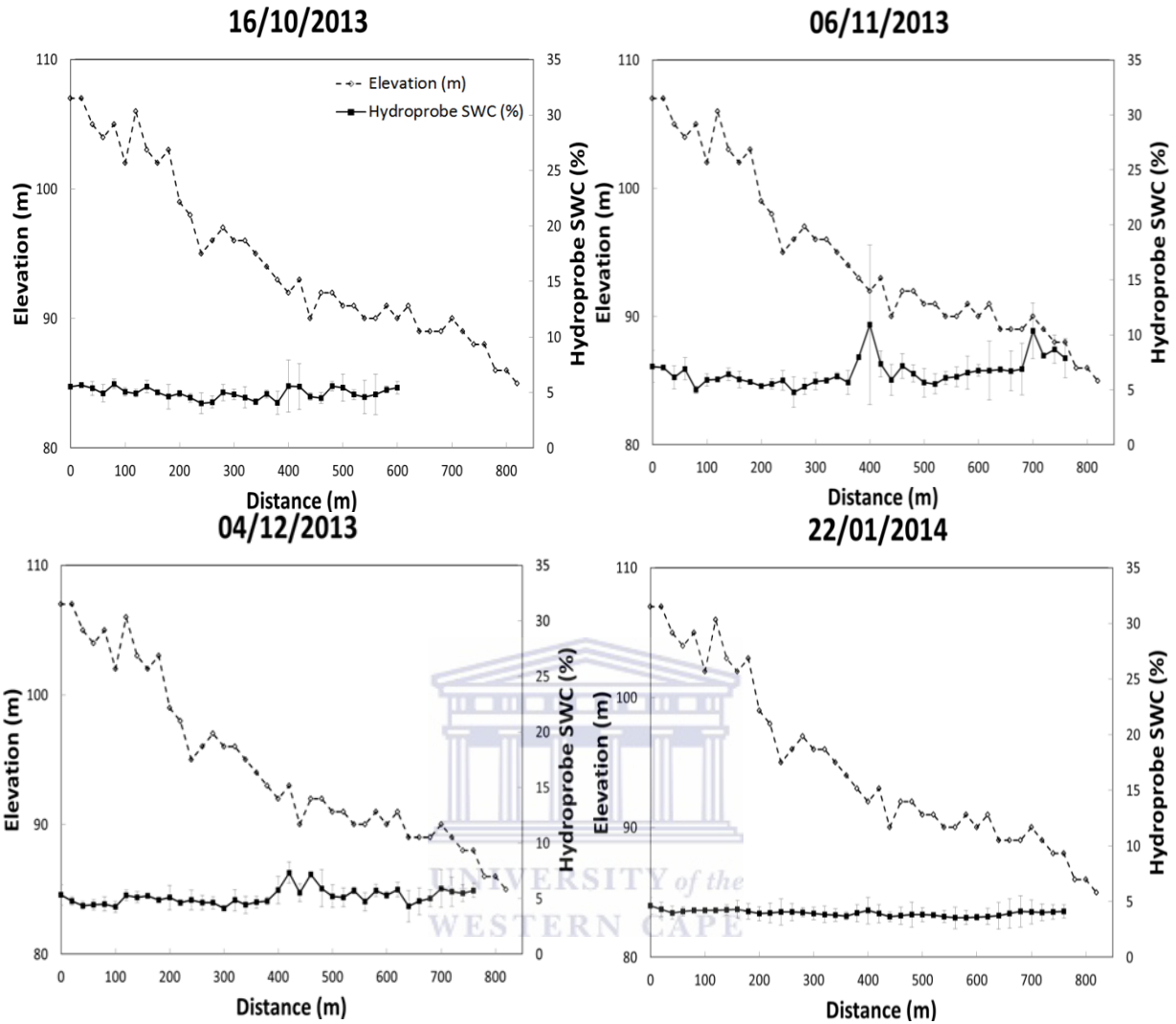


Figure 4.13: Variation of Hydroprobe soil water content along Transect D from 16 October 2013- 22 January 2014. The error bars indicate the standard deviation of the three measurements used to obtain the soil moisture estimate at each point.

There was a gradual decrease in soil moisture along Transect E from July till December/January (Figure 4.14 and 4.15). There are marked peaks in the middle and at the end of the transect, which are caused by water accumulating on flat locations along the transect. By January 2014 the soil had almost dried out. Grape vines at this transect were bare during the winter period and only started growing from November 2013. Tillage occurred between vineyard rows during October and there sparse amounts of wheat cultivated between rows during the wet period.

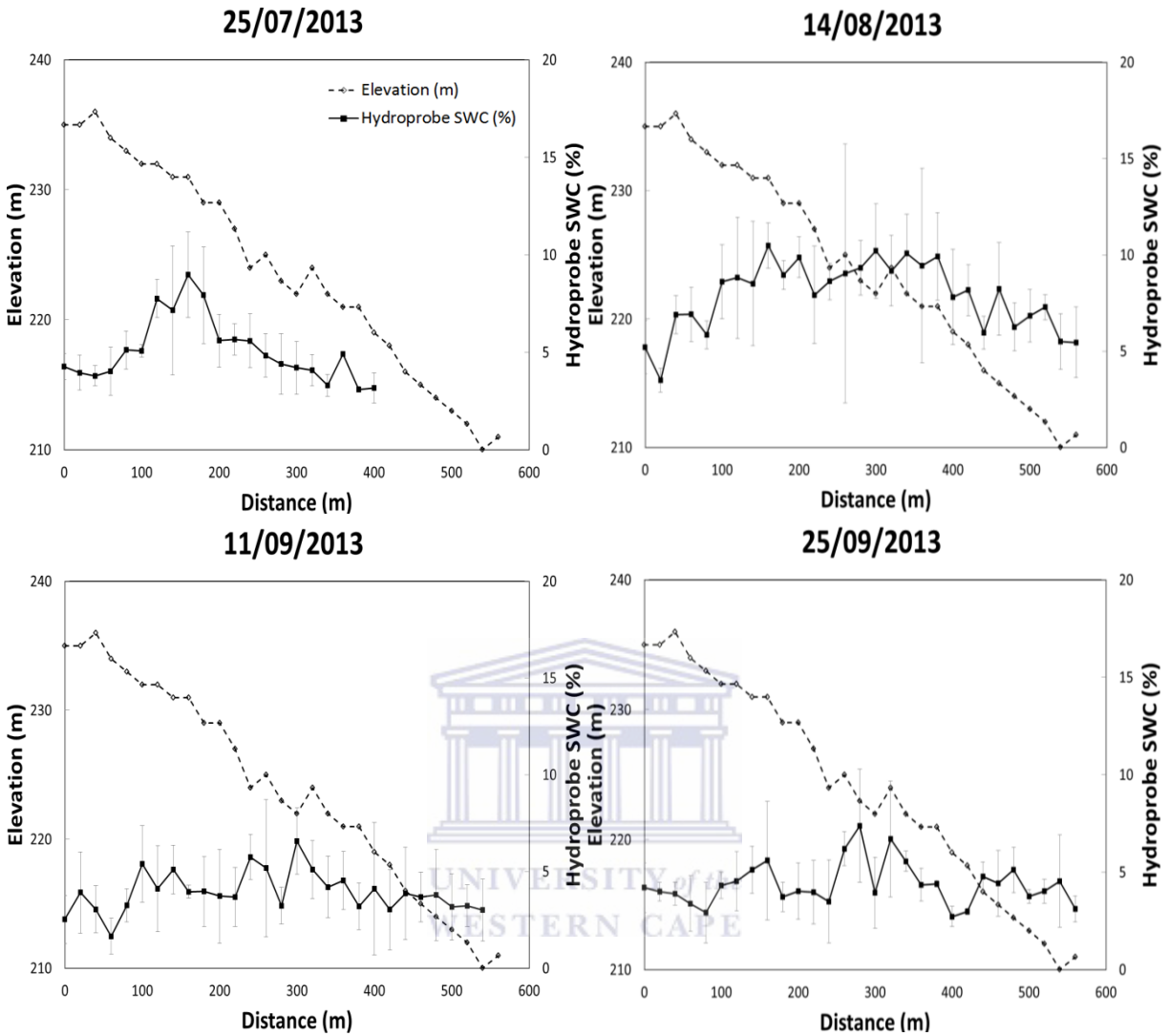


Figure 4.14: Variation of Hydroprobe soil water content along Transect E from 25 July 2013-25 September 2013. The error bars indicate the standard deviation of the three measurements used to obtain the soil moisture estimate at each point.

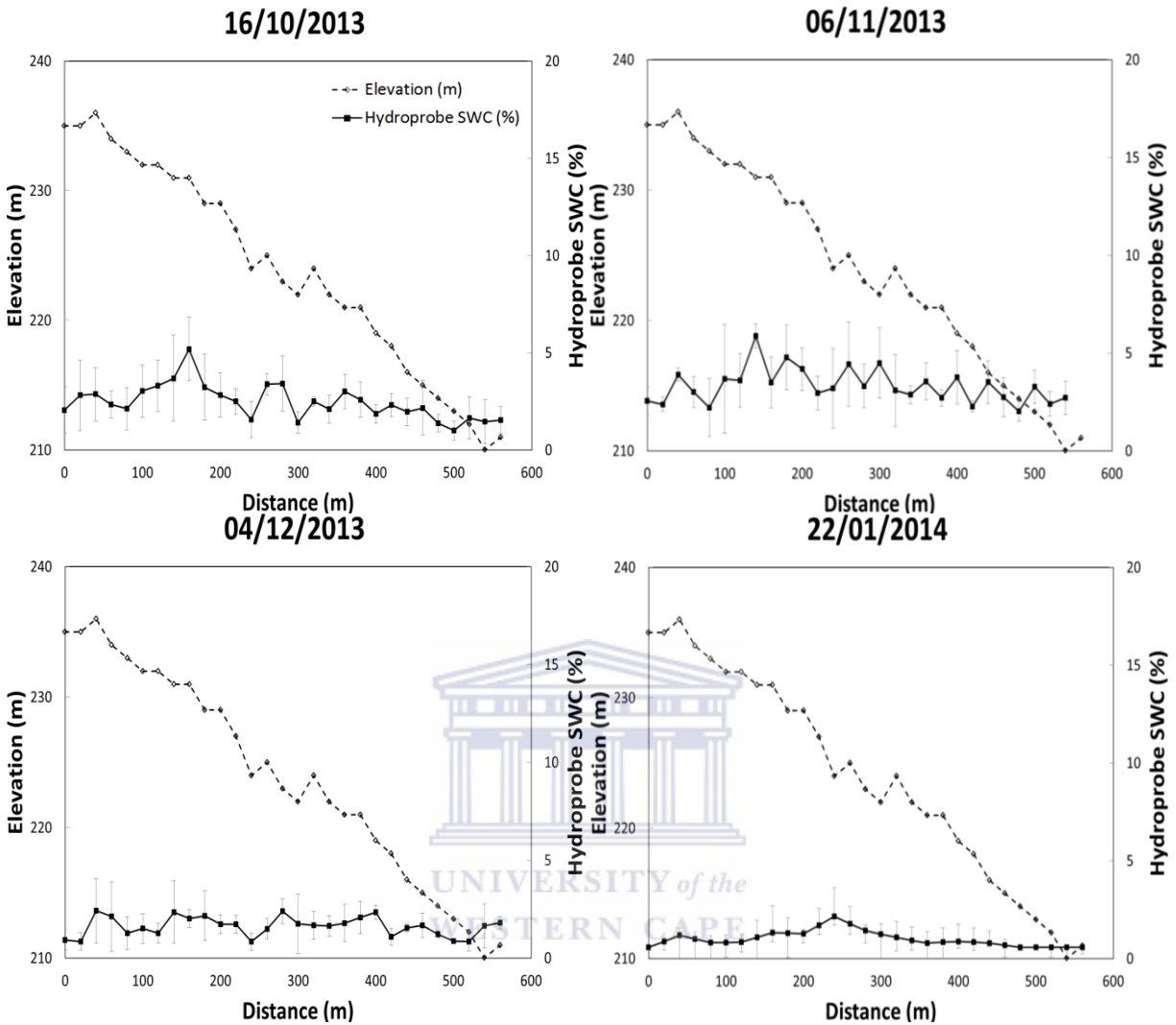


Figure 4.15: Variation of Hydroprobe soil water content along Transect D from 16 October 2013- 22 January 2014. The error bars indicate the standard deviation of the three measurements used to obtain the soil moisture estimate at each point.

Transect F had higher soil water content compared to Transects D and E (Figure 4.16 and 4.17). There was also a well-defined trend showing the increase of soil moisture as one moves down the transect. High soil moisture values in the middle of the transect during the wet period (August-September 2013) were indicative of ponding of water at the surface. There was a gradual decrease in soil moisture values from July 2013 till January 2014. There was also a decrease in soil moisture variability between points in the transect during this period. There was a slight decrease in vegetation density at transect F from the wet to dry period. The stream near

the bottom of the transect may have contributed to the high soil water content in that area up until December 2013.

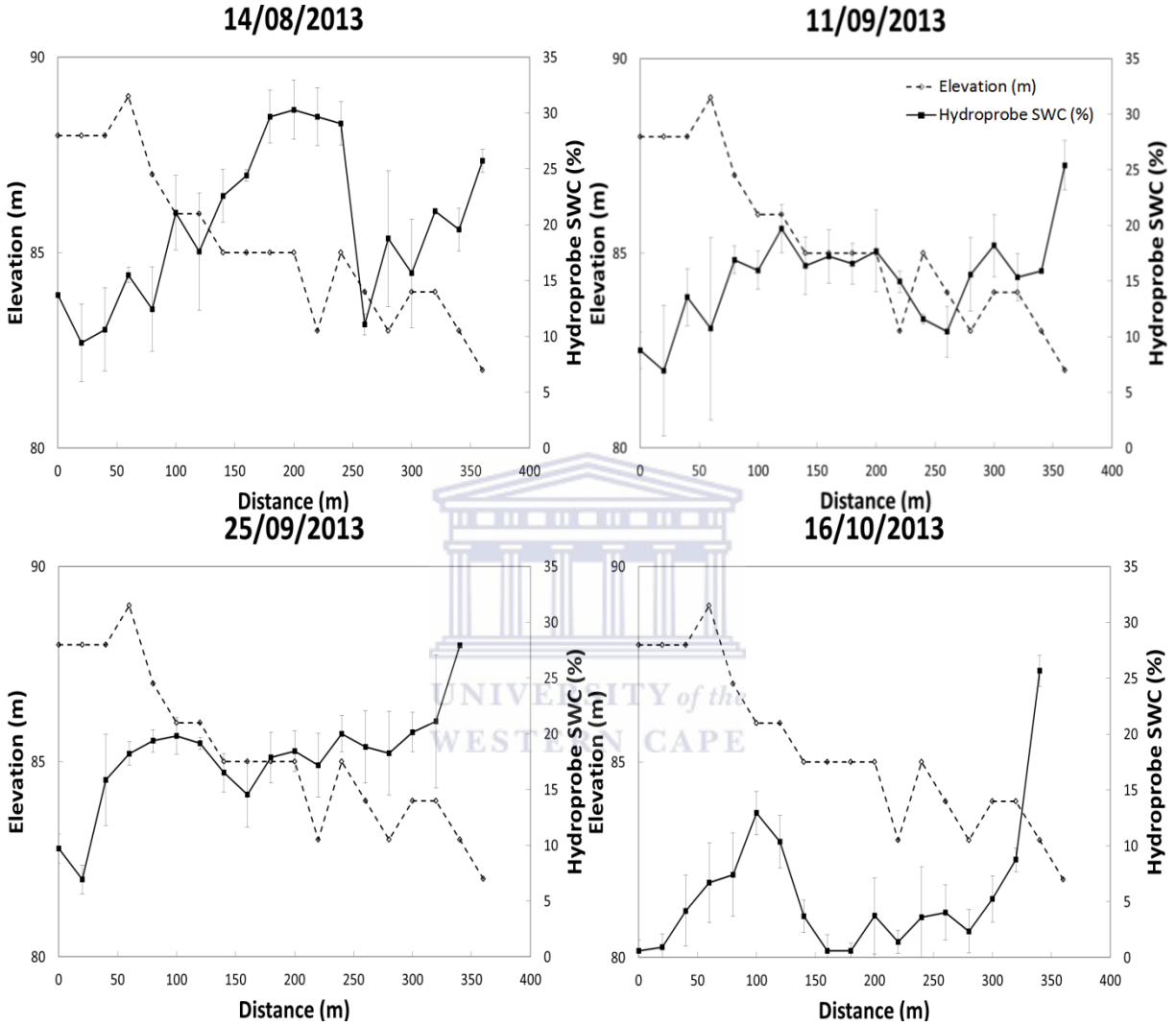


Figure 4.16: Variation of Hydroprobe soil water content along Transect E from 8 August 2013- 16 October 2013. The error bars indicate the standard deviation of the three measurements used to obtain the soil moisture estimate at each point.

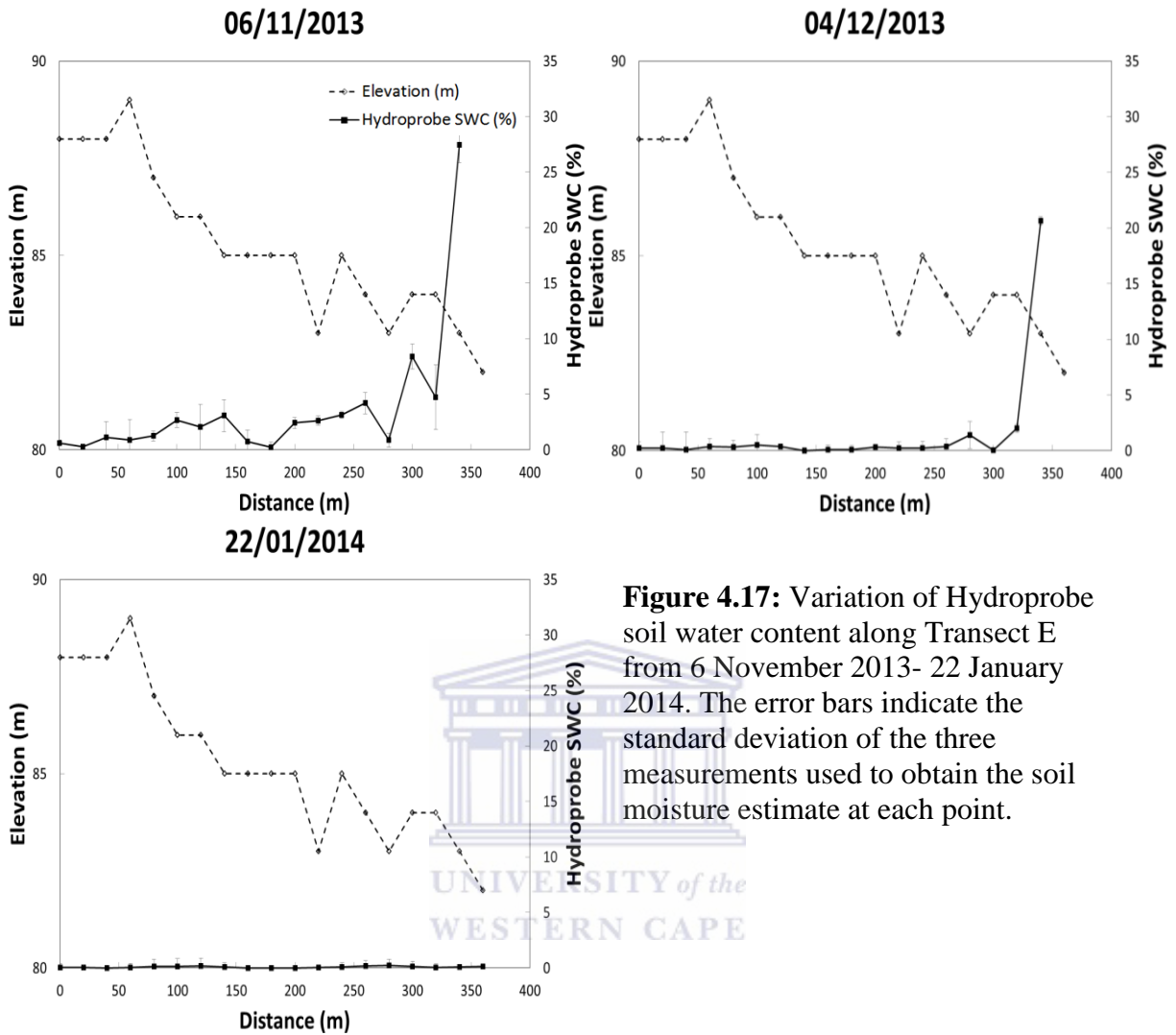
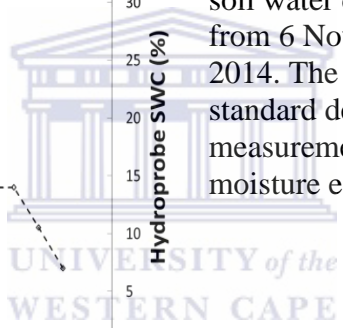


Figure 4.17: Variation of Hydroprobe soil water content along Transect E from 6 November 2013- 22 January 2014. The error bars indicate the standard deviation of the three measurements used to obtain the soil moisture estimate at each point.



4.9. Transect physical properties and soil moisture

The correlation between soil physical properties and soil water content was investigated. To achieve this, static soil physical properties were compared to the dynamic soil water contents at each of the sampling transects for all sampling days. This was done so as to assess how the correlation varies between soil physical properties and soil water content from the wet to the dry period.

Soil physical properties were determined using composite samples made up of soil samples collected at the first 4 and last 4 points at each transect. Thus, soil water content was calculated as the average soil water content for the upslope and downslope regions of each transect corresponding to the points used for soil sampling. The comparison comprises of soil moisture, percentage of sand, silt and clay, organic matter (%), slope (%) and relative elevation. Relative elevation was derived for each transect segment by using its average elevation values and normalising it with maximum and minimum elevation for the study site by:


$$E_R = \frac{E - E_{min}}{E_{max} - E_{min}} \quad (4.1)$$

where E denotes elevation and the subscript R denotes relative, while max and min denote maximum and minimum values for the study site. Correlation values were grouped together and are colour coded, ranging from high correlation (red- >0.8), to moderately high correlation (orange- $0.65-0.8$), to moderately correlated (yellow- $0.5-0.65$) and poorly correlated (green- <0.5).

There was found to be very poor correlation between soil moisture and silt, clay and sand, with soil moisture correlation values approaching negatively moderate. Slope is also poorly negatively correlated with correlation values approaching 0 during the dry period. Relative elevation has the strongest correlation of all physical properties with soil moisture, which is strongly negative during the wet period and decreased to poorly correlated as soil becomes drier towards the end of the study period.

Table 4.7: Correlation matrix for transect physical properties and soil moisture averages for both study sites- depicting *slope*, *silt-clay-sand* proportions, *bulk density*, *relative elevation (E_R)* and *soil moisture* for all sampling days. Used to compare soil moisture to depict the change in relationship between soil moisture and transect physical properties throughout the study period.

	<i>Slope %</i>	<i>Silt %</i>	<i>Clay %</i>	<i>Sand %</i>	<i>Bulk density</i>	<i>Elevation_{rel}</i>	7/25/13	8/14/13	9/11/13	9/25/13	10/16/13	11/6/13	12/4/13	1/22/14
<i>Slope %</i>	1													
<i>Silt %</i>	-0.22405	1												
<i>Clay %</i>	-0.12685	0.212153	1											
<i>Sand %</i>	0.237392	-0.94234	-0.52538	1										
<i>Bulk density</i>	-0.11959	-0.25313	0.064371	0.205193	1									
<i>Elevation_{rel}</i>	0.532036	-0.53467	0.058362	0.452307	-0.04482496	1								
7/25/13	-0.22121	-0.4598	-0.33651	0.424165	0.910720519	-0.610312	1							
8/14/13	0.469902	0.848484	-0.3912	-0.64836	-0.53567944	-0.8975572	0.994023	1						
9/11/13	-0.3131	-0.23618	-0.42136	0.366542	0.632487084	-0.3980282	0.789204	0.929645	1					
9/25/13	-0.4122	0.022401	-0.44059	0.134146	0.49339772	-0.5148128	0.777036	0.826445	0.939733	1				
10/16/13	-0.43818	0.381651	-0.50642	-0.202	0.27647401	-0.7205232	0.693676	0.890836	0.798661	0.935121	1			
11/6/13	-0.42829	0.467211	-0.12401	-0.36598	-0.28736637	-0.4909562	-0.12568	0.912367	0.319369	0.456005	0.63848	1		
12/4/13	-0.23391	0.642303	-0.16112	-0.50532	-0.39233525	-0.4158434	-0.45614	0.851716	0.167497	0.323277	0.591073	0.881305	1	
1/22/14	-0.12367	0.411374	0.642484	-0.5953	-0.24037005	-0.4146395	-0.26507	0.288889	-0.30748	-0.28768	-0.20679	0.2848	0.250389	1

There is a moderate correlation between relative elevation and slope with a moderately negative correlation between slope and organic matter. There is also a high correlation between organic matter and silt, with a high negative correlation between organic matter and sand. Similarly sand has a high negative correlation with silt. Bulk density did not correlate with any physical parameters but did show good correlation with soil water contents at the start of the study which decreased as soils became drier.

4.10. Summary of Hydroprobe soil moisture estimates

It was observed from the Hydroprobe soil moisture estimates that both study sites experienced the same seasonal trend dominated by a wet period (July –September 2013), followed by a drying period (October –November 2013) and lastly a dry period (December 2013-January 2014). Soil moisture values were found to be generally higher at the sandier Malmesbury study site during the wet and drying periods but were also lower during the dry period in comparison to the loamier Riebeek site. Transects A and F, which had natural vegetation, were found to have higher soil water content during the wet periods as compared to other transects. Transect C however, had high soil water content during the wet period, but this may also be as a result of the correction of the Hydroprobe estimates for this transect.

Soil and transect physical properties for the most part showed poor correlation with soil moisture, with the exception of relative elevation and bulk density, which showed good correlation during the wet period.

5. Remote sensing derived soil moisture and downscaling

5.1. Introduction

In this chapter the remote sensing derived soil moisture estimates will be presented. Firstly, the coarse resolution microwave soil moisture product handling procedures will be described, which will be followed by the presentation and discussion of the coarse resolution microwave soil moisture estimates. Thereafter the data preparation for the downscaling will be discussed, which will include the NDVI and LST products' processing procedures, a look at the NDVI-LST relationship and the calibration of the downscaling coefficients for the algorithm. This will be followed by the downscaled soil moisture estimates for all the sampling transects.

5.2. Coarse resolution soil moisture product processing

The coarse resolution, remote sensing derived soil moisture product has global coverage with a nearly daily coverage. This data is freely available from Eumetsat and can be downloaded via (EUMETSAT, 2013). ASCAT soil moisture data was downloaded in Binary Universal Form for the Representation of meteorological data (BUFR) and comprises of a full disc image of point measurements at a ~12.5km resolution grid structure. This data format is not routinely supported by Geographical Information System (GIS) software packages. Images were thus imported into ILWIS 3.7.2, an open source GIS software package, using the GEONETCast plug-in, which is available for all versions of ILWIS above 3.7 (ILWIS, 2013).

During this process, images are read as tables, which are then converted to point maps with a WGS84 geographic projection and the WGS84 datum. Once in ILWIS format, the images were converted to raster maps using nearest neighbour interpolation, with an Alberts Equal Area projection, which again made use of the WGS84 datum for further processing.

5.3 Coarse resolution soil moisture analysis

Once the data were prepared, coarse resolution satellite volumetric soil moisture content (θ_c) was derived by using the coarse resolution satellite estimate (SM_c) field capacity (F_c) and wilting point (W_p), as determined by the Hydroprobe soil moisture measurement for each pixel. This was achieved by making use of field capacity (F_c) and wilting point (W_p) observed values for the entire study period and was determined through:

$$\theta_c = (SM_c \times (F_c - W_p)) + W_p \quad (5.1)$$

This was done, as the coarse resolution soil moisture product is determined using a change detection algorithm (Naeimi et al., 2009) and thus each pixel value is only representative of the relative percentage of surface moisture for that specific pixel location. Once converted, ASCAT soil water content estimates were graphically compared to Hydroprobe soil moisture estimates for the entire study period (19 July 2013- 22 January 2014) (Figure 5.2 and 5.4). Thereafter, ASCAT soil moisture estimates were compared in Hydroprobe values using the coefficient of determination (r^2) and the root mean square error (RMSE) at all transects as well as the average values for the entire study site (Figure 5.3 and 5.5). Hydroprobe average soil water content estimates for each study site/ASCAT pixel were obtained from the mean of Hydroprobe estimates for all transects within a specific study site/ASCAT pixel.

During the wet period (July-September 2013), the ASCAT soil moisture estimates generally vary between 15 and 28 % for the Malmesbury site. This is again followed by a drying period (October-November 2013), which stabilises around December, when values varied between 3 and 7 %. The ASCAT soil water content averaged between 15 and 25 % during the wet period (July-September 2013), and then gradually declined until stabilising during the dry period (December 2013-January 2014) at around 3 %.

ASCAT soil moisture estimates at both sites showed high sensitivity to rainfall, resulting in high daily soil moisture variability (Figure 5.1)

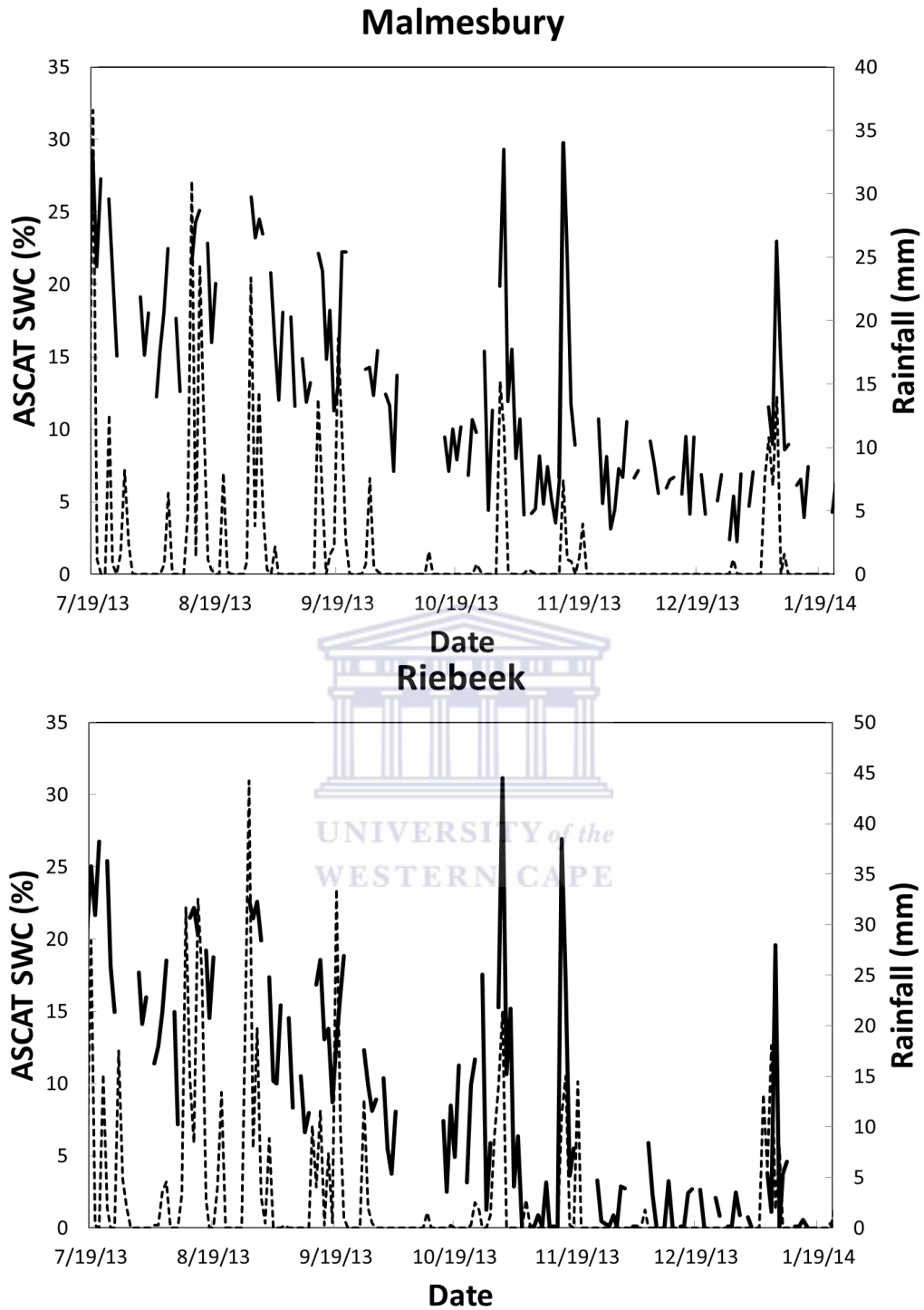


Figure 5.1: Comparison of ASCAT 12.5km course resolution soil moisture estimates and rainfall (mm) for the Mamlesbury site (above) and Riebeeck site (below) for the period of 19 July 2013- 22 January 2014, with soil water content given in percentage.

ASCAT soil moisture estimates at the Malmesbury site, were generally similar to the values obtained from Hydroprobe estimates (Figure 5.2). Transect A shows the best agreement between ASCAT soil moisture and Hydroprobe estimates. Unfortunately, there are no Hydroprobe estimates for the wet period (July-August 2013), to evaluate the remote sensing estimates for Transect A during this period. Transect B showed the worst agreement between the ASCAT soil moisture estimates and Hydroprobe soil moisture estimates. At this transect, the ASCAT estimates overestimated the Hydroprobe soil water content estimates for most of the study. At transect C, ASCAT soil moisture underestimated Hydroprobe estimates during the wet and drying periods but values are overestimated during the dry period by ~5%.



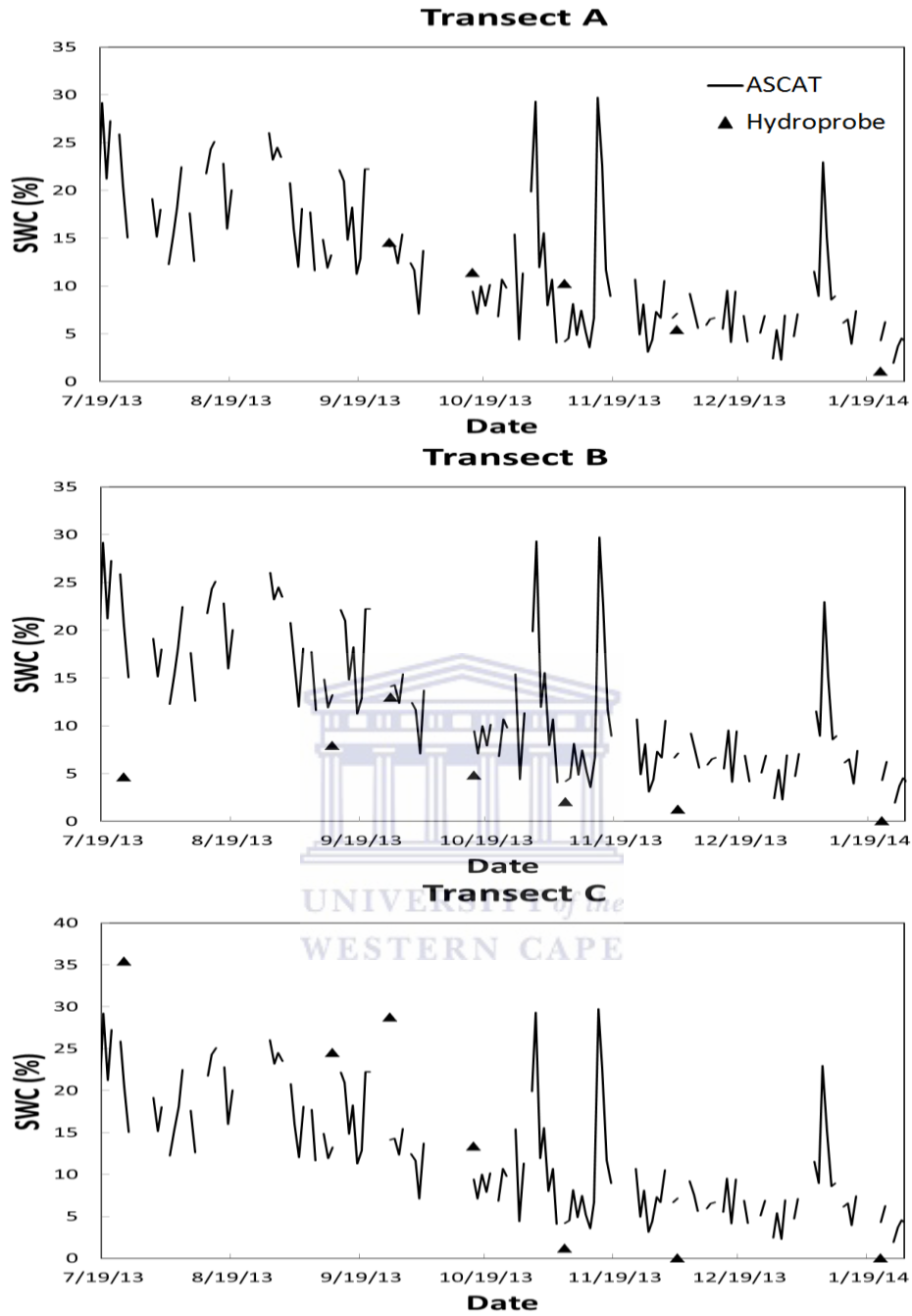


Figure 5.2: ASCAT 12.5km coarse resolution soil moisture estimates (solid line) and in Hydroprobe moisture estimates (triangles) at Transect A, B and C for the Malmesbury site for the period 19 July 2013 to 27 January 2014, with soil water content (SWC) given in percentage.

For Transect A, Hydroprobe soil moisture and ASCAT soil moisture had moderate r^2 with low RMSE while at Transect B there was a low r^2 value and high RMSE (Figure 5.2). For transect C there was a high r^2 values with a relatively high RMSE. The averaged Hydroprobe estimates for all transects in the Malmesbury site had both a high r^2 value as well as a low RMSE compared to ASCAT soil moisture estimates.

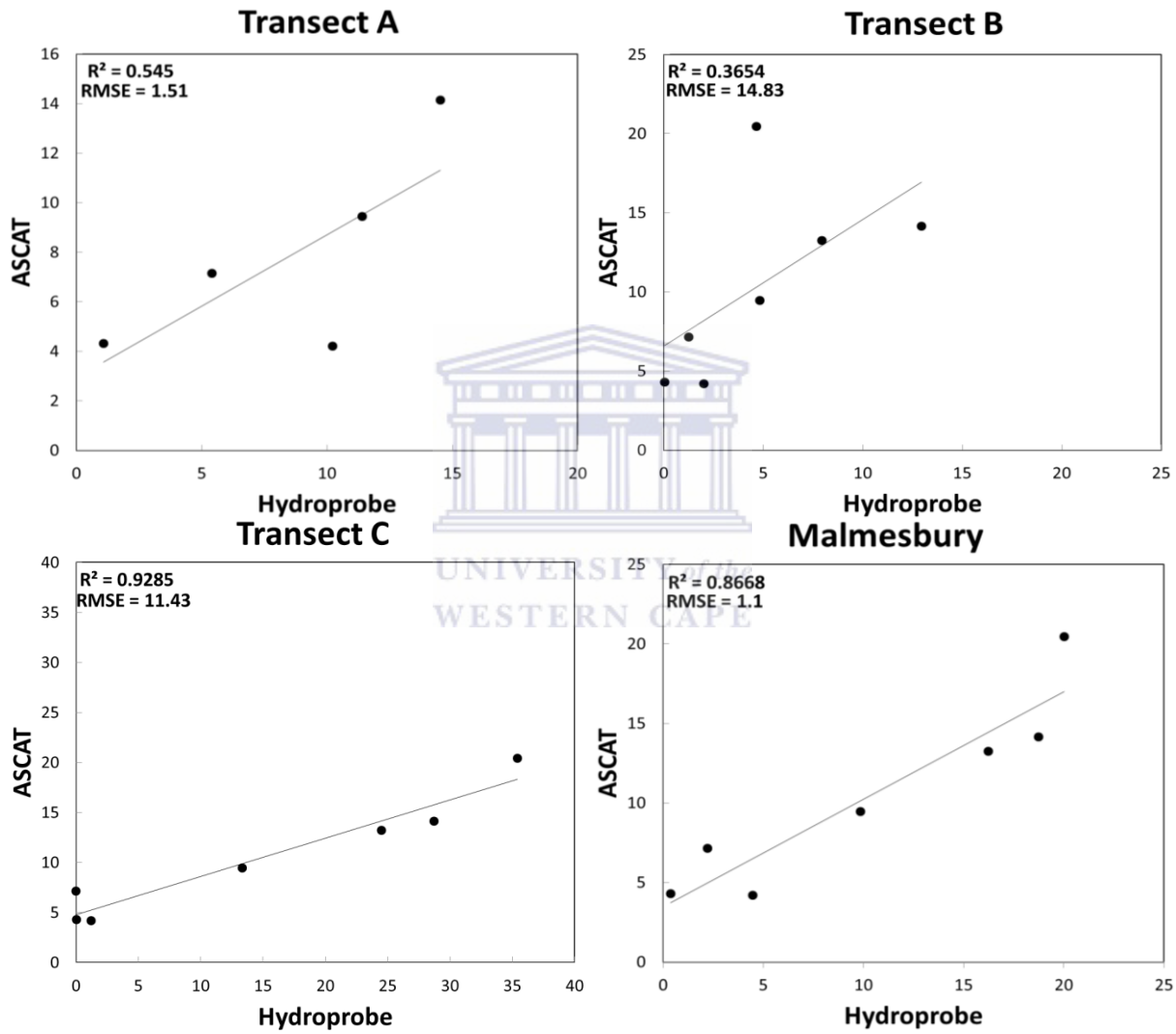


Figure 5.3: ASCAT 12.5km coarse resolution soil moisture estimates and Hydroprobe soil moisture estimates at Transect A, B, C and averages for the Malmesbury site for the period 19 July 2013- 27 January 2014, with soil water content given in percentage.

The general decrease in situ soil moisture was well captured by the ASCAT soil moisture estimates for the Riebeek site, with the exception of 3 abnormally wet days during the drying and dry periods on the 31 October 2013, 16 November 2013 and 8 January 2014. Transect D (Figure 5.4) shows the best overall fit during wet (July-September 2013), drying (October- November 2013) and dry (December 2013-January 2014) periods. Transect B shows that ASCAT overestimated soil moisture values at this transect during the wet period and dry periods. Transect C shows the highest deviation between measured and microwave estimated soil moisture content of the three transects. There however seems to be reasonable agreement between the in situ and remote sensing soil moisture during the dry period at 2 of the three transects (Transect E and F) (Figure 5.4).



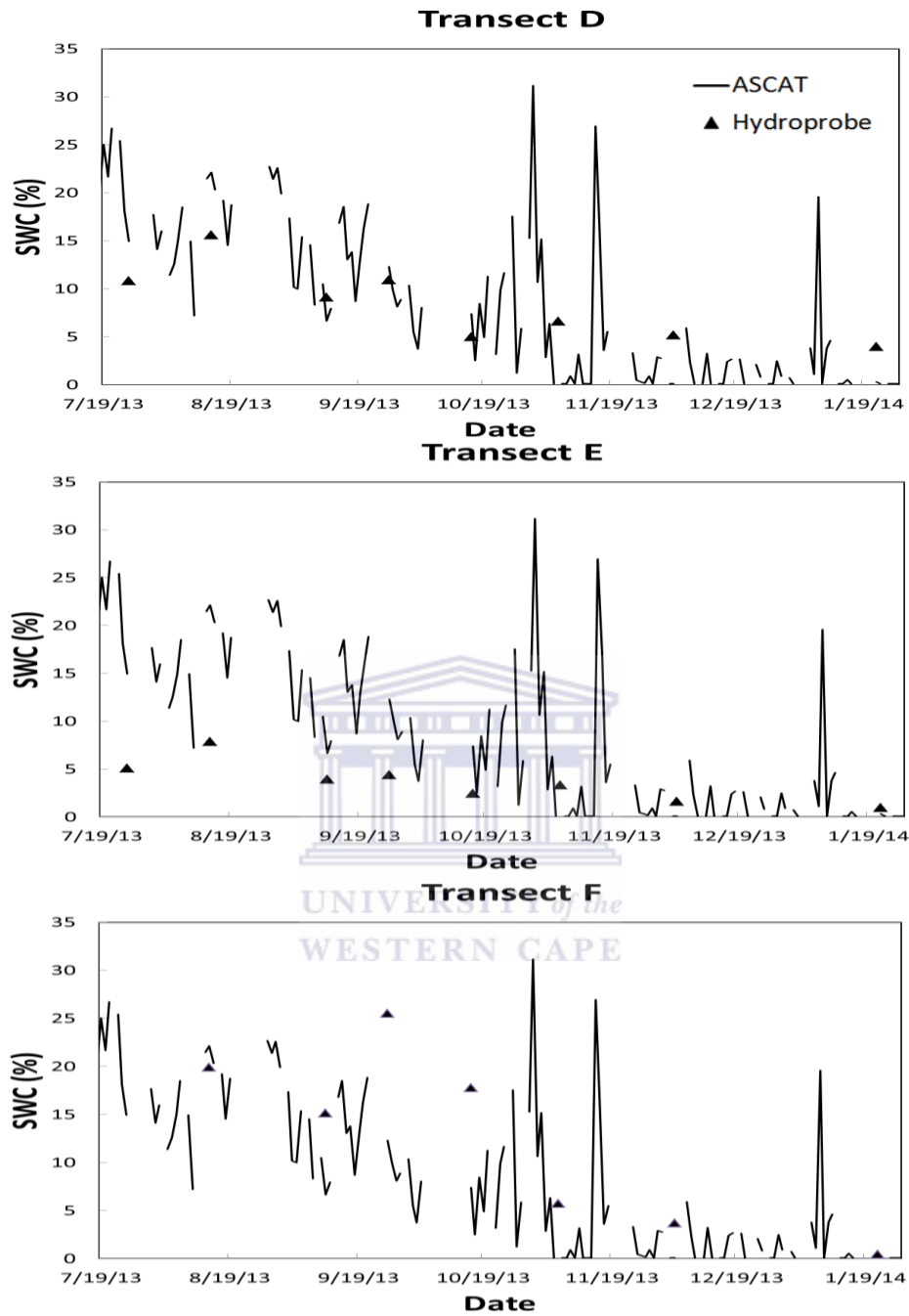


Figure 5.4: ASCAT 12.5km coarse resolution soil moisture estimates (solid line) and Hydroprobe soil moisture estimates (triangles) at Transect D, E and F for the Riebeeck site for the period 19 July 2013 to 27 January 2014, with soil water content (SWC) given in percent.

All three transects at Riebeek show moderately high to high r^2 values when comparing ASCAT soil moisture estimates to Hydroprobe soil moisture estimates. At transect D there is a low RMSE value, while transects E and F had moderately high to high RMSE values respectively. The averaged Hydroprobe soil moisture estimates for all transects at the Riebeek site had a moderately high r^2 and a very low (almost negligible) RMSE compared to ASCAT soil moisture.

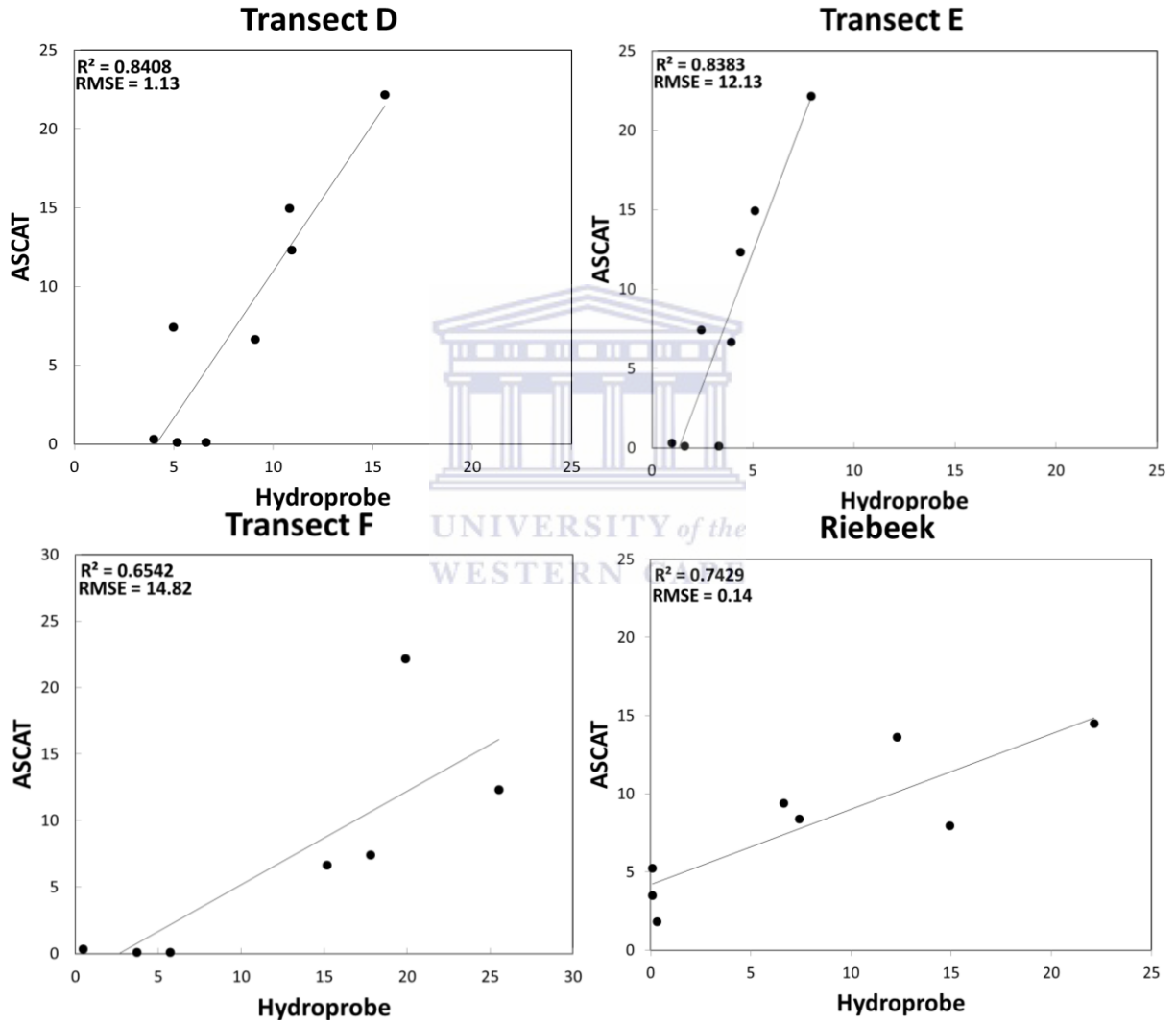


Figure 5.5: ASCAT 12.5km coarse resolution soil moisture estimates and Hydroprobe soil moisture estimates at transect D, E, F and averages for the Riebeek site for the period 19 July 2013 to 27 January 2014, with soil water content given in percent.

5.4 Data preparation- LST and NDVI

The data sets used for the downscaling algorithm, namely land surface temperature (LST) and the Normalised Difference Vegetation Index (NDVI) at ~1km resolution were acquired from National Aeronautics and Space Administration Agency (NASA) through their data dissemination portal at (U.S Geological Survey, 2014) which was accessed on 25 January 2014. The images are directly downloaded via ftp links sent as a list to the client.

These images are in a standardized data format which MODIS uses, namely the Hierarchical Data Format (HDF). The HDF data format is not routinely supported by many GIS software packages. Thus, before processing took place, images were imported into the GIS software package ENVI version 4.7, as ENVI is able to read this data format. Once in ENVI, LST images were georeferenced and the projection was converted from sinusoidal to a geographic Lat/Lon projection with the WGS84 datum. NDVI images can be imported already georeferenced and thus, only the reprojection was done for the NDVI images. Also, a gain of 0.02 was applied to LST images to convert the pixel values from emissivity to temperature in Kelvin. Once completed, LST pixel values were then converted from Kelvin to degrees Celsius by subtracting 272.15 from the pixel values. NDVI and LST images were then saved in geotiff format which were then imported to ILWIS version 3.3, for final processing.

5.5 LST-NDVI relationship

In order to calibrate the coefficients a_{00} - a_{22} for the downscaling, all NDVI pixel values were plotted against LST values for the entire study period to produce the universal triangle. This was only done for pixel values of the corresponding transects, as plotting all pixel values would be too many for one graph. A triangle was produced for each coarse resolution pixel, so as to determine the NDVI-LST relationship with soil moisture for that pixel. From these triangles, one can observe the maximum and minimum NDVI and LST values for the scaling of these values, which are needed for the downscaling algorithm presented in Chapter 3.5. These triangles are given in Figures 5.6, for the Malmesbury and Riebeeck pixels.

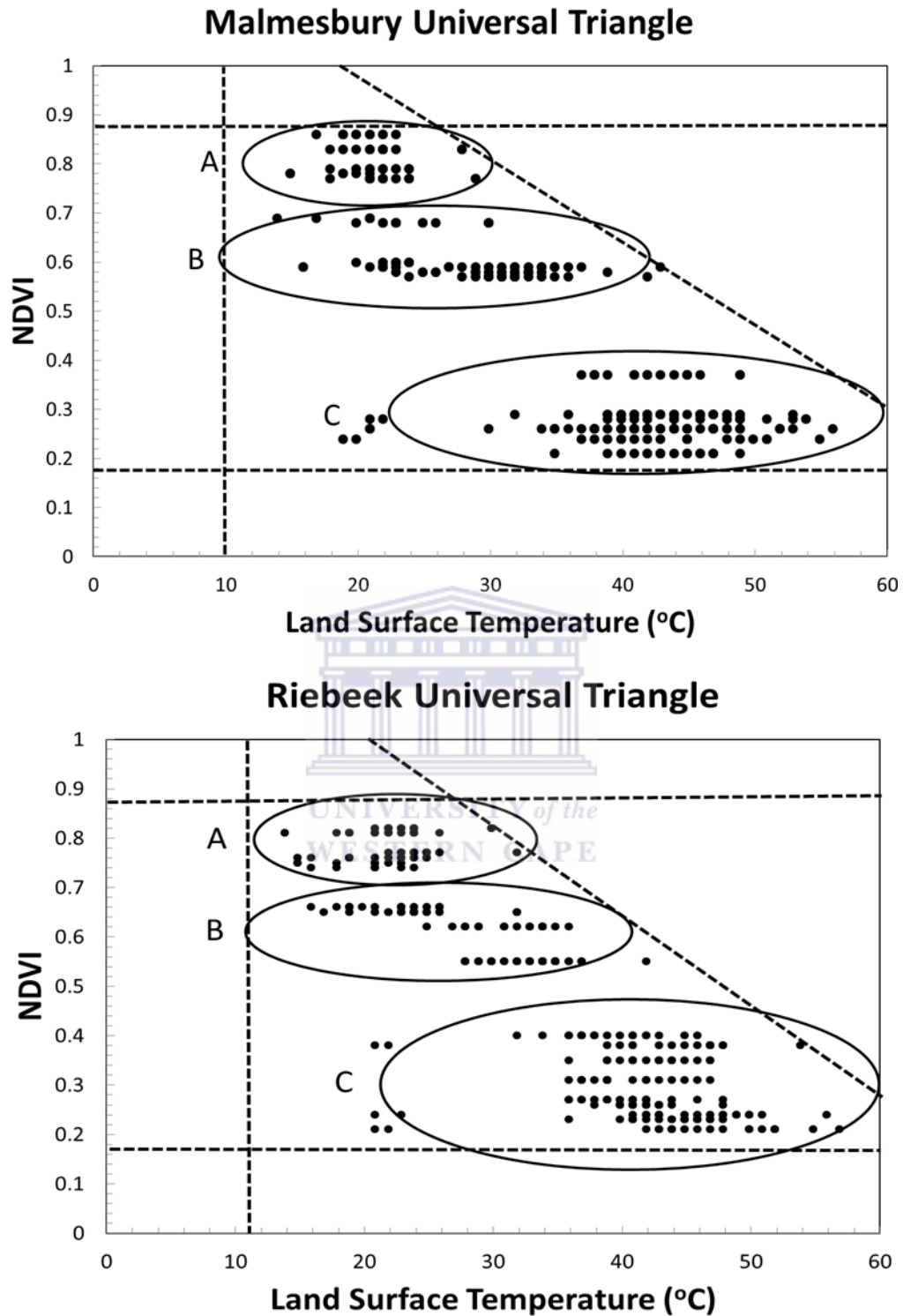


Figure 5.6: Universal triangle depicting soil moisture relationship with Normalized Difference Vegetation Index (NDVI) and Land Surface Temperature (LST) (°C) at Malmesbury (above) and Riebeeek (below)

The universal triangle for Malmesbury and Riebeeck (Figure 5.6) are very similar, with regards to maximum and minimum values for LST and NDVI as depicted by the dotted lines on the top, bottom and left sides of the graphs. The top left corners of the triangles represent wet conditions where surface temperature is low and NDVI values are high as experienced during late July- early September. The bottom right hand corner of the triangles is indicative of pixel values that are dry- high LST and low NDVI. Three groups of pixels are formed in which generally represent wet, drying and dry conditions as depicted by A, B and C (Figure 5.6). Even though the MODIS LST product was reported to give surface temperature values within 1°C accuracy (Wang and Liang, 2009), values in these triangles exceed 50°C, which is more than 10°C above summer maximum air temperature values in this region.

Maximum and minimum LST and NDVI values were then used to determine their scaled values using Equations 3.3 and 3.4. Once these values are obtained, these, values are used in equation 3.6, and coefficients a_{00} - a_{22} are calibrated by inserting ASCAT soil moisture on the left hand side of the equation. The calibration was done using the least two squares method. Calibrated coefficients were obtained for each pixel, as each pixel has a unique relationship between LST-NDVI and soil moisture. The calibrated coefficient values are given in Table 5.1.

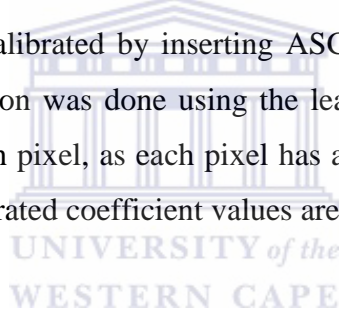
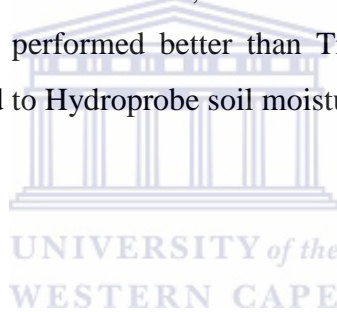


Table 5.1: Calibrated coefficients for brightness temperature linear regression model for Malmesbury and Riebeeck study sites

Site	a_{00}	a_{01}	a_{10}	a_{11}	a_{02}	a_{20}	a_{12}	a_{21}	a_{22}
Riebeeck	4.76	-3.8	4.75	16.09	-2.04	5.19	-4.43	4.17	-1.14
Malmesbury	9.91	-8.94	12.69	17.21	-3.91	2.33	-2.47	4.05	-2.28

Once obtained, these coefficients were inserted into Equation (3.6) using the 1km LST and NDVI pixel values for each transect to obtain a 1km estimation of the volumetric soil moisture. Line graphs and scatter plots were then generated for the study period depicting downscaled soil moisture and in situ soil moisture measurements as can be seen in Figure 5.7 to 5.10.

Hydroprobe soil moisture measurements were closely predicted by downscaled soil moisture estimates throughout the study period for Transect A (Figure 5.7). At transect B, the trend of downscaled soil moisture estimates moderately estimated the trend of soil moisture measurements for the study period, but overestimated them by 5-10%, with the exception of the in situ measurement on 26 September which was close to the downscaled estimate. Transect C shows that downscaling soil moisture estimates underestimated in situ measurements during the wet period, overestimated them during the dry period and failed to capture the seasonal trend of soil moisture. Thus, downscaling at Transect A, which has natural vegetation cover and the smallest slope gradient, generally performed better than Transects B and C which are grass covered pasture lands, as compared to Hydroprobe soil moisture estimates.



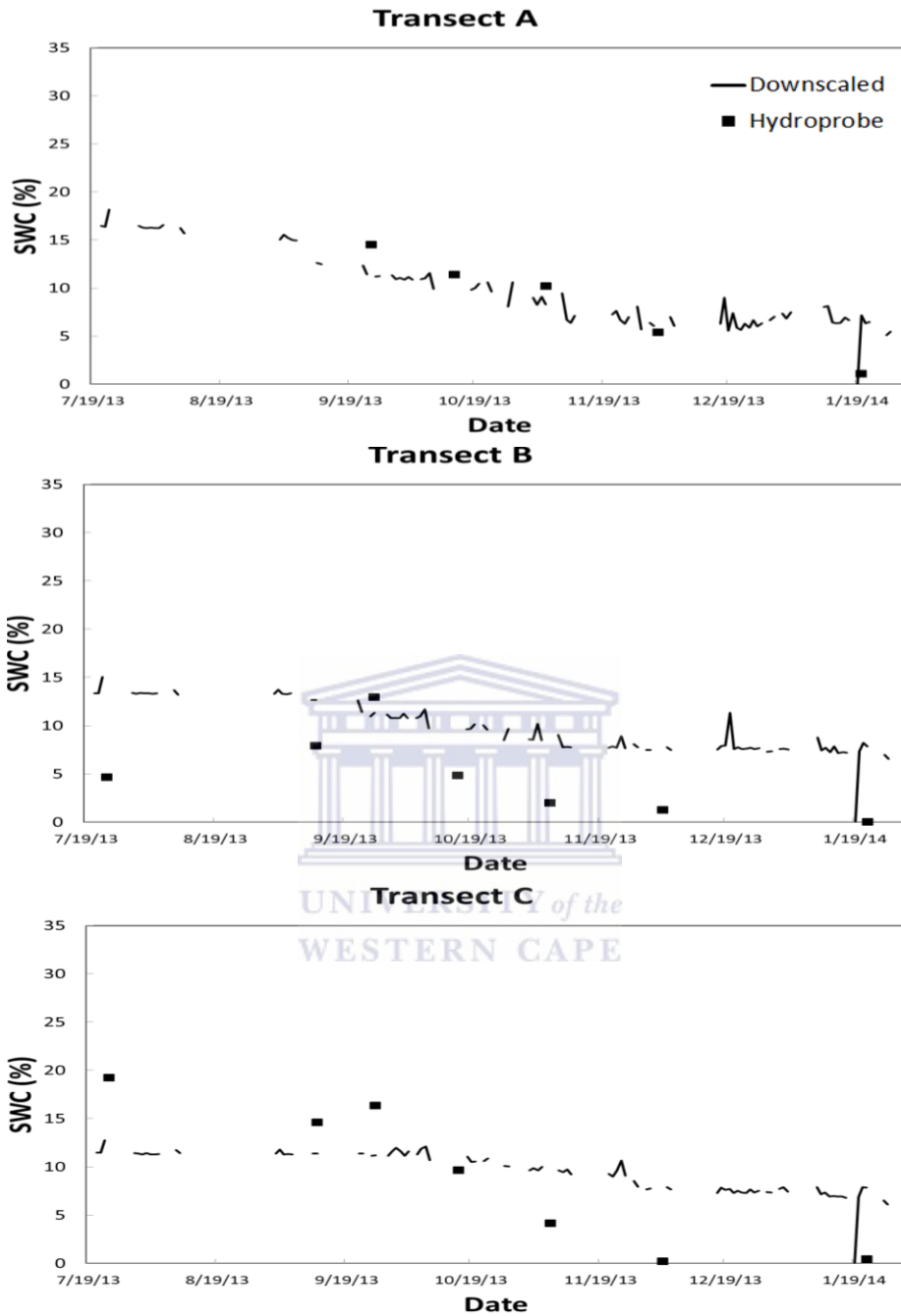


Figure 5.7: Downscaled 1km fine resolution soil moisture estimates (solid line) and Hydroprobe soil moisture estimates (squares) for Transects A, B and C at the Malmesbury site for the period 19 July 2013 to 27 January 2014, with soil water content (SWC) given in percent.

Comparison of downscaled soil moisture estimates and Hydroprobe soil moisture estimates showed that they had very high r^2 value at Transect A and almost negligible RMSE (Figure 5.8). At transect B the comparison of soil moisture values revealed a low r^2 value with a high RMSE,

because of the constant overestimation of in situ measurements by the downscaling results. At transect C downscaled soil moisture estimates had a high r^2 value as compared to in situ soil moisture measurements, with a low RMSE value.

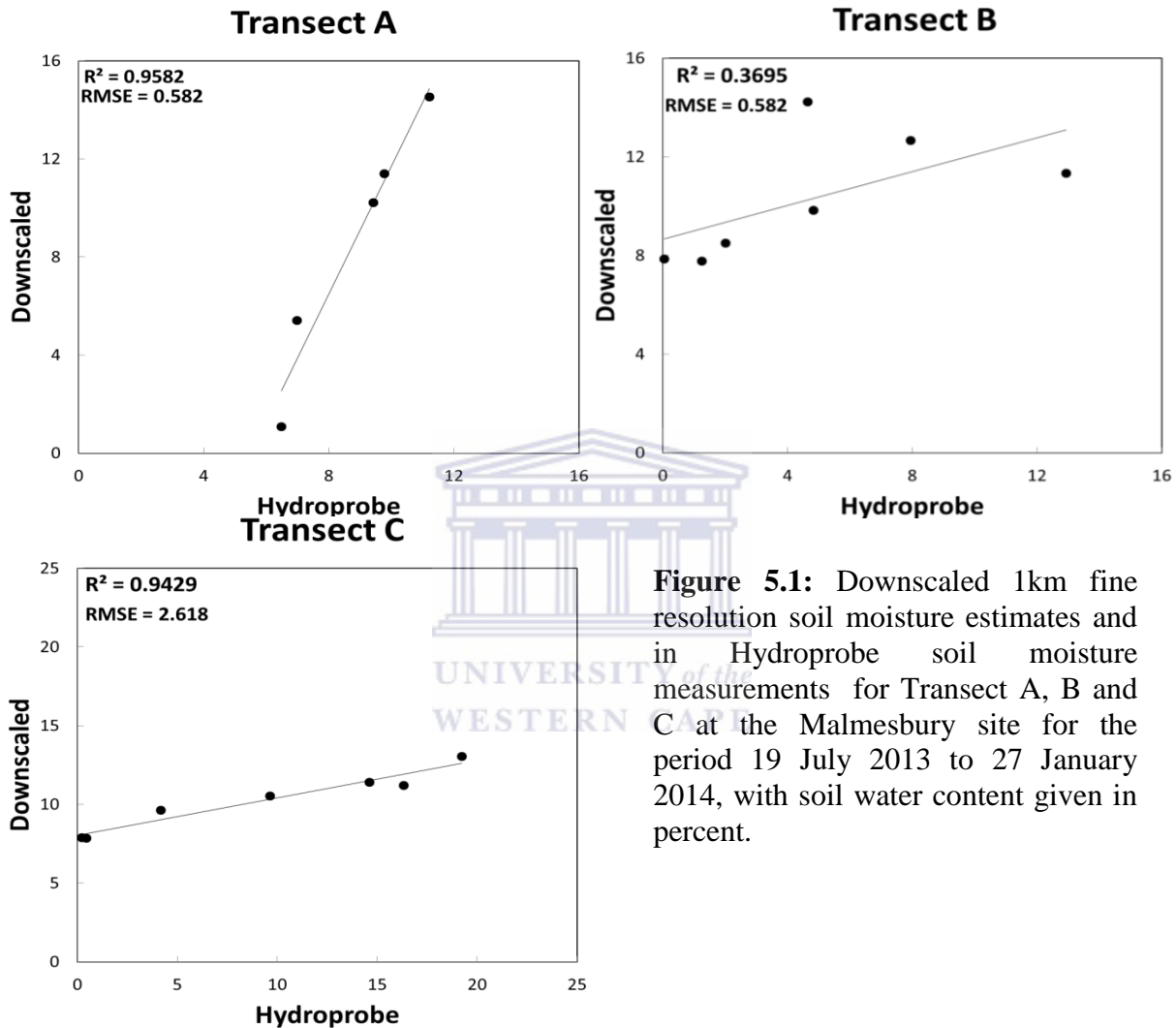


Figure 5.1: Downscaled 1km fine resolution soil moisture estimates and in Hydroprobe soil moisture measurements for Transect A, B and C at the Malmesbury site for the period 19 July 2013 to 27 January 2014, with soil water content given in percent.

At Riebeek study site, for all three transects, Hydroprobe soil moisture values were moderately to closely estimated by downscaled soil moisture estimates during the period November 2013 to January 2014 (Figure 5.9). Downscaled soil moisture estimates fit Hydroprobe estimates well during wet and dry periods and the seasonal trend was well represented. For Transect E however downscaled values overestimated Hydroprobe soil moisture during the wet period, while underestimating Hydroprobe soil moisture for Transect F during this same period. Downscaling

for Transect D which had grass covered pasture lands and a moderate slope gradient performed better than Transect E and F, as compared to Hydroprobe soil moisture estimates.

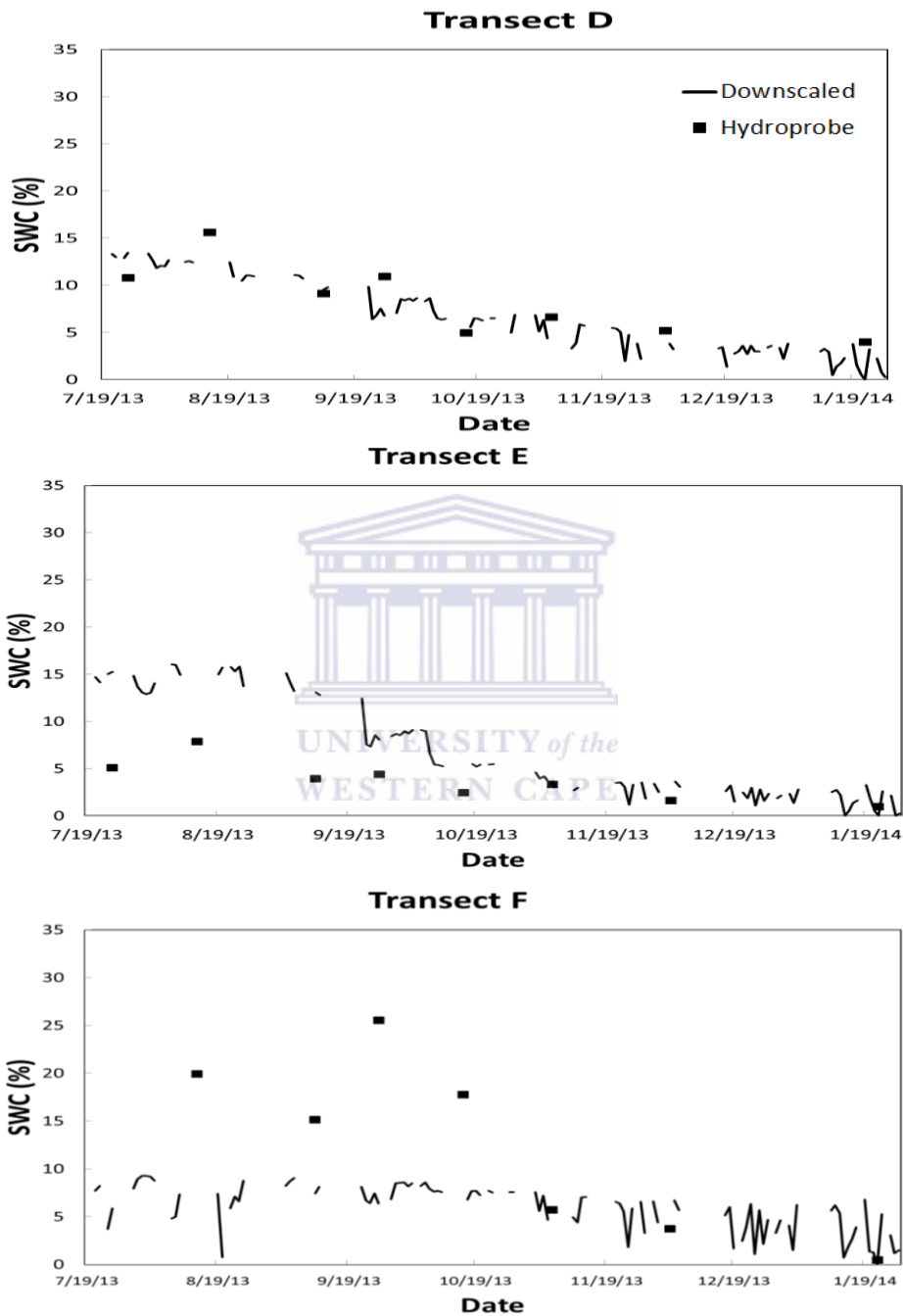


Figure 5.2: Downscaled 1km soil moisture estimates (solid line) and in Hydroprobe soil moisture estimates (square) for Transects D, E and F at the Riebeeck site for the period 19 July 2013 to 27 January 2014. Soil water content (SWC) is given in percent.

Transect D had a moderate r^2 value between downscaled soil moisture estimates and Hydroprobe soil moisture estimates with a relatively low RMSE (Figure 5.10). Transect E had a relatively high r^2 value between downscaled soil moisture estimates and Hydroprobe soil moisture estimates with a relatively high RMSE. For Transect F however there is a low r^2 coefficient between downscaled soil moisture estimates and Hydroprobe soil moisture estimates with a high RMSE.

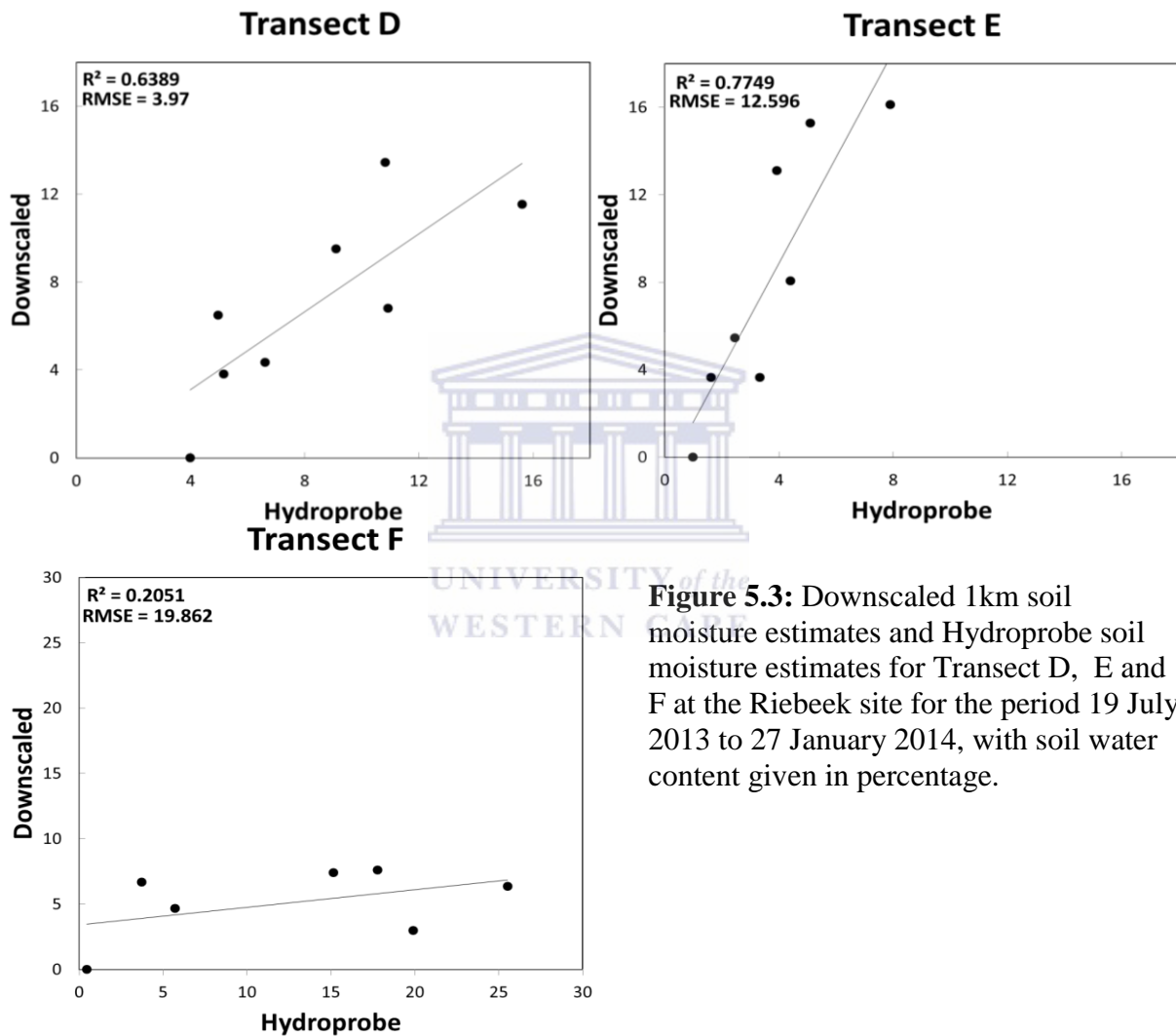


Figure 5.3: Downscaled 1km soil moisture estimates and Hydroprobe soil moisture estimates for Transect D, E and F at the Riebeek site for the period 19 July 2013 to 27 January 2014, with soil water content given in percentage.

5.6 Summary

ASCAT soil moisture estimates compared reasonably well at both sites to in Hydroprobe estimates with regards to seasonal variation, which is evident in the resulting r^2 value, 0.8668. Daily variations in soil moisture were also well represented by the ASCAT soil moisture estimates as is evident by the moderate to low RMSE values observed. ASCAT thus performed well at the sandy Malmesbury site as well as the loamy sand dominated Riebeek site. ASCAT soil moisture estimates were very responsive to precipitation at both sites.

Downscaled soil moisture estimates only compared well to Hydroprobe soil moisture estimates at transects A at the Malmesbury site, while performing reasonably at transect C poorly at transect B which is evident from the comparison of R^2 and RMSE values. At the Riebeek study site, downscaled soil moisture estimates also only compared well at one transect (D), while comparing reasonably at transect E and poorly at transect F. There was no evidence to suggest that soil texture had any appreciable effect on the results of the comparison between downscaled soil moisture estimates and Hydroprobe soil moisture estimates, when comparing the results obtained for the Malmesbury and Riebeek sites. There was also no conclusive evidence that the downscaling model performed better under any specific land cover type or slope conditions. The downscaling model was not responsive to rainfall as there were slight variation in daily LST values which may have been influenced by rainfall events, but NDVI has no daily response to rainfall and thus downscaled soil moisture shows less daily variations as compared to ASCAT soil moisture estimates.

6. Soil Water Balance Model

6.1 Introduction

This chapter will deal with the soil water modelling. Included will be the rainfall data, reference evapotranspiration and soil retention curves used in the soil water balance model. A model sensitivity analysis of all calibrated parameters is discussed, followed by a discussion of the procedure followed and considerations made for the model calibration. This will be followed by the model simulation results.

6.2 Daily rainfall and evapotranspiration

The two study sites, Malmesbury and Riebeek, have very similar seasonal rainfall pattern from winter to summer (Figure 6.1). They also had a very similar number of rainfall days often experiencing rainfall on the same day. Riebeek however had slightly higher rainfall than Malmesbury on all days they both received rainfall.

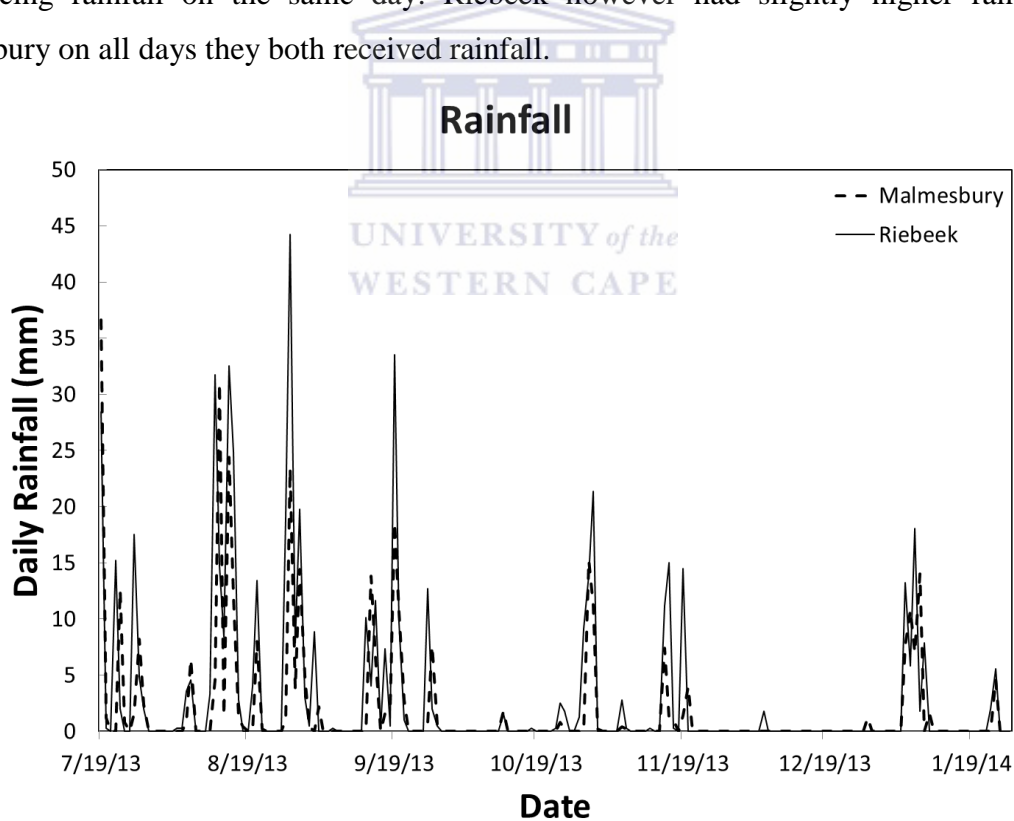


Figure 6.1: Daily rainfall for the Malmesbury (dotted line) and Riebeek (solid line) sites from 17 July 2013 to 27 January 2014

Malmesbury had peak rainfall during July with the highest amount totalling 36.6mm/day on 19 July 2013 while Riebeeck experienced peak rainfall during August with a peak daily amount of 33.53 mm/day on 19 September 2013. Both sites received almost no rainfall from December 2013 to January 2014 excluding the period of the 5th-10th January 2014 where each site had a few consecutive days with rainfall with the maximum values exceeding 10mm/day.

Reference evapotranspiration was calculated for each of the sites using the Hargreaves and Samani (1985) Equation (3.10) and is presented in Figure 6.2. When examining the reference evapotranspiration values, obtained using Equation (3.10), there was a general increase in values from July to January for both sites. These daily variations observed over shorter periods of time were a result of the increases and decreases in air temperature values observed between consecutive days. Malmesbury had generally higher evapotranspiration rates.

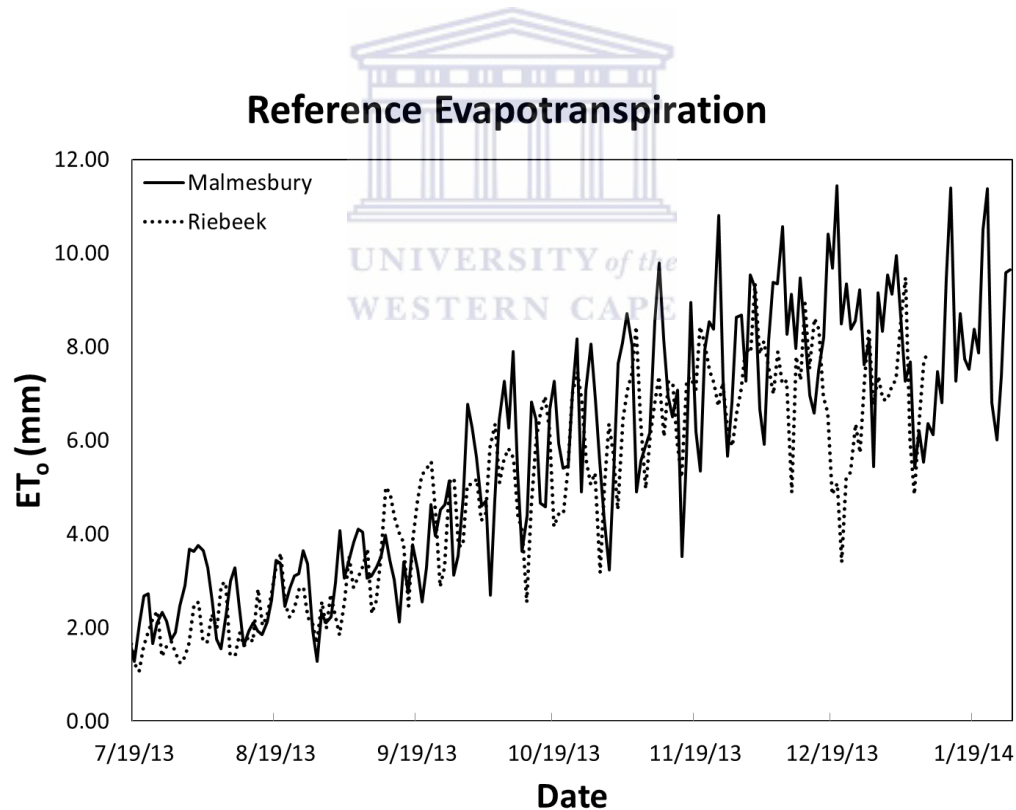


Figure 6.2: Reference evapotranspiration in mm calculated using the Hargreaves and Samani (1985) method at the Malmesbury and Riebeeck sites for the period 19 July 2013 to 27 January 2014

6.3 Soil hydraulic properties for the Malmesbury and Riebeek sites

Figure 6.3 shows the relationship between hydraulic conductivity (K) and volumetric soil moisture (θ) at Malmesbury and Riebeek. These relationships are assumed to be uniform at all transects within the specified study sites as the soil types were very similar for all transects within a specific study site. Hydraulic conductivity was estimated using the van Genuchten-Maulem single porosity model with the initial conditions set to an upper boundary with a constant pressure head and a lower boundary experiencing free drainage (Van Genuchten, 1980). Other inputs for this model were physical soil properties observed in the field as presented in Table 4.4 as well as field capacity and wilting point values observed during Hydroprobe soil moisture measurements.

Malmesbury has higher hydraulic conductivity values for lower volumetric water content values than Riebeek (Figure 6.3). Malmesbury has sandy soils and Riebeek has loamy soils. It is assumed in the soil water balance model that there are no additions of water to the soil column being investigated from the groundwater table as this area has a deep water table and no capillary rise.

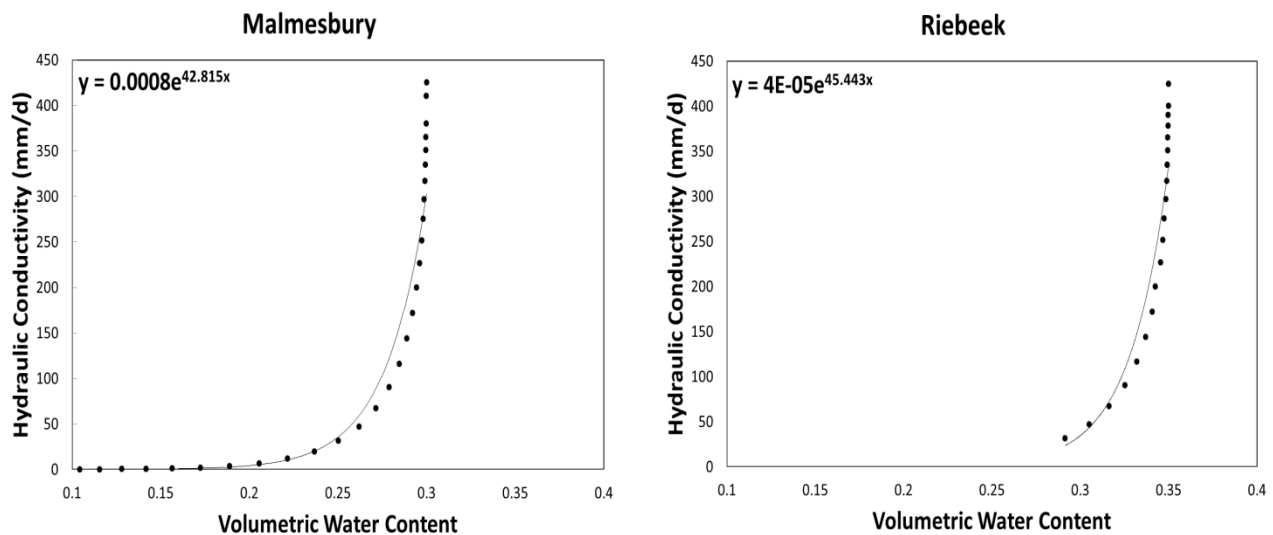


Figure 6.3: Hydraulic conductivity-soil water content relationships for Malmesbury and Riebeek fitted with an exponential trend line (equations displayed on graphs).

6.4 Method of model calibration

Model calibration was done for four model parameters, namely, field capacity (F_c), runoff coefficient (β), rainfall interception (P_i) and evapotranspiration coefficient (ET_c). Due to the low number of in situ sampling days, model calibration was done in two phases. Initially, the calibrated parameters were constrained using values obtained from the literature after which manual calibration was done, by fitting simulated soil moisture estimates to Hydroprobe estimates along each of the transects.

Field capacity values were assumed to be the highest Hydroprobe soil moisture estimates observed at each transect during the study period, as certain agricultural practices, such as livestock grazing and tillage are known to result in soil compaction (Lipiec and Hatano, 2003), which would then lower the soil's water holding potential in addition to other effects. It was noted by De Clerq et al. (2010) that infiltration rates in these areas were a function of land use and agricultural practices. These effects were then also taken into consideration as compaction of the soil surface would also lower rainfall infiltration capacity. Runoff coefficients were guided by Oregon Department of Transportation (2005), as they provide runoff indices for a wide range of land uses.

Rainfall interception values were based on recommendations of Thurow et al. (1987), who proposed interception values for short and medium grasses. This was suitable as none of the transects had dense vegetation, with the thickest vegetation occurring in transects with natural land cover, which were dominated by grasses, shrubs and medium size bushes (1-1.5m tall).

Studies by Jovanovic et al. (2013) investigated the relationship between potential and actual evapotranspiration in this region. This information was used to guide calibration. There were however marked land cover changes for transects on pasture land, they showed short-medium grass and shrub growth during winter-spring, but became almost bare soil going into summer. Wallace et al. (1990), however shows that there is a close relationship between evapotranspiration rates of fallow shrubland and bare soil experiencing the same meteorological conditions.

Once the possible range of parameter values was established, adjustments of parameters was then done by comparing simulated and Hydroprobe soil water content estimates.

The Field capacity (Figure 6.4), shows that simulated soil moisture estimates during the wet period reached field capacity within this parameter's constrained range. As soil moisture decreases, the influence of field capacity on simulated soil moisture estimates decreases. Thus, for the Runoff Coefficient, Rainfall Interception and Evapotranspiration Coefficient (Figure 6.4), all maximum simulated soil moisture values were constrained by the field capacity used for these simulations. Runoff coefficient changes shows differences in simulated soil moisture values, with the magnitude of the difference directly related to the amount of rainfall received, which is highest during the wet period. Rainfall interception parameter values (Figure 6.4) show very little change in simulated soil moisture estimates during rainfall periods. Evapotranspiration coefficient increases create decreases in simulated soil moisture estimates during wet and dry periods. These simulation differences were found to be the largest during dry periods, where reference evapotranspiration is the highest.

All final calibrated parameter values for each transect are given in Table 6.1, based on best fit of simulated to the Hydroprobe soil moisture estimates.

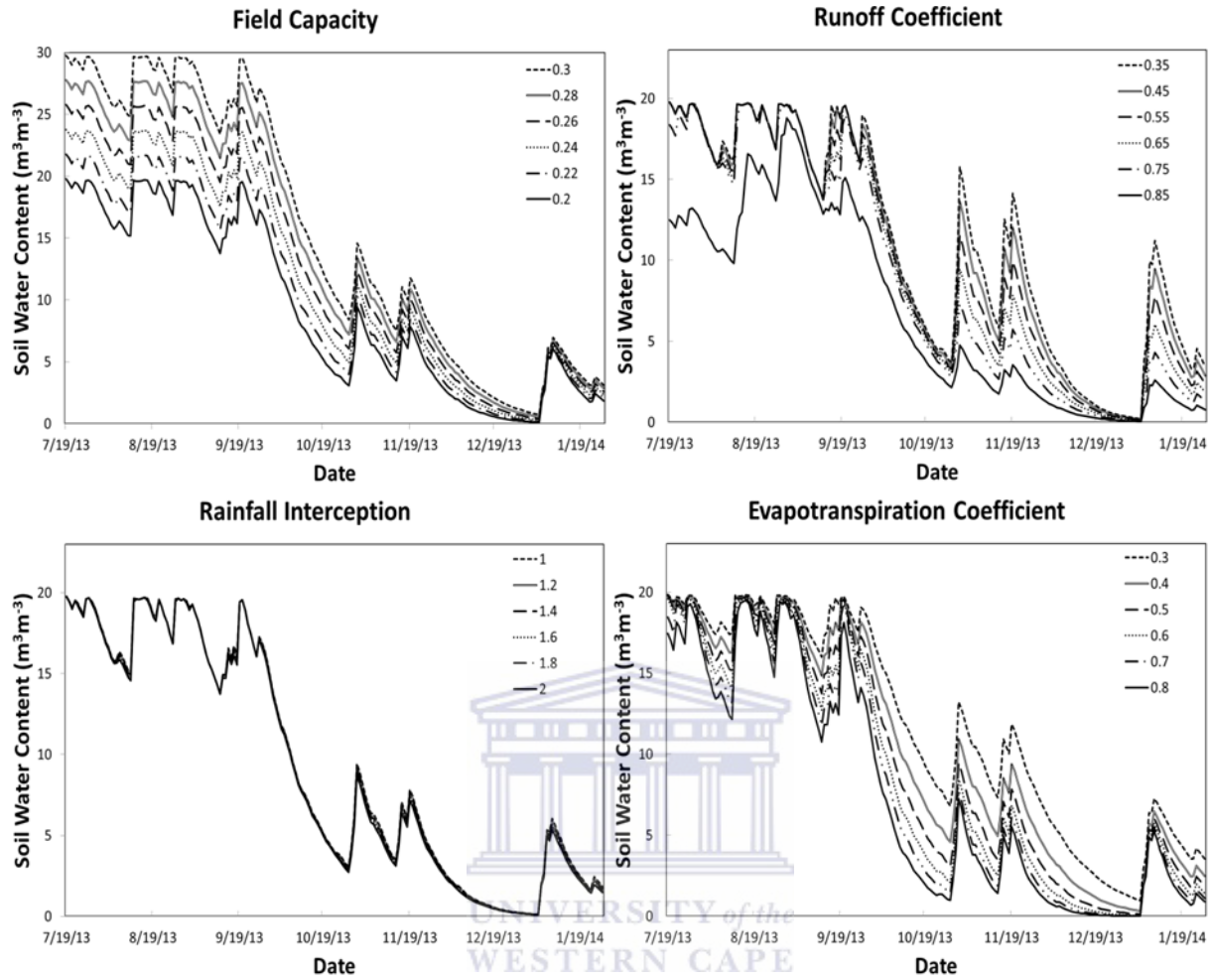


Figure 6.4: Soil water balance model simulation variations as observed with changes in field capacity, runoff coefficient, rainfall interception and evapotranspiration coefficient for the period of 19 July 2013 to 27 January 2014, with soil water content (SWC) given in percent.

Table 6.1: Calibrated parameter values for field capacity (F_c), runoff coefficient (β), rainfall interception (P_i) and evapotranspiration coefficient for all transects

Transect	F_c	β	P_i	ET_C
A	0.20	0.65	1	0.5
B	0.20	0.85	2	0.55
C	0.26	0.40	2	0.80
D	0.27	0.07	2	0.80
E	0.23	0.50	2	0.70
F	0.22	0.20	2	0.90

6.5 Simulation results

The soil water balance model simulated soil water content for the entire study period and the results were compared to Hydroprobe soil moisture estimates, which were average soil moisture values obtained for each of the transects for each sampling day.

The model captured the seasonal trend, as well as shorter variability at each of the three transects in Malmesbury (Figure 6.5) compared to Hydroprobe estimates. Wet and dry simulated soil moisture values matched Hydroprobe soil moisture values well, with the exception of 24 July 2013 and 16 October 2013 for Transects B and C. On 24 July 2013 simulation results overestimated Hydroprobe soil moisture estimates for Transect B and underestimated Hydroprobe soil moisture estimates for Transect C, and on 16 October 2013 simulation results underestimated Hydroprobe soil moisture estimates for both transects.

During the dry period however, for Transects B and C the model overestimated in Hydroprobe soil moisture while for Transect A Hydroprobe soil moisture was underestimated. Soil moisture simulation for Transect A, which has natural vegetation cover, and a small slope gradient performed the best of the three transects in comparison to Hydroprobe soil moisture estimates. Simulated soil moisture estimates for Transect C, which had a bare soil surface during the dry period compared most poorly to Hydroprobes estimates during this time.

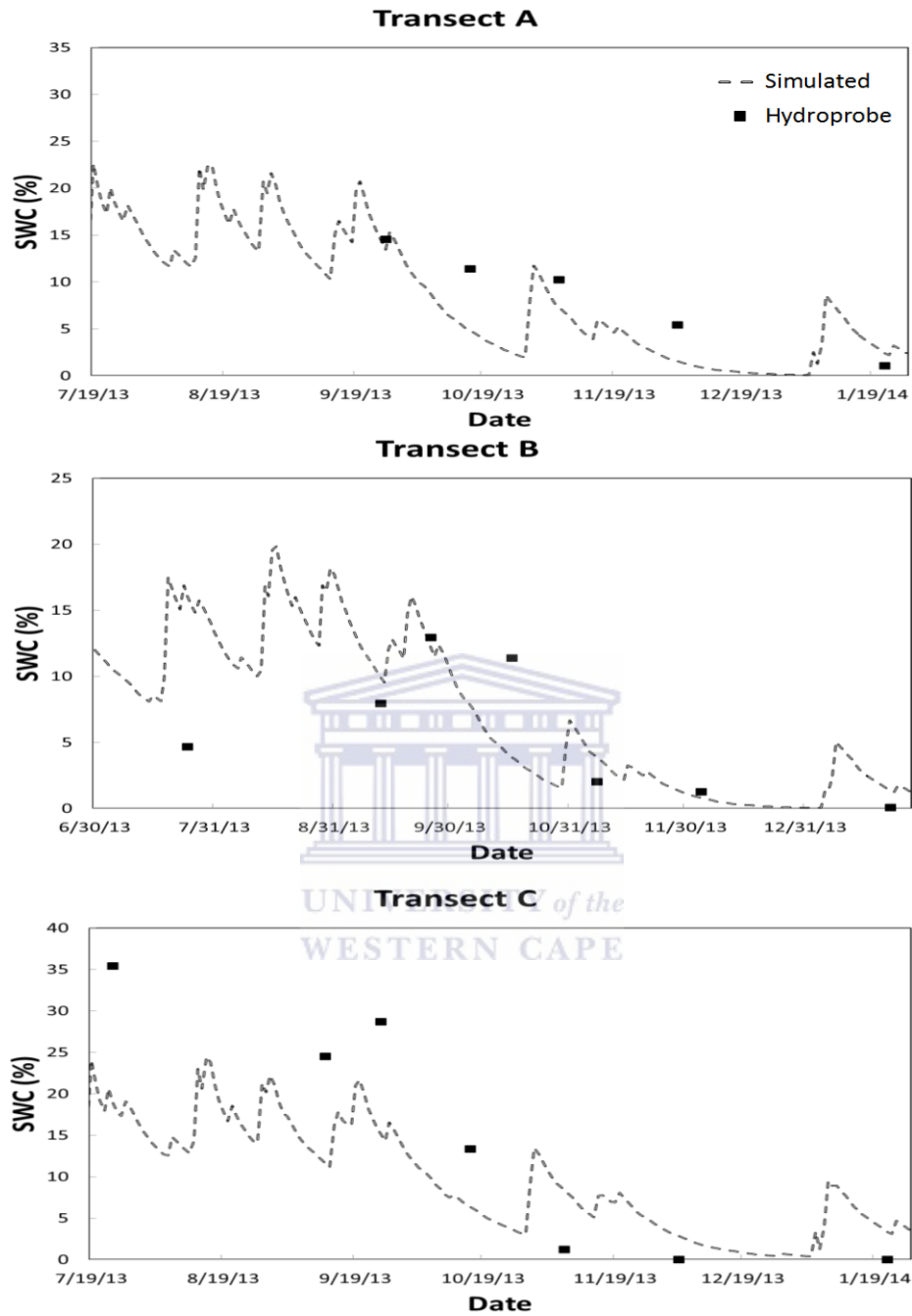


Figure 6.5: Simulated soil moisture estimates (dotted line) and Hydroprobe soil moisture estimates (squares) for Transects A, B and C at the Malmesbury study site for the period 19 July 2013 to 22 January 2014, with soil water content (SWC) given in percent.

The simulated and Hydroprobe soil moisture content values have a high coefficient of determination (r^2) for Transect C (>8), a low r^2 for C and a moderate r^2 for Transect A. The RMSEs however are the lowest for Transect B and the highest for Transect C. The high RMSE for Transect C is due to the model overestimation of in Hydroprobe estimates for all sampling days.

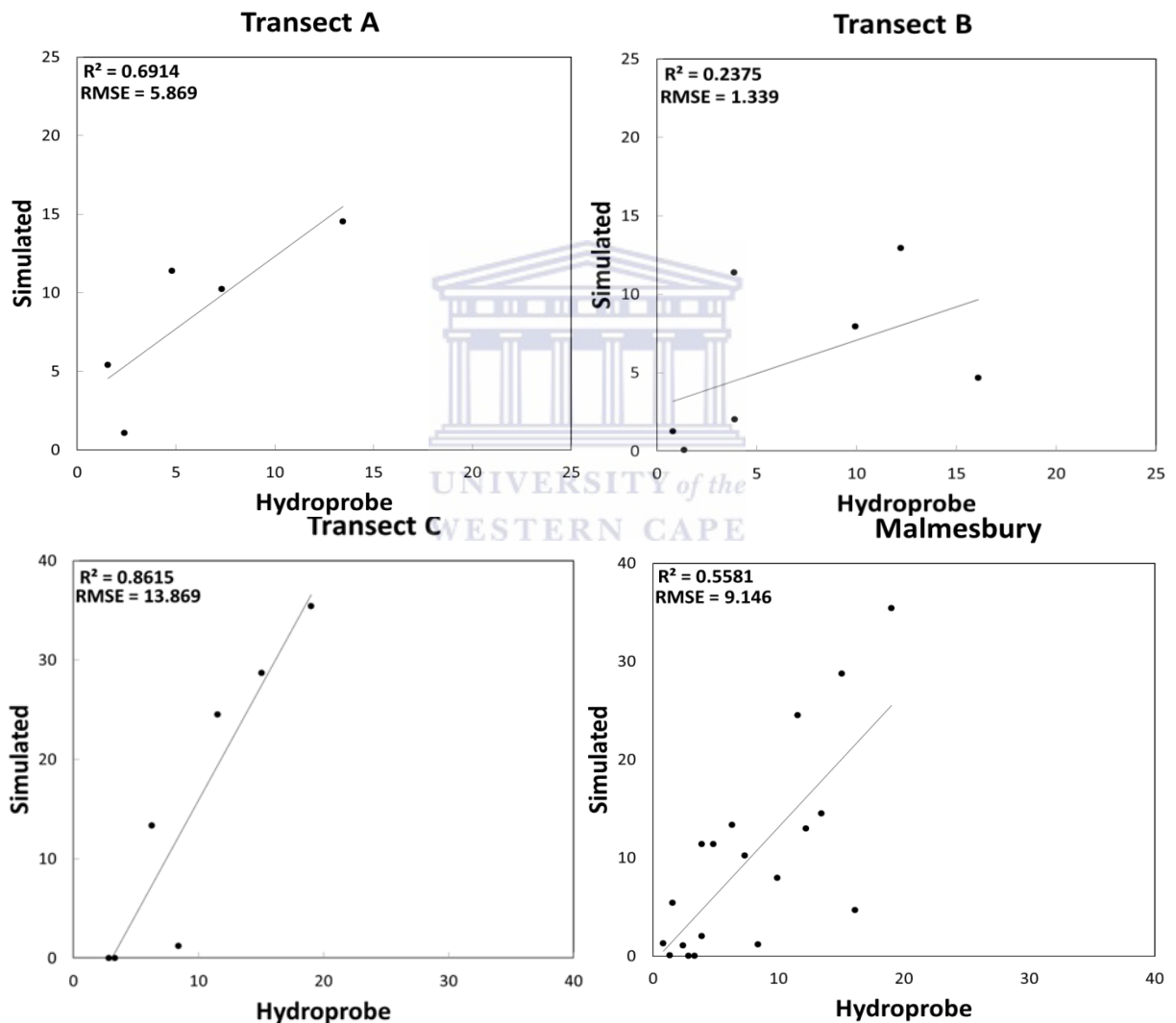


Figure 6.6: Simulated soil moisture estimates and Hydroprobe soil moisture estimates for Transect A, B, C and overall at the Malmesbury site for the period 19 July 2013 to 27 January 2014, with soil water content is given in percent.

The simulated soil moisture has a similar variation over time as compared with with the Hydroprobe soil moisture estimates for all transects in the Riebeek site (Fig. 6.7). The model overestimated Hydroprobe soil moisture of Transect D and E during the wet period, July 2013- September 2013. The model performed well on Transect F throughout the study. The model produced accurate results during the drier period (November 2013- January 2014) for all three transects. Transect F has natural vegetation cover with the lowest slope gradient of the three transects, while transects D and E were grass covered pastureland and vineyard respectively. The model performed poorly on transect E, which has vineyards as vegetal cover.



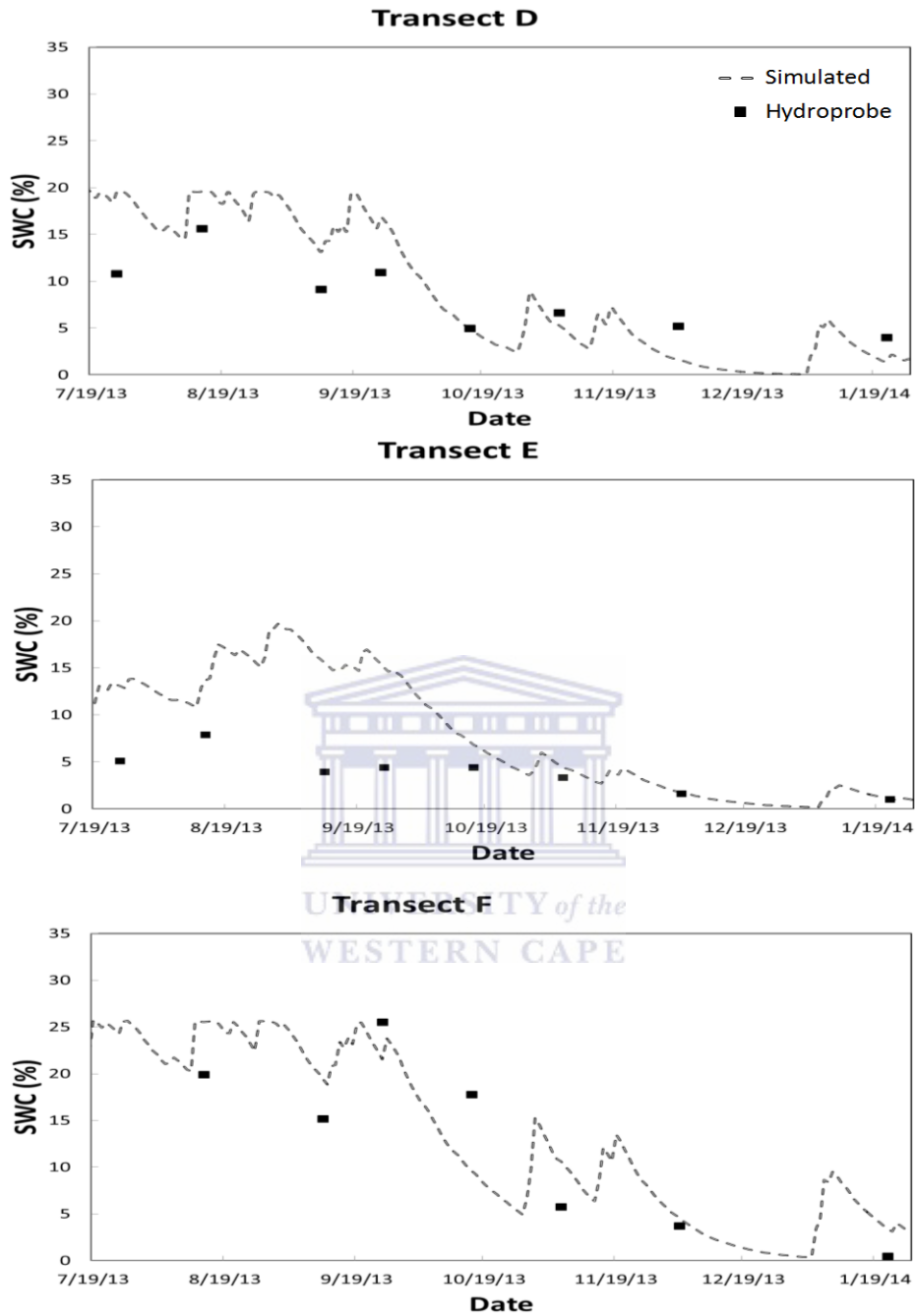


Figure 6.7: Simulated soil moisture estimates (dotted line) and Hydroprobe soil moisture (squares) for Transects D, E and F at the Riebeeck study site for the period 19 July 2013 to 22 January 2014, with soil water content (SWC) given in percent.

The observed and simulated values for all of the transects had moderate (0.58) to high (0.87) r^2 , with the highest r^2 on Transect A and the lowest for Transect B. The overall evaluation of all simulated and Hydroprobe soil moisture for transects in the Riebeek site also had a moderate r^2 (0.63). The RMSEs for all of the transects was generally low (>7). The Hydroprobe and simulated soil moisture was however also generally low throughout the study period (soil water content $<26\%$), potentially leaving less room for high values of RMSE.

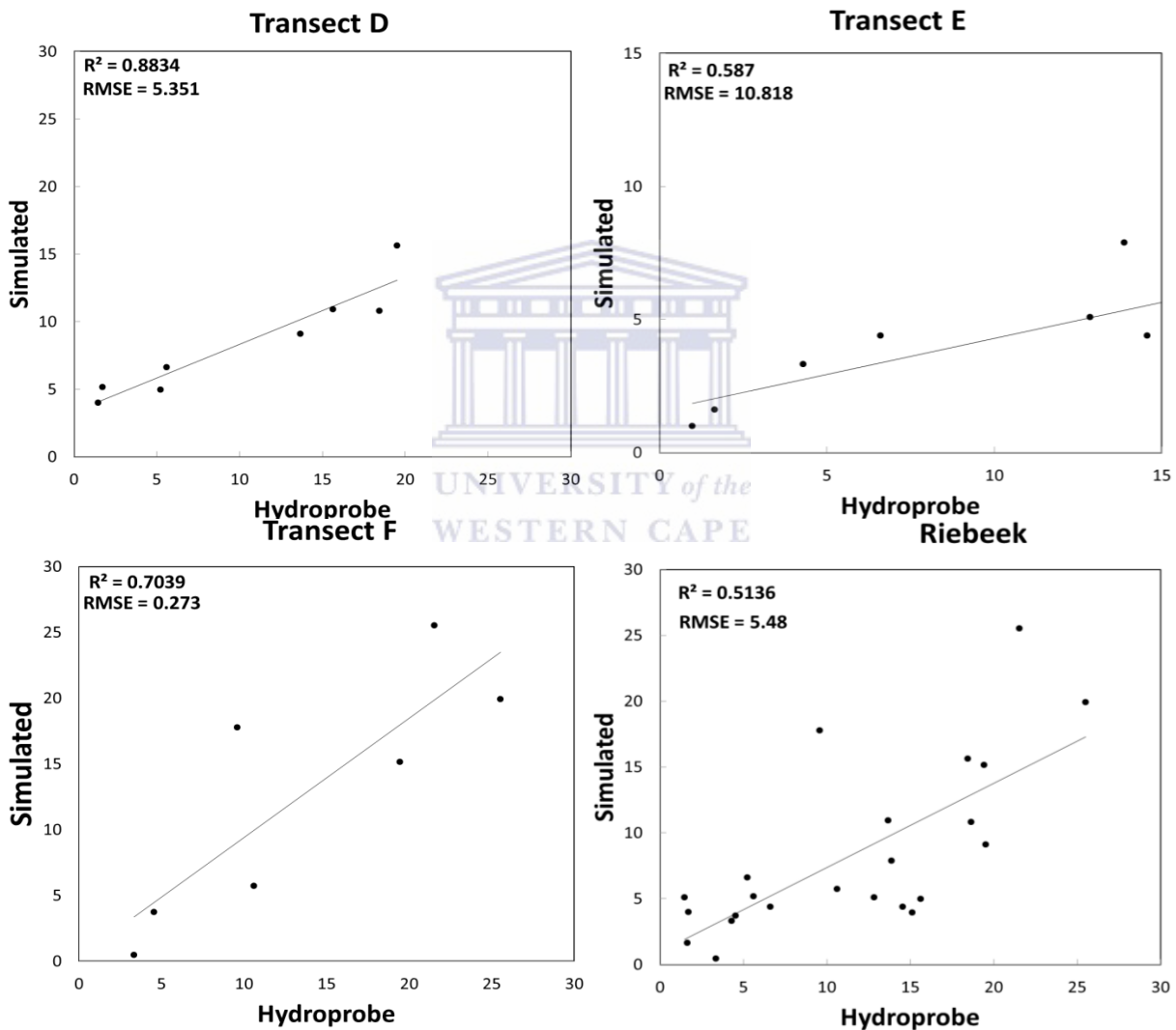


Figure 6.8: Simulated soil moisture estimates and Hydroprobe soil moisture estimates at Transect D, E, F and overall for the Riebeek site for the period 19 July 2013 to 27 January 2014, with soil water content given in percent.

6.6 Sensitivity analysis

Simulated values and observed values were used to determine the RSME, deviation percentages for adjustments of the calibrated values as presented in Figure 6.9.

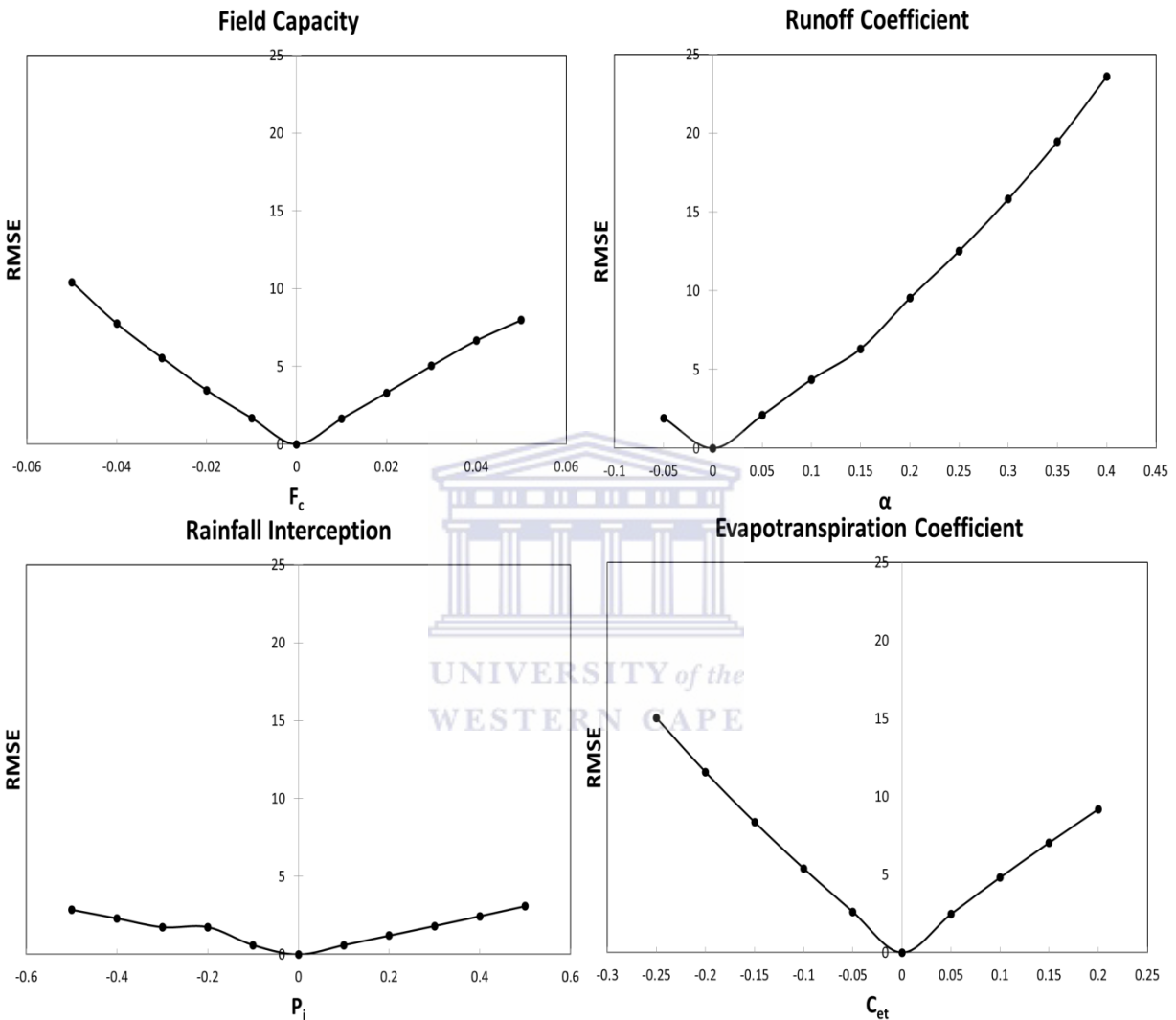


Figure 6.9: Sensitivity analysis of soil water balance model to *field capacity*, *runoff coefficient*, *rainfall interception* and *evapotranspiration coefficient*. The root mean square error (RMSE) is given in soil water content (%).

The sensitivity analysis was done by comparing model simulation to historic in situ data for the year of 2008 for transect D, as this was the only extended time series of available soil moisture data, which was representative for a depth of ~10cm of the soil profile. This is due to the fact that sampling incorporated an extensive spatial element during the field work section of the study

but due to time and budget constraints the number of sampling days were limited to approximately 1 day every 2-3 weeks.

The sensitivity analysis revealed that the most sensitive parameters in the hydrological model are the evapotranspiration coefficient and runoff coefficient, with field capacity being moderately sensitive and rainfall interception being the least sensitive. Because of the runoff coefficient's dependency on rainfall, this parameter was found to have a large influence on RMSE during the wetter period. Similarly, the evapotranspiration is dependent on potential evapotranspiration and thus this parameters has a more pronounced influence on RMSE during the summer period.

6.7 Summary

From the comparison of simulated soil moisture estimates it observed that all soil water balance model simulations at both the Malmesbury and Riebeek sites captured the seasonal trend reasonably well excluding Transect C. For Transect C Hydroprobe soil moisture estimates were underestimated by the model during the wet period (July-September 2013). This may be due to the ponding of water between contour bunds during the wet period. At the Malmesbury site, the seasonal trend was preserved by the model estimates, r^2 values were generally moderate (5-6) with moderate to high RMSE values (4-19). At the Riebeek site the comparison of in situ measurements to simulated results was also dominated by moderate r^2 values (6), but RMSE stayed quite low for all transects (>6.5).

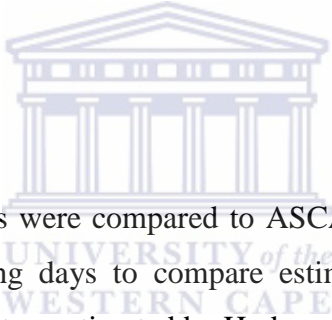
The model performed better at the Riebeek site, which is characterised by sandy loam soils than at the Malmesbury site which has sandy soils. This is evident from observing r^2 values between simulated and Hydroprobe soil moisture estimates for all transects. The model also performed better at transects with natural vegetation cover and low slope gradients as compared to transects dominated by agricultural practices with steeper slope gradients.

7. Remote sensing derived and simulated soil moisture

7.1 Introduction

In this chapter remote sensing derived soil moisture estimates will be compared to (a) soil moisture estimated using a soil water balance model and (b) Hydroprobe soil moisture estimates. The coarse (ASCAT 12.5km) and fine (downscaled 1km) resolution remote sensing derived soil moisture was compared to the Hydroprobe estimates and simulated estimates for each of the days when field measurement was done. Correlation matrices comparing estimates made using these different methods are presented.

7.2 In situ soil moisture results



Hydroprobe soil moisture estimates were compared to ASCAT, downscaled and simulated soil moisture estimates for all sampling days to compare estimated soil moisture values to soil moisture variation along the transect as estimated by Hydroprobe measurements.

For Transect A, ASCAT soil moisture values generally fit the average of the transect well throughout the sampling period with the exception of 7 November 2013, for soil moisture is underestimated. The downscaled soil moisture closely mirrors the ASCAT soil moisture with the exception of 7 November 2013, when it better fits the Hydroprobe soil moisture measurement. The simulated soil moisture similarly, fits the seasonal trend of the Hydroprobe soil moisture well. The comparison of these soil moisture estimates for Transect A suggests that all three methods of soil moisture estimation compared well to Hydroprobe soil moisture measurements at Transect A which has shrubland vegetation cover and a low slope gradient.

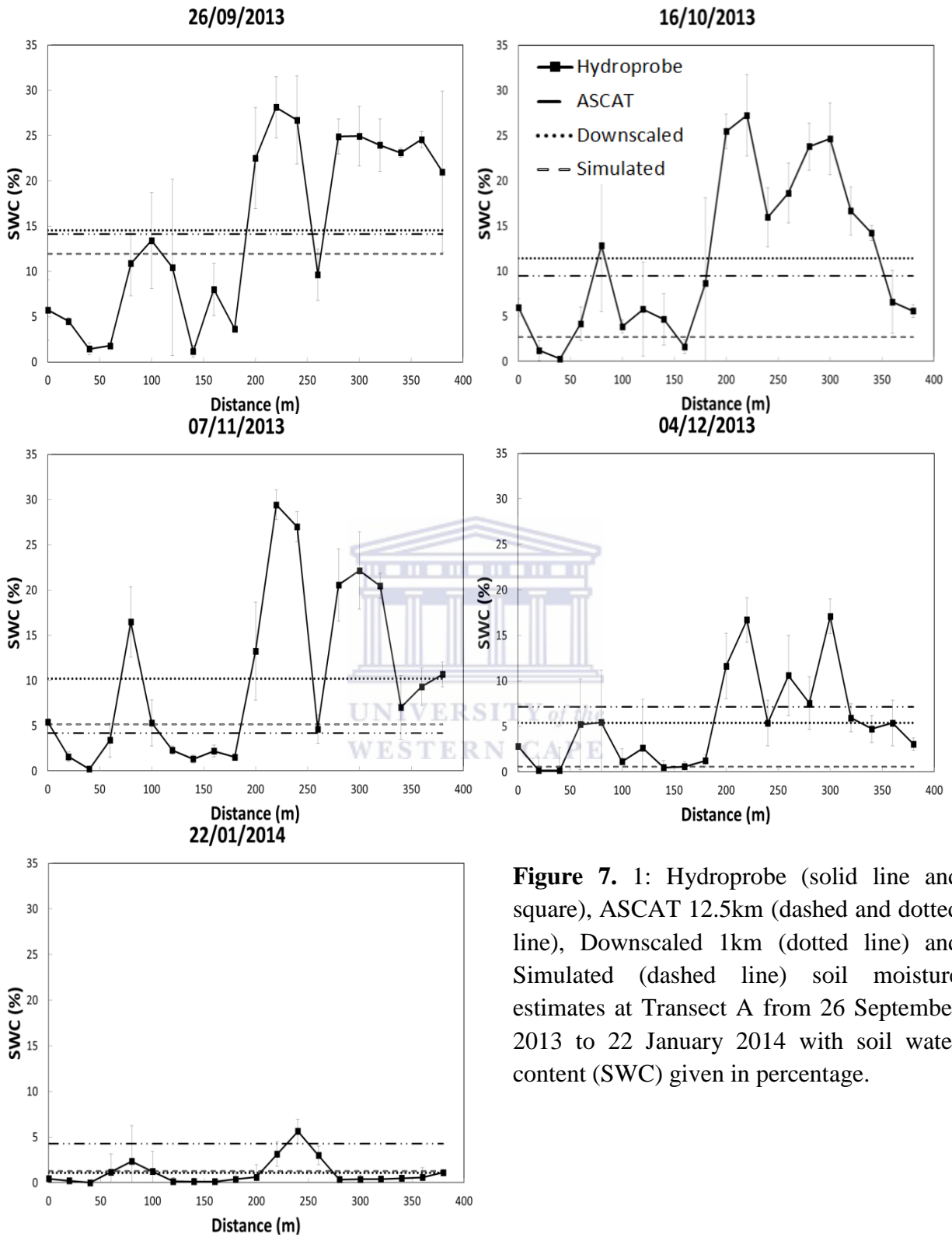


Figure 7. 1: Hydroprobe (solid line and square), ASCAT 12.5km (dashed and dotted line), Downscaled 1km (dotted line) and Simulated (dashed line) soil moisture estimates at Transect A from 26 September 2013 to 22 January 2014 with soil water content (SWC) given in percentage.

ASCAT, downscaled and simulation soil moisture estimation generally overestimated soil moisture throughout the study at Transect B (Figure 7.2 and 7.3), with the exception of 26 September 2013, where the aforementioned estimates more accurately represent Hydroprobe soil moisture. The most seasonal variation of ASCAT, downscaled and simulated soil moisture datasets was the downscaled soil moisture estimates, which shows the largest overestimation of Hydroprobe soil moisture during the dry period (Figure 7.3), while the simulated soil moisture estimates more accurately predicted soil moisture during the same period. ASCAT and simulated soil moisture estimates compared moderately well to Hydroprobe soil moisture estimates at Transect B. Comparison of ASCAT, downscaled and simulated soil moisture to Hydroprobe soil moisture did better at this transect during the wetter periods when there was some ponding of water at the surface at certain parts of the transect and grass cover was more dense (Figure 7.2).



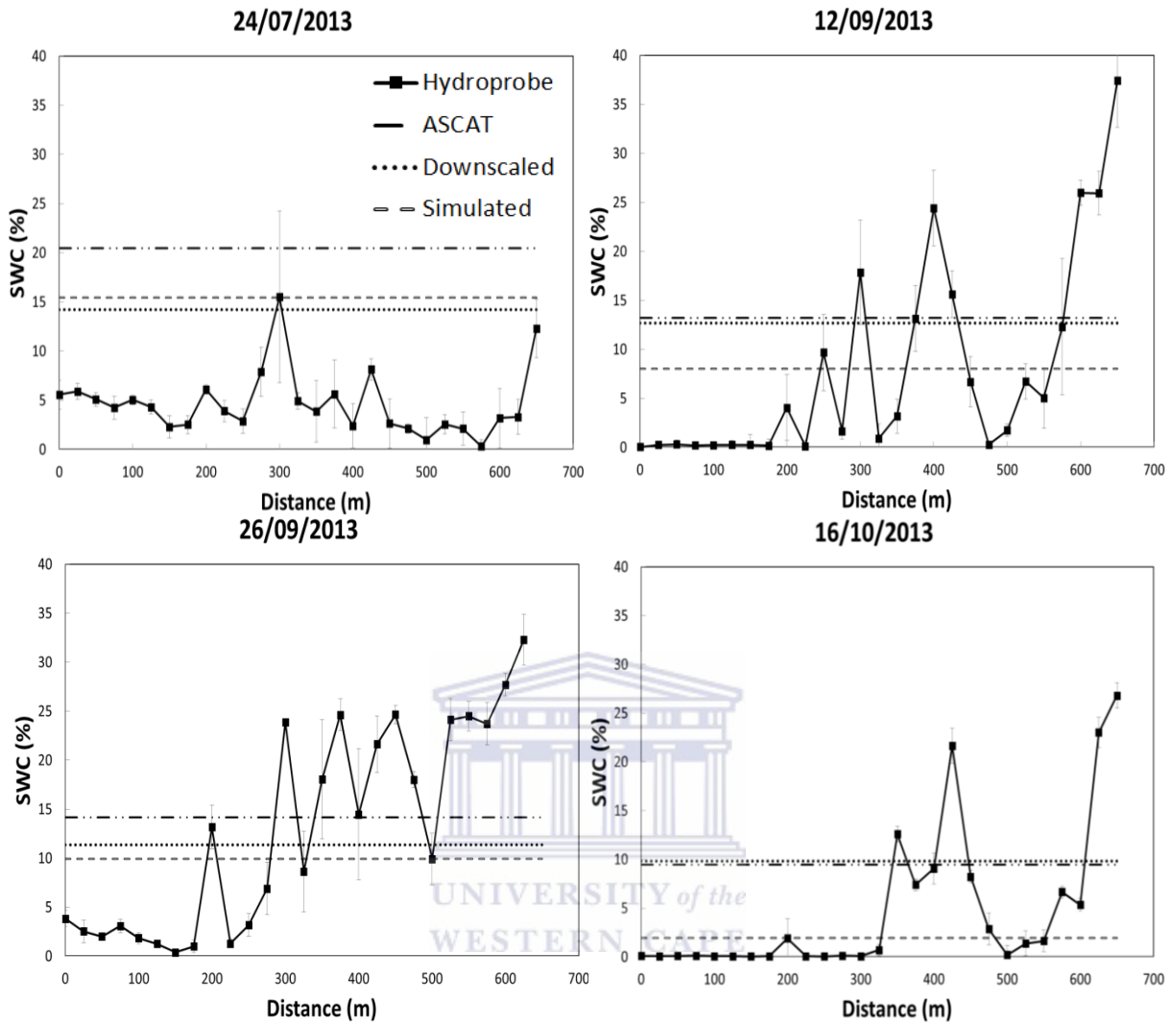


Figure 7.2: Hydroprobe (solid line and square), ASCAT 12.5km (dashed and dotted line), Downscaled 1km (dotted line) and Simulated (dashed line) soil moisture estimates at Transect B from 24 July 2013 to 16 October 2013 with soil water content (SWC) given in percentage.

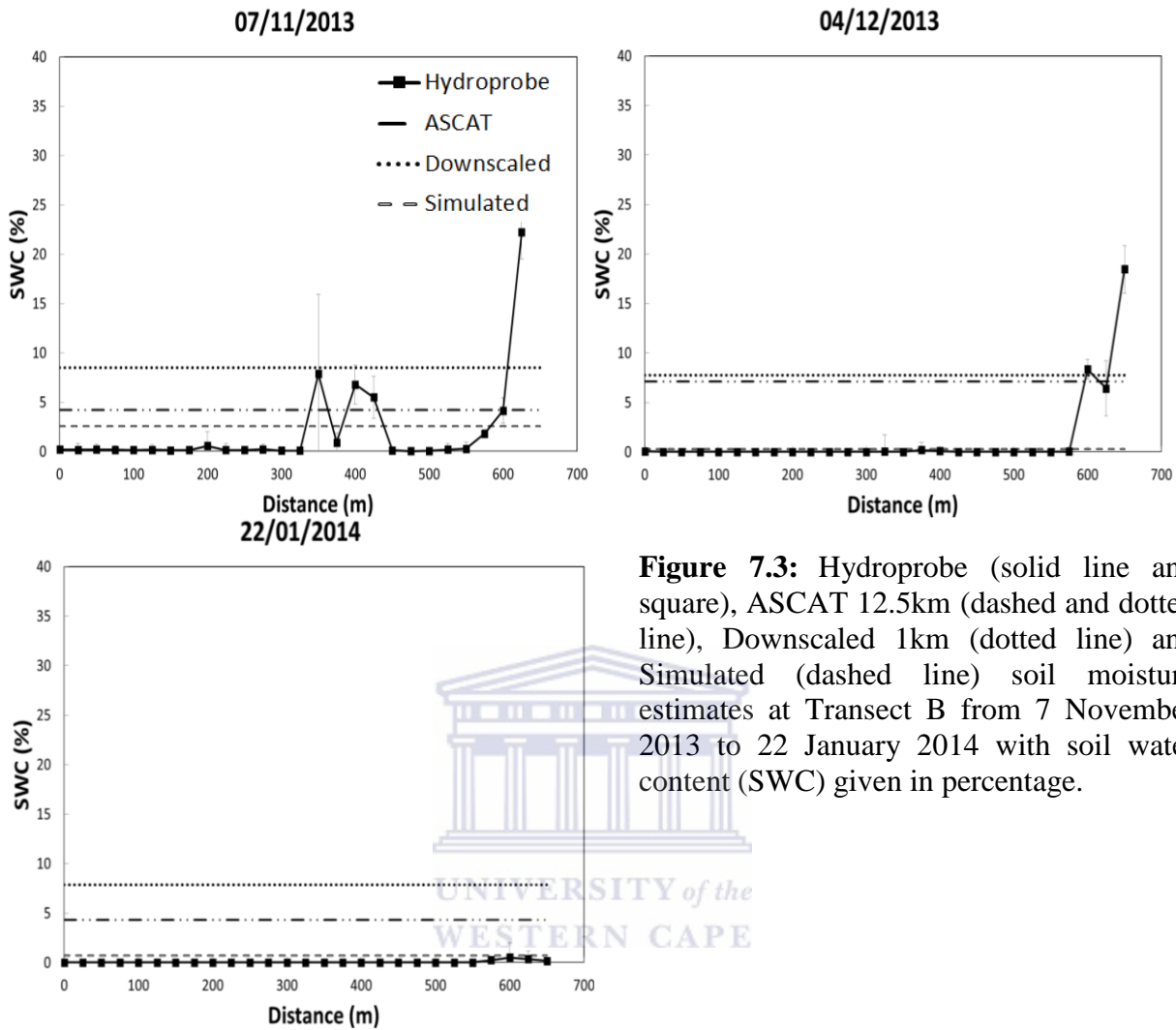


Figure 7.3: Hydroprobe (solid line and square), ASCAT 12.5km (dashed and dotted line), Downscaled 1km (dotted line) and Simulated (dashed line) soil moisture estimates at Transect B from 7 November 2013 to 22 January 2014 with soil water content (SWC) given in percentage.

ASCAT, downscaling and simulation soil moisture estimation underestimated Hydroprobe soil moisture on all days from 7 July 2013 to 26 September 2013 for Transect C (Figure 7.4). It is also noted that Hydroprobe soil moisture measurements were extremely high during the wet period for Transect C. These conditions are completely the opposite during the dry period (Figure 7.5), when Hydroprobe soil moisture values were very low and soil moisture values derived ASCAT, downscaling and simulation all overestimated Hydroprobe soil moisture. ASCAT downscaled and simulation results plot closely together throughout the study for Transect C and are closer to Hydroprobe measurements during the dry period as opposed to the wet and drying periods. ASCAT, downscaled and simulation soil moisture all poorly estimated soil moisture at this transect while water was ponded between contours.

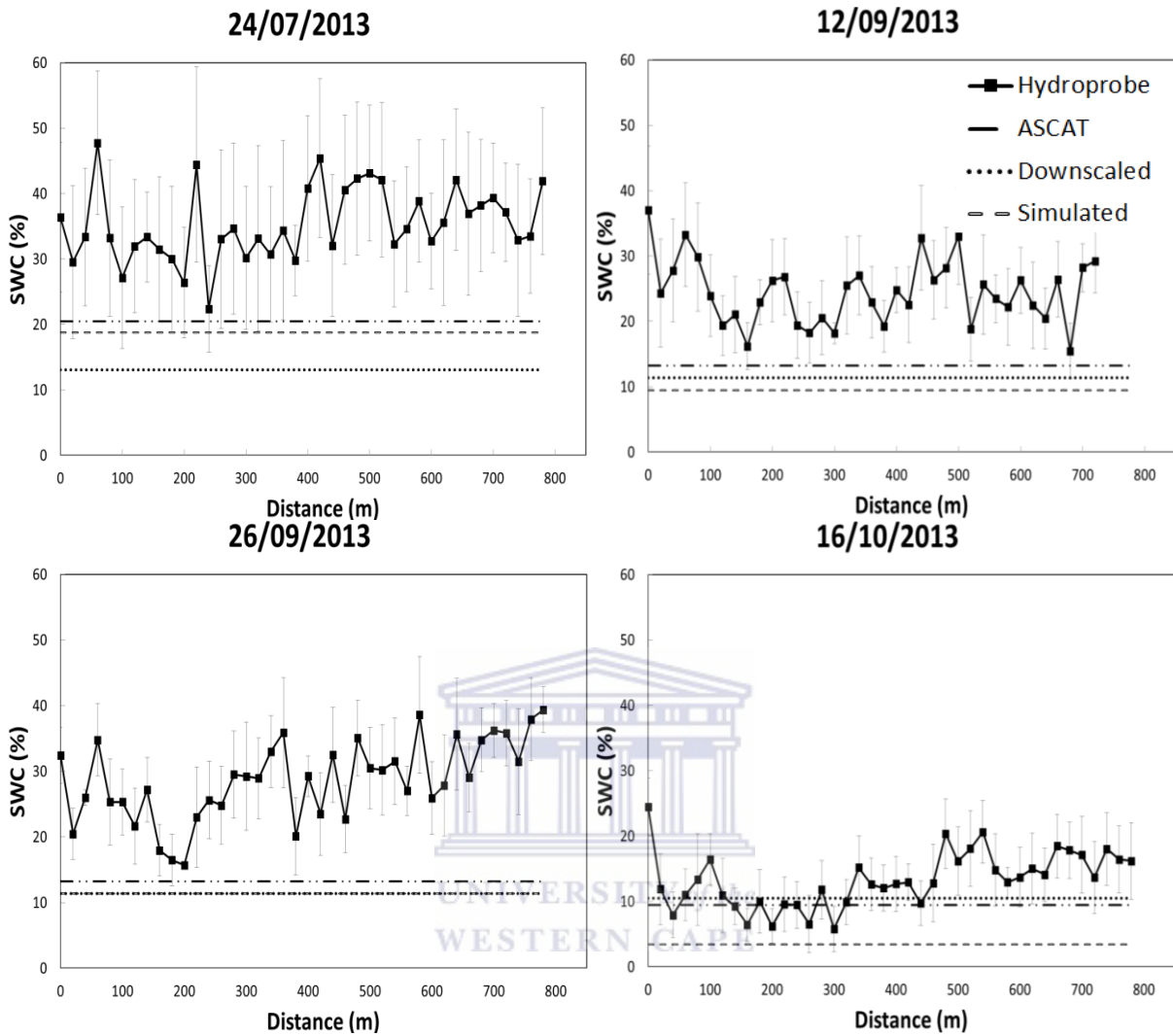


Figure 7.4: Hydroprobe (solid line and square), ASCAT 12.5km (dashed and dotted line), Downscaled 1km (dotted line) and Simulated (dashed line) soil moisture estimates at Transect C from 24 July 2013 to 16 October 2013 with soil water content (SWC) given in percentage.

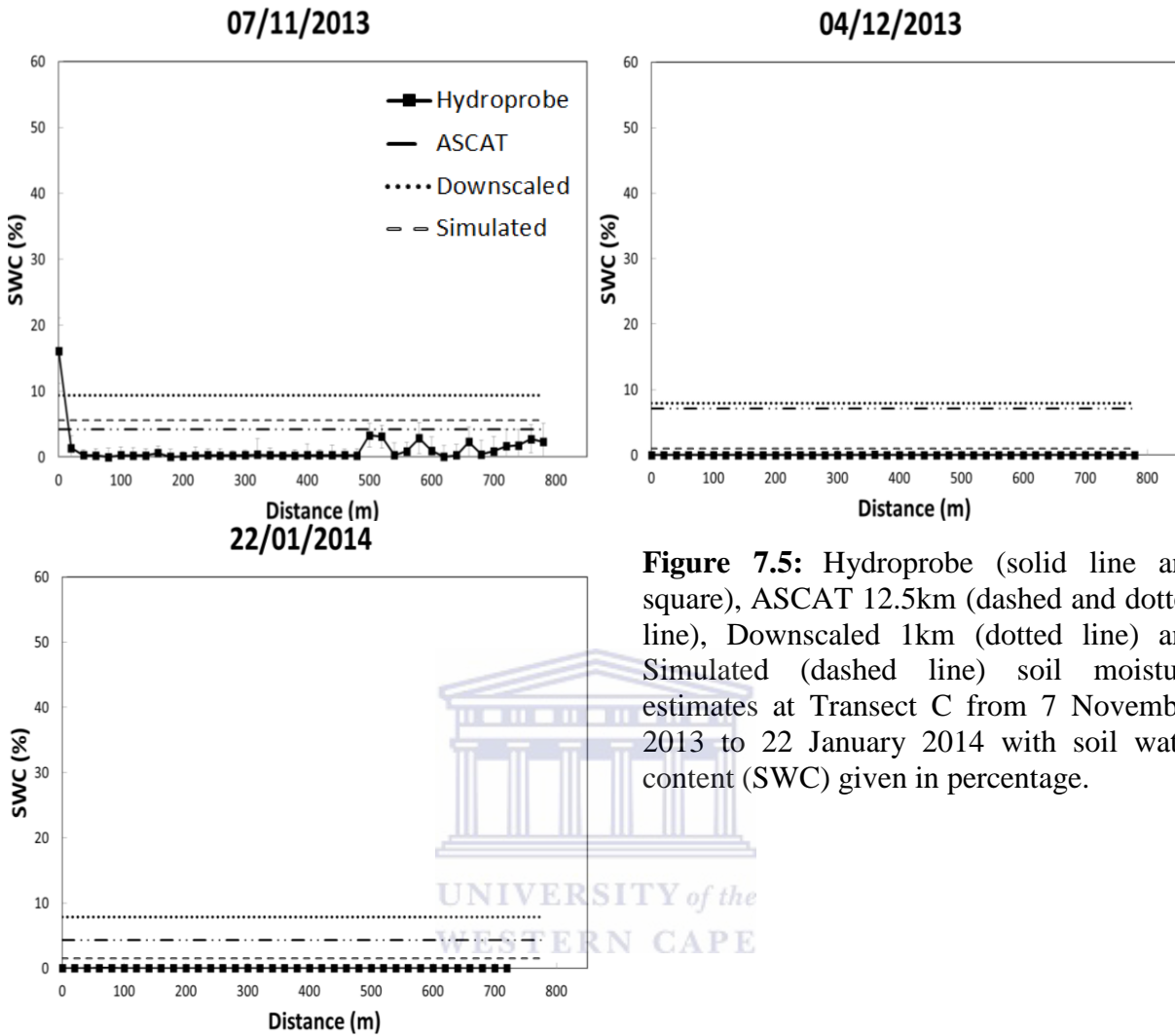


Figure 7.5: Hydroprobe (solid line and square), ASCAT 12.5km (dashed and dotted line), Downscaled 1km (dotted line) and Simulated (dashed line) soil moisture estimates at Transect C from 7 November 2013 to 22 January 2014 with soil water content (SWC) given in percentage.

Soil moisture estimates derived from ASCAT, downscaling and simulation, capture the seasonal trend and closely match Hydroprobe average estimates on most days well at transect D (Figure 7.6 and 7.7). Simulated values however, overestimate soil moisture during the wet period (Figure 7.6), while downscaled soil moisture best represents soil moisture during the same period. During the drier period (Figure 7.7), ASCAT, downscaled and simulated soil moisture estimates are in good agreement with Hydroprobe soil moisture measurements on 16 October and 6 November 2013 (drying period), but all three methods underestimate Hydroprobe soil moisture measurements on 4 December 2013 and more so on the 22 January 2014 (dry period). There is good agreement between ASCAT, downscaled, and simulated soil moisture and Hydroprobe soil moisture during wetter periods when there is grass cover at this transect, but the three methods underestimated soil moisture when the grass cover dried out at Transect D.

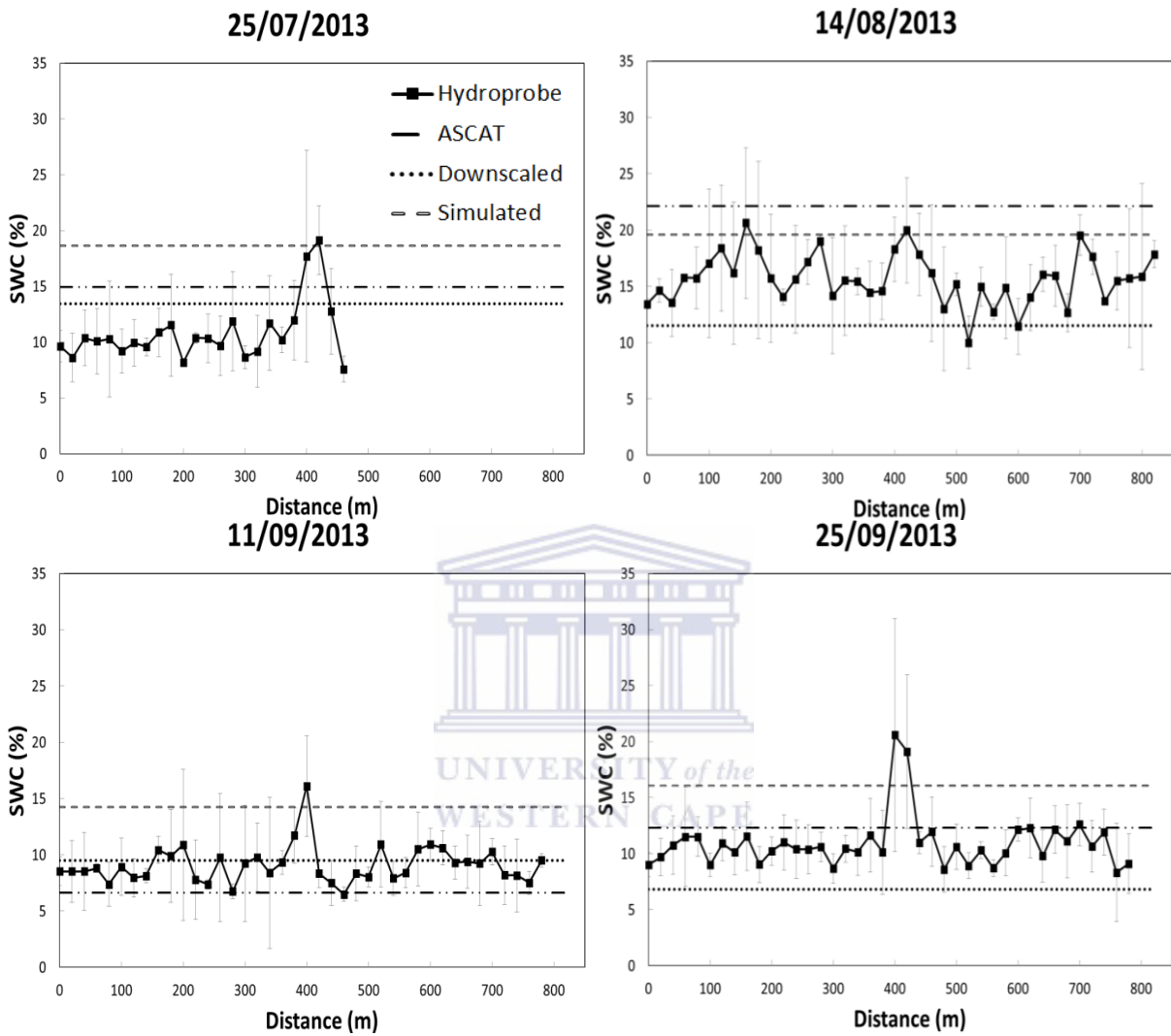


Figure 7.6: Hydroprobe (solid line and square), ASCAT 12.5km (dashed and dotted line), Downscaled 1km (dotted line) and Simulated (dashed line) soil moisture estimates at Transect D from 25 July 2013 to 25 September 2013 with soil water content (SWC) given in percentage.

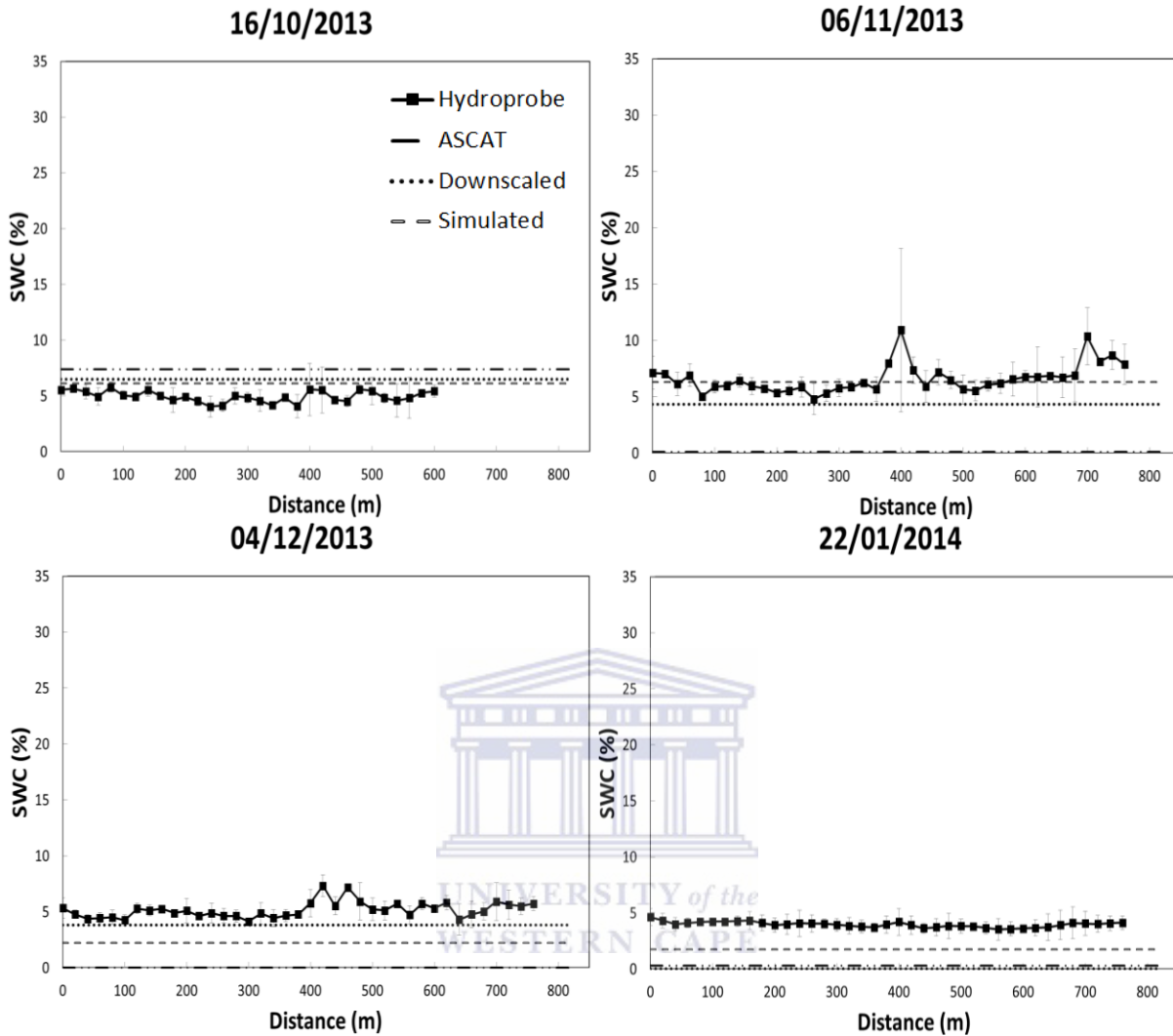


Figure 7.7: Hydroprobe (solid line and square), ASCAT 12.5km (dashed and dotted line), Downscaled 1km (dotted line) and Simulated (dashed line) soil moisture estimates at Transect D from 16 October 2013 to 22 January 2013 with soil water content (SWC) given in percentage.

For Transect E (Figure 7.8 and 7.9), seasonal soil moisture patterns are poorly represented by remote sensing derived and simulated soil moisture during the wet period (Figure 7.8), with ASCAT soil moisture, generally showing the highest overestimation (except for 11 September 2013- where it best represents Hydroprobe soil moisture conditions as compared to the downscaled and simulated soil moisture). During the dry period (Figure 7.9), simulated and downscaled soil moisture estimates closely mirror in situ soil moisture measurements while ASCAT soil moisture estimates underestimate Hydroprobe soil moisture on 11 September 2013, 4 December 2013 and 22 January 2014. ASCAT, downscaled and simulated soil moisture

estimates perform poorly during the wet period period when grape vines are dormant and vegetation density is low, as compared to Hydrorpobe soil moisture values. Downscaled and simulated soil moisture however perform better in the drier period where there is more prominent vegetation cover and grape vines are growing.

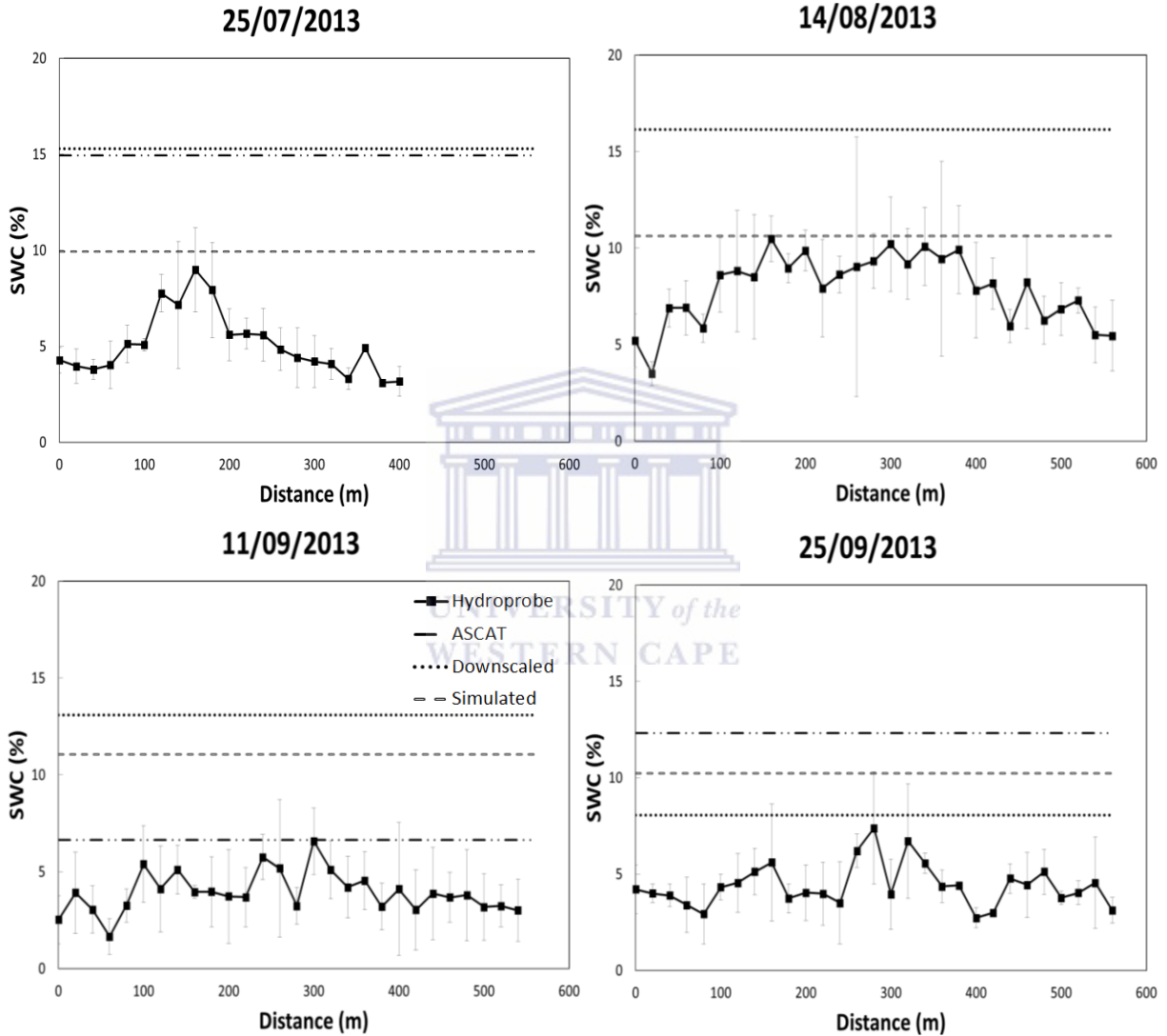


Figure 7.8 Hydroprobe (solid line and square), ASCAT 12.5km (dashed and dotted line), Downscaled 1km (dotted line) and Simulated (dashed line) soil moisture estimates at Transect E from 25 July 2013 to 25 September 2013 with soil water content (SWC) given in percentage.

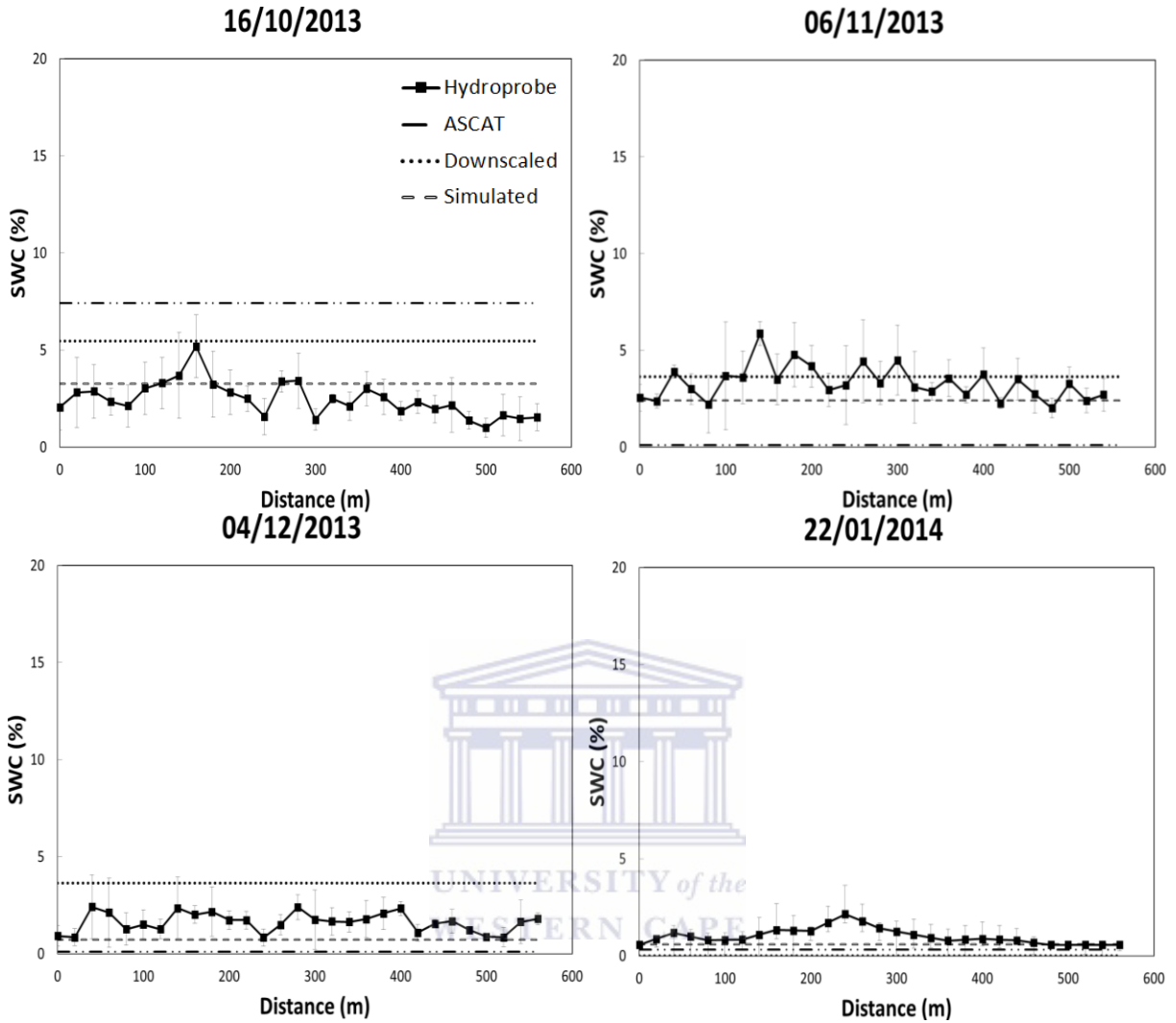


Figure 7.9 Hydroprobe (solid line and square), ASCAT 12.5km (dashed and dotted line), Downscaled 1km (dotted line) and Simulated (dashed line) soil moisture estimates at Transect E from 16 October 2013 to 22 January 2013 with soil water content (SWC) given in percentage.

For transect F, simulated and remote sensing derived soil moisture captures the seasonal trend of Hydroprobe soil moisture reasonably well (Figure 7.10 and 7.11). Downscaled soil moisture underestimated Hydroprobe soil moisture values during the wet period (14 August 2013, and 11 and 25 September 2013), while simulated results overestimated Hydroprobe soil moisture on these days. ASCAT, downscaled and simulated soil moisture methods more accurately depicted soil moisture during the drier period (Figure 7.11). ASCAT and simulated soil moisture

compared well to Hydroprobe measurements in the natural vegetation conditions found at Transect F (which did not have appreciable changes in vegetation cover during the study).

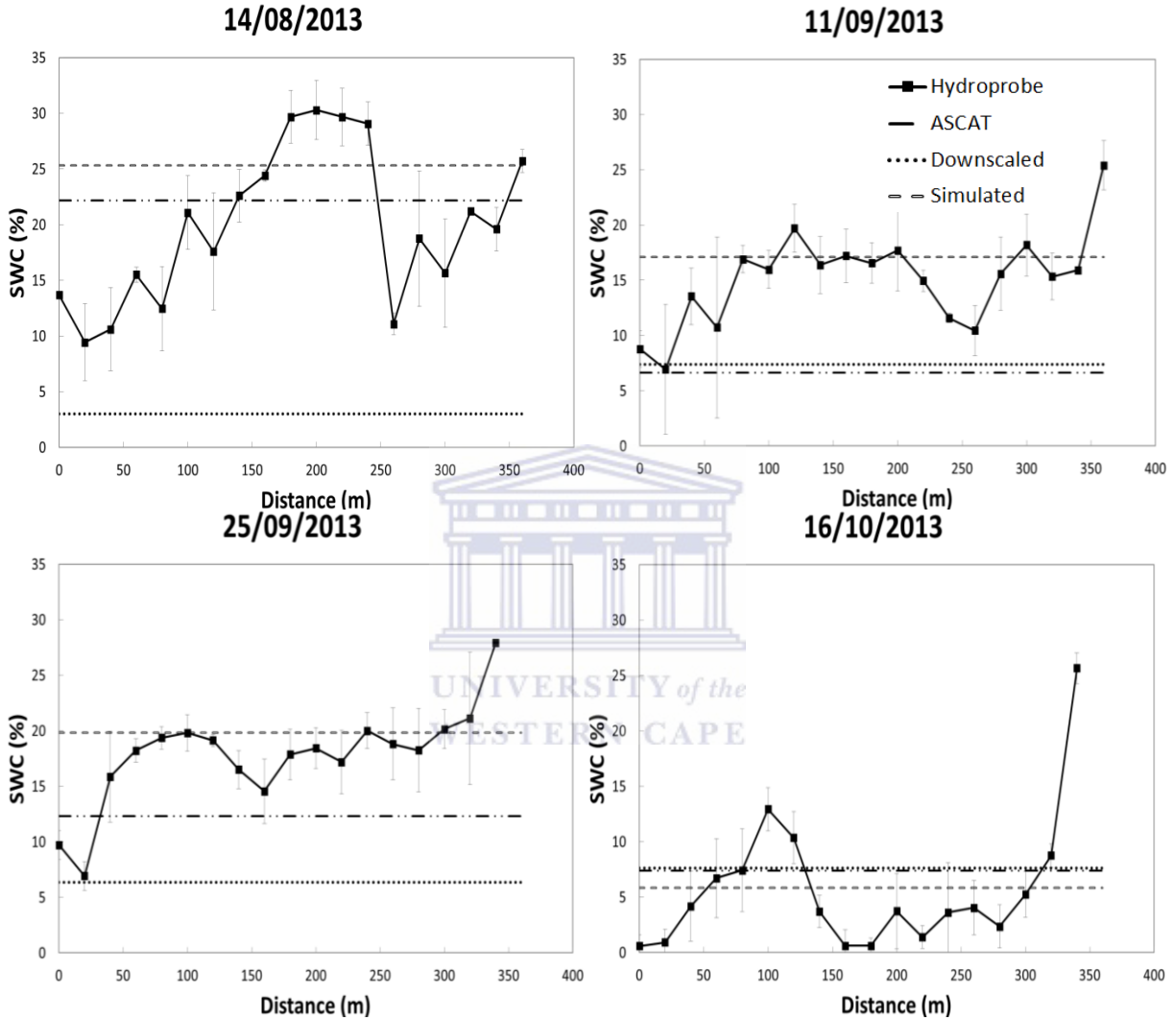


Figure 7.10: Hydroprobe (solid line and square), ASCAT 12.5km (dashed and dotted line), Downscaled 1km (dotted line) and Simulated (dashed line) soil moisture estimates at Transect F from 14 August 2013 to 16 October 2013 with soil water content (SWC) given in percentage.

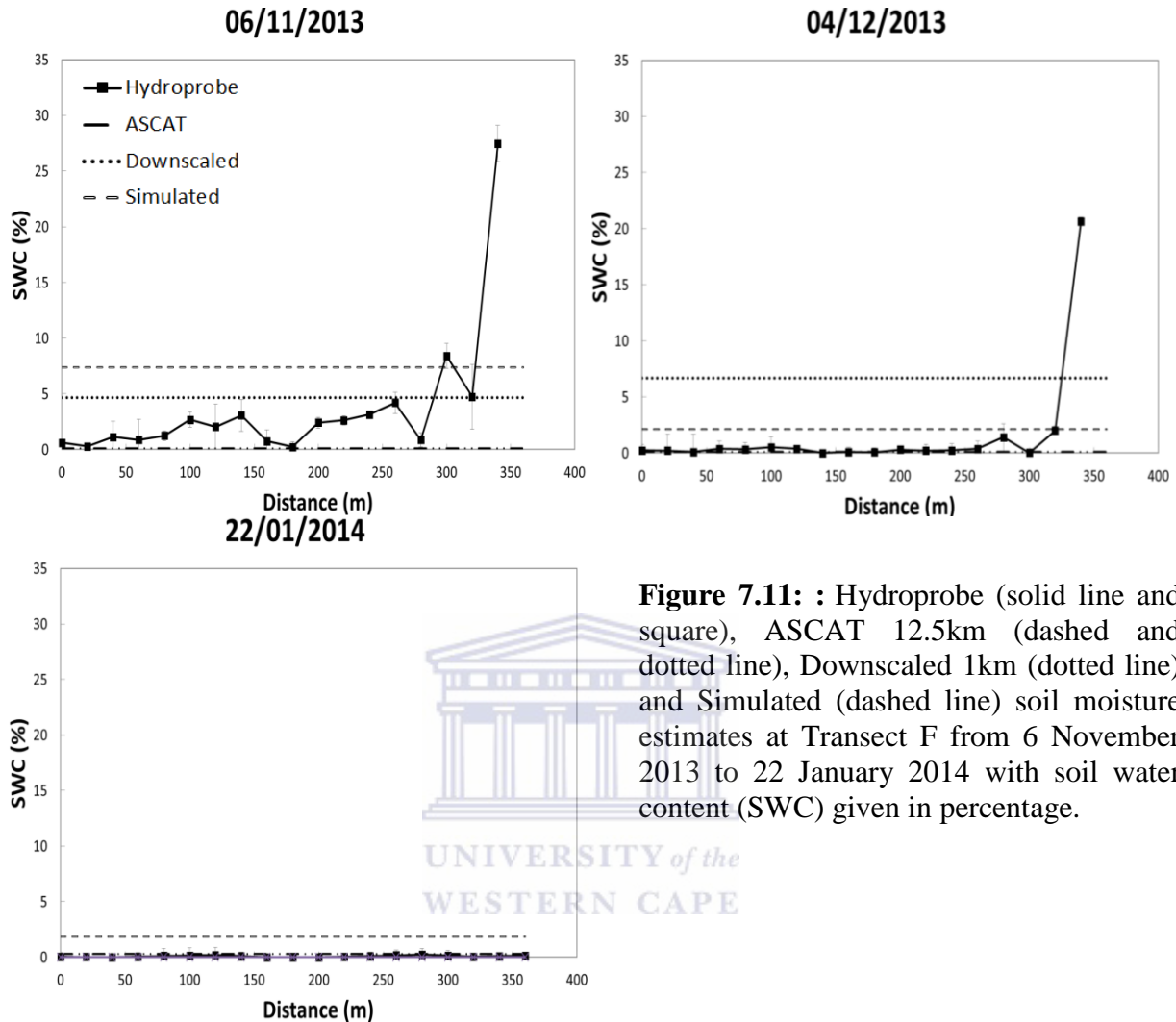
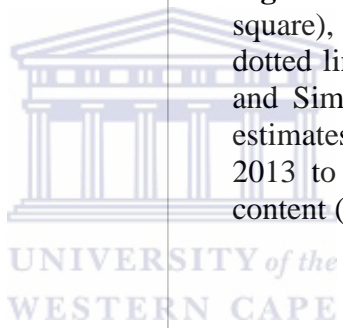


Figure 7.11: Hydroprobe (solid line and square), ASCAT 12.5km (dashed and dotted line), Downscaled 1km (dotted line) and Simulated (dashed line) soil moisture estimates at Transect F from 6 November 2013 to 22 January 2014 with soil water content (SWC) given in percentage.



7.3 Simulated and remotely sensed soil moisture

Simulated soil moisture was compared to coarse resolution remotely sensed soil moisture as well as fine resolution remotely sensed soil moisture. This was done by plotting the simulated and remotely sensed soil moisture values on line graphs for the period from 19 July 2013 to 22 January 24 (Figure 7.12 to 7.15). This analysis was undertaken in order to graphically compare the seasonal and daily variations of the methods selected for estimation of soil moisture.

Malmesbury: simulated and ASCAT soil moisture

At Transects A, B and C the ASCAT soil moisture estimates very closely compared to the simulated soil moisture (Figure 7.12). The biggest similarities were observed during the wet and drying period. The peak soil moisture values of ASCAT however, were consistently higher than those of the model, while the model also had consistently lower values than those of the remotely sensed soil moisture during the dry periods. The model at Transect B and C however did show similarly high soil moisture peaks, during wet and dry periods with the simulated soil moisture peaks at Transect B having lower values, as compared to ASCAT soil moisture estimates. The model at Transect A however did also have the fastest drying occurring between rainfall events, while Transect C being the slowest in this regard as a result of evapotranspiration rates in both cases. From the general trend, there is very little to separate the modelled values from the remote sensing derived values, but when examining the daily soil moisture variation, the ASCAT soil moisture has large variations for all transects, compared to simulated soil moisture.

Malmesbury: Simulated and downscaled soil moisture

When comparing the simulated soil moisture to the downscaled soil moisture, for all the three transects the downscaled soil moisture estimates were generally lower than simulated values during the wet period and higher during the dry period (Figure 7.13). There is generally good agreement for all three transects between modelled and downscaled soil moisture estimates. The downscaled values however better fit simulated values during the wet season for the three transects, while only fitting the peak values during the dry season. The largest disparity between the two soil moisture estimates is noticed for Transect B, where the downscaled values were appreciably higher than simulated estimates. There is less daily variation in downscaled soil moisture for all transects compared to ASCAT soil moisture, as the downscaled soil moisture values are less sensitive to rainfall events.

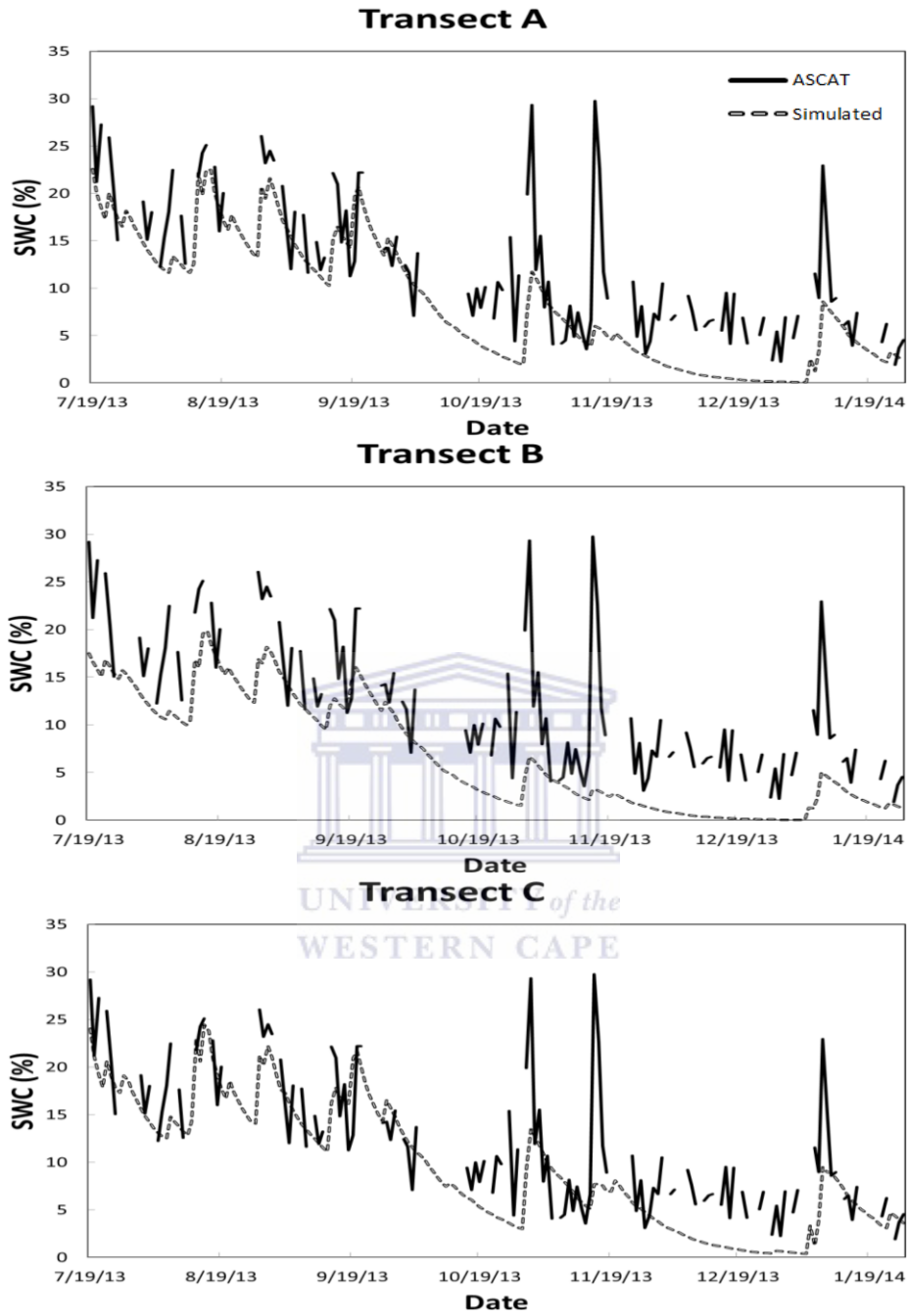


Figure 7.12: Soil water balance model simulated soil moisture estimates and ASCAT 12.5km soil moisture estimates for Transect A, B and C at the Malmesbury study site for the period 19 July 2013 to 22 January 2014 with soil water content (SWC) given in percentage.

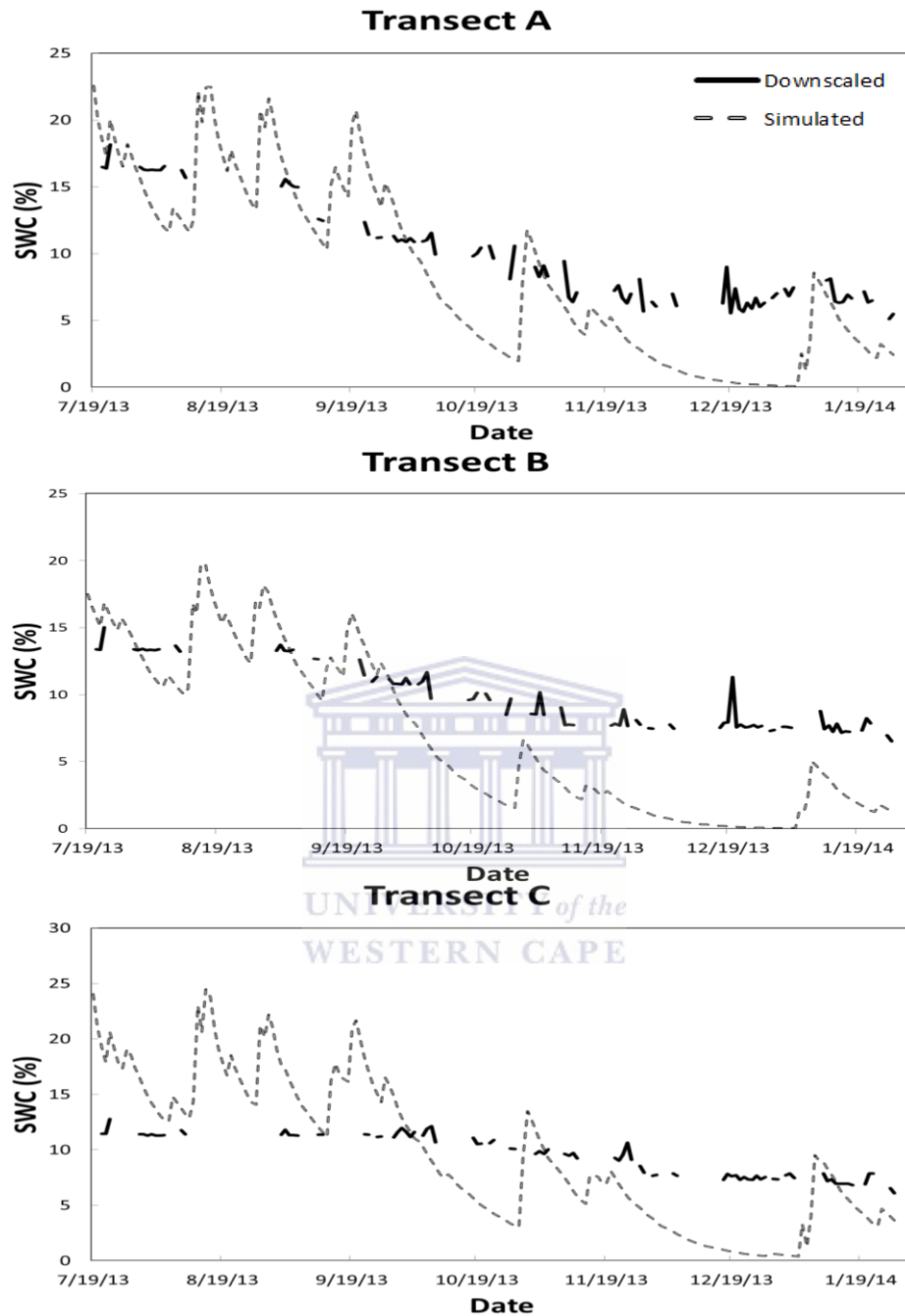


Figure 7.13: Soil water balance model simulated soil moisture estimates and downscaled 1km soil moisture estimates for Transect A, B and C at the Malmesbury study site for the period 19 July 2013 to 22 January 2014 with soil water content (SWC) given in percentage.

Riebeek: Simulated and ASCAT soil moisture

The simulated and ASCAT soil moisture estimates have similar seasonal variation for Transect D, E and F (Figure 7.14). During the wet period, the average values compare very well between the two estimates for transect D. For Transect E during the wet period, simulated values compare better to ASCAT soil moisture peaks than simulated soil moisture at Transect D and F during the wet period. For Transect F simulated values for the wet period compare well to the lower range of ASCAT soil moisture estimates. During the dry period there is good agreement between the two estimates for the three transects. The ASCAT soil moisture estimates, however do show more pronounced peak values during the drier period at for three transects, with Transect F simulation showing the least difference between drier period peak values and Transect E showing the biggest difference between peaks during this period. There is greater daily variation in ASCAT soil moisture values for all transects, compared to simulated values, which become more prominent during the dry period.

Riebeek: Simulated and downscaled soil moisture

For Transect D, the comparison between the simulated and downscaled soil moisture estimates is reasonable (Figure 7.15). The simulated soil moisture estimates are however higher than the downscaled estimates during the wet period but show very good agreement during the drier period. For Transect E there is very good agreement between simulated and downscaled soil moisture for the duration of the study with simulated soil moisture being about ~5% greater than the downscaled soil moisture during September 2013. Transect F shows poor agreement between modelled and downscale soil moisture estimates throughout the study period. The downscaled soil moisture estimates are considerably lower than simulated estimates during the wet period and higher during the dry period. There is low daily variation between ASCAT and downscaled soil moisture during the wet period, but similar variation during the dry period. The daily variations in downscaled soil moisture values during the dry period, is attributed to great variations in land surface temperature during this period.

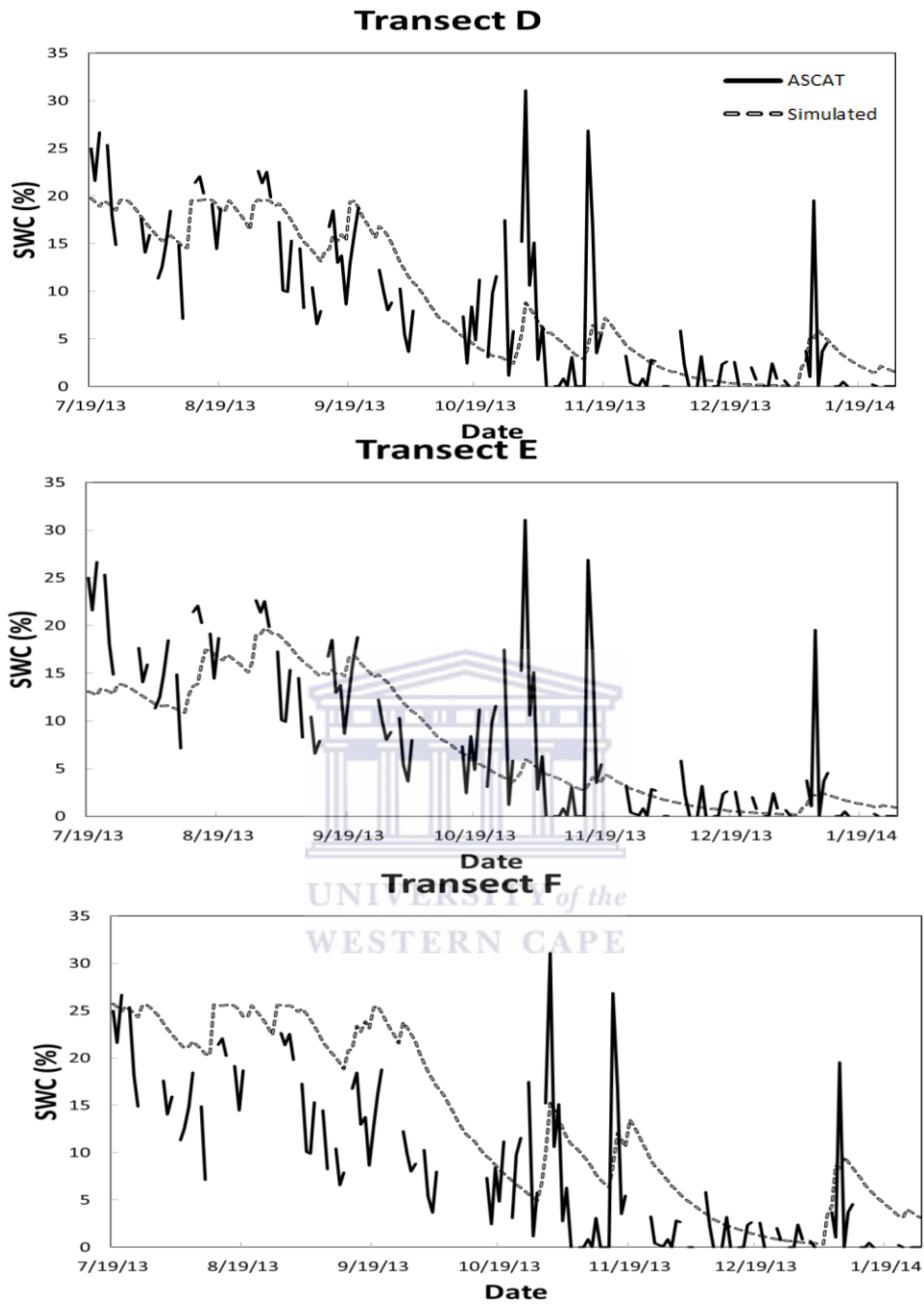


Figure 7.14: Soil water balance model simulated soil moisture estimates and ASCAT 12.km soil moisture estimates for Transect D, E and F at the Riebeek study site for the period 19 July 2013 to 22 January 2014 with soil water content (SWC) in percent.

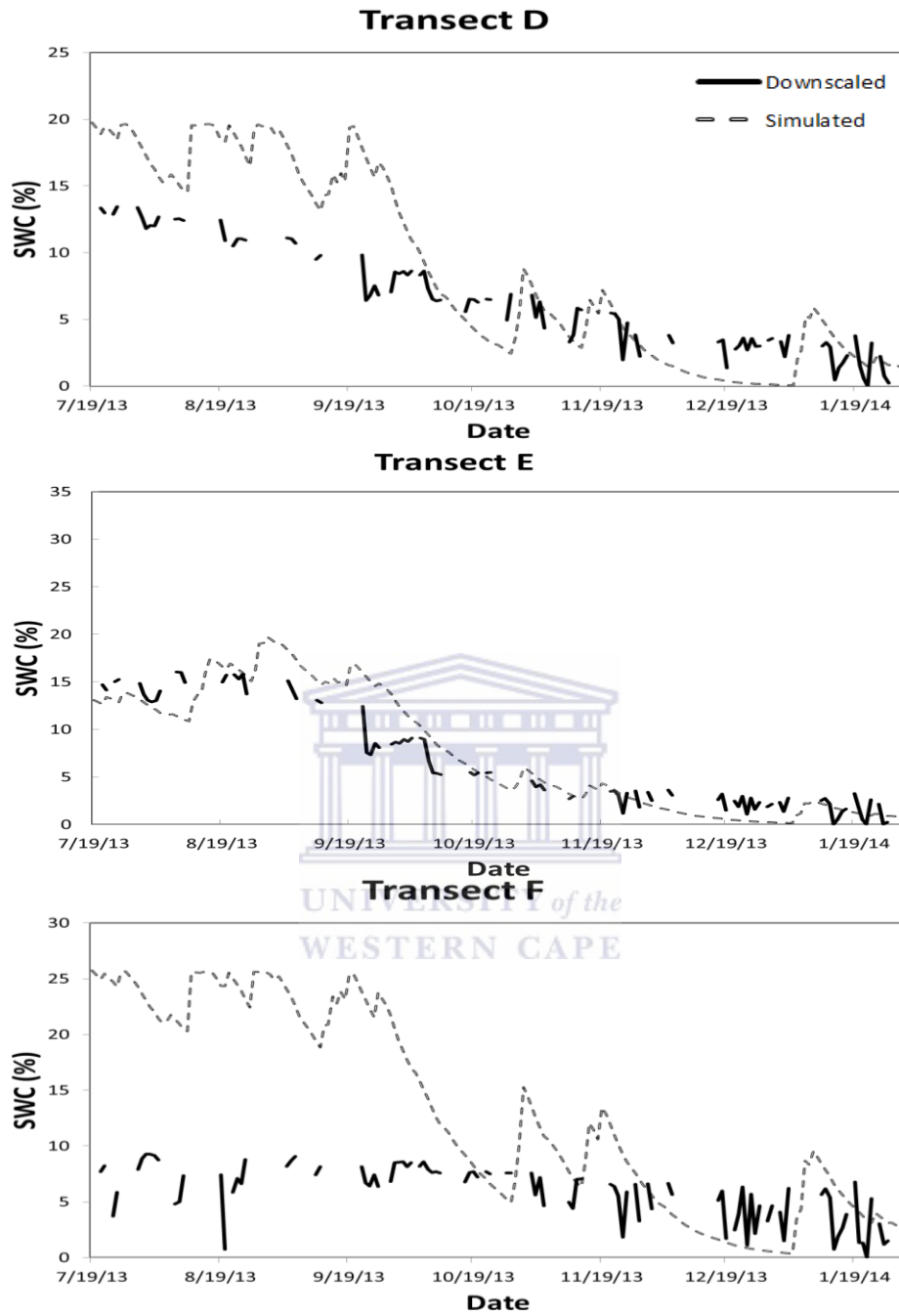
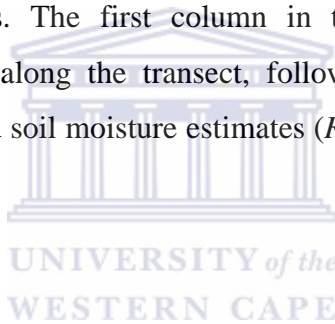


Figure 7.15: Soil water balance model simulated soil moisture estimates and downscaled 1km soil moisture estimates for Transect D, E and F at the Riebeeek study site for the period 19 July 2013 to 22 January 2014 with soil water content (SWC) given in percent.

7.4 Comparison of ASCAT, downscaled and simulated soil moisture to Hydroprobe measurement points

In situ soil moisture measurements at each point for all six transects were compared to coarse resolution satellite, downscaled and simulated soil moisture estimates for the entire study period. This was achieved by calculating the Pearson's correlation coefficient (r), which was used to determine the relationship between the changes in the in situ point measurements and the three methods of soil moisture estimation. From this analysis, the relationships were determined between ASCAT, downscaled and simulated soil moisture estimation and Hydroprobe soil moisture estimates for various points where measurements were taken along the transect. This is presented in the form of Table 7.1 to 7.6 with values in red indicating high correlation values, orange indicating moderately high values, yellow indicating moderate values and green indicating low correlation values. The first column in the tables represents the relevant Hydroprobe measurements point along the transect, followed by the ASCAT soil moisture estimates (*RS 12.5km*), downscaled soil moisture estimates (*RS 1km*) and simulated soil moisture estimates (*Sim*).



Transect A

For Transect A, there is low correlation between points located the middle area of the transect indicating a high degree of soil moisture spatial heterogeneity (Table 7.1), with higher r values between the last four points along this transect. The ASCAT soil moisture estimates showed the lowest r with Hydroprobe soil moisture. The downscaled soil moisture estimates had the highest r values. Even so, ASCAT, downscaling and simulation soil moisture estimation methods showed low correlation with Hydroprobe estimates at points 8, 10 and 14 in the transect, where higher soil moisture was measured on most sampling days. For the rest of the Hydroprobe sampling points, downscaled soil moisture r values were moderately high to high, simulated soil moisture r values were mostly moderate to high and ASCAT soil moisture r values were a mixture of low to high. The ASCAT, downscaling and simulation methods of soil moisture estimation have moderately high correlation when compared to one another. This indicates that there were low r values between ASCAT, downscaled and simulated soil moisture and

Hydroprobe soil moisture estimates at local elevation anomalies where water was ponded at the surface during the wet period.



Table 7.1: Pearson’s correlation matrix for Hydroprobe soil moisture sampling points (1-20) along the transect and ASCAT 12.5km (*RS 12.5km*), downscaled 1km (*RS 1km*) and simulated (*Sim*) soil moisture estimates for Transect A for all sampling days.

	1	2	3	4	5	6	7	8	9	10	11	12	13	14	15	16	17	18	19	20	<i>RS 12.5km</i>	<i>RS 1km</i>	<i>Sim</i>				
1	1.00																										
2	0.59	1.00																									
3	0.55	0.96	1.00																								
4	-0.69	-0.97	-0.88	1.00																							
5	0.90	0.25	0.28	-0.44	1.00																						
6	0.59	1.00	0.96	-0.98	0.26	1.00																					
7	0.72	0.89	0.94	-0.78	0.40	0.87	1.00																				
8	0.61	-0.11	-0.18	0.09	0.38	-0.14	0.14	1.00																			
9	0.59	0.99	0.99	-0.94	0.38	0.99	0.91	-0.19	1.00																		
10	0.62	0.08	0.06	-0.04	0.23	0.05	0.39	0.96	0.02	1.00																	
11	0.92	0.51	0.60	-0.45	0.67	0.48	0.83	0.76	0.59	0.90	1.00																
12	0.95	0.60	0.38	-0.74	0.91	0.60	0.39	0.40	0.50	0.36	0.52	1.00															
13	0.82	0.75	0.64	-0.88	0.86	0.76	0.61	0.01	0.74	0.01	0.59	0.92	1.00														
14	0.18	-0.19	-0.09	0.30	-0.23	-0.22	0.26	0.81	-0.19	0.88	0.71	-0.12	-0.44	1.00													
15	0.99	0.71	0.64	-0.77	0.87	0.70	0.78	0.54	0.68	0.59	0.92	0.93	0.85	0.17	1.00												
16	0.97	0.70	0.57	-0.75	0.64	0.69	0.71	0.59	0.63	0.66	0.86	0.88	0.74	0.28	0.99	1.00											
17	0.94	0.83	0.71	-0.93	0.87	0.84	0.77	0.17	0.78	0.22	0.80	0.94	0.95	-0.22	0.96	0.88	1.00										
18	0.66	0.90	0.91	-0.83	0.14	0.89	0.99	0.24	0.89	0.46	0.81	0.54	0.54	0.25	0.76	0.81	0.72	1.00									
19	0.65	0.98	0.98	-0.93	0.44	0.98	0.91	-0.27	0.99	-0.06	0.63	0.46	0.76	-0.25	0.72	0.57	0.81	0.86	1.00								
20	0.68	0.98	0.93	-0.98	0.54	0.99	0.85	-0.24	0.97	-0.08	0.59	0.61	0.86	-0.36	0.75	0.63	0.87	0.81	0.98	1.00							
<i>RS 12.5km</i>	0.56	0.76	0.90	-0.61	0.18	0.742	0.97	0.12	0.84	0.40	0.76	0.16	0.40	0.38	0.63	0.54	0.59	0.92	0.83	0.73	1.00						
<i>RS 1km</i>	0.96	0.89	0.77	-0.91	0.79	0.881	0.87	0.32	0.80	0.45	0.91	0.84	0.85	0.08	0.98	0.95	0.97	0.91	0.83	0.84	0.74	1.00					
<i>Sim</i>	0.60	0.99	0.94	-0.99	0.46	0.996	0.84	-0.19	0.98	-0.02	0.53	0.62	0.83	-0.31	0.69	0.67	0.81	0.84	0.97	0.99	0.73	0.79	1				

Transect B

For Transect B, the upper part of the transect had r values between Hydroprobe measurement points while showing low correlation between points in the upper part of the transect compared to points in the lower part of the transect (Table 7.2). There is also high r between sampling points in the lower part of the transect. The soil moisture changes are homogenous in the upper and lower extents of the transect but heterogeneous when compared to each other. ASCAT, downscaling and simulation methods of soil moisture estimation correlated poorly to points in the lower extent of the transect, but correlated well with points in the upper extent of the transect. ASCAT and simulated soil moisture estimates have high r values with the upper extent of the transect, while downscaled soil moisture estimates have moderately high correlation values in the same area. ASCAT, downscaling and simulation methods of soil moisture estimation have high r values when compared to each other. It is evident that variation in ASCAT, downscaled and simulated soil moisture compared better with variations at Hydroprobe soil moisture measurement points for the upper section of the transect. This section had a steeper slope gradient and did not have ponding of surface water, compared to the lower section, which was flatter and did have some water ponding at the surface during the wet period. The lower section of the transect also had more dense grass cover throughout the study period.

Transect C

For Transect C, all Hydroprobe measurement points along the transect had high r values between points along the transect and ASCAT, downscaled and simulated soil moisture estimation, with the exception of three sampling points (1, 6 and 28), which had moderately high r values compared to simulated results (Table 7.3). All three methods of soil moisture estimation correlated highly with each other. This transect was relatively flat, and had very little vegetal variation along it, which indicated that there was very little variation in the amount of soil moisture change experienced throughout the sampling period at the various sampling points. The change in ASCAT, downscaled and simulated soil moisture values was also thus uniform when compared to Hydroprobe soil moisture variations along the transect.



Transect D

Transect D, had high r values between most Hydroprobe soil moisture measurement points with the exception of a few points in the middle of the transect, which experienced high soil moisture during wet and drying periods (Table 7.4). At these points, r values were mostly moderately high. ASCAT and simulated soil moisture estimates correlated highly with Hydroprobe measurements at most sampling points in the transect, while downscaled soil moisture estimates had moderately high r values with most sampling points. ASCAT, downscaling and simulation methods of soil moisture estimation had high r values compared to each other. The grass cover at Transect D experienced uniform drying during the study which was reflected in the uniform seasonal soil moisture variation for most of the transect. This was reflected in the seasonal changes in soil moisture estimates obtained from ASCAT, downscaling and simulation, which also had uniform decreases.



Transect E

For Transect E, there is high r between Hydroprobe soil moisture sampling points throughout most of the transect with each other, with the exception of point 2 which has moderate to moderately high r with the rest of the transect (Table 7.5). ASCAT and downscaled soil moisture had high r values with most sampling points in the transect, while simulated soil moisture values had moderately high r values with most Hydroprobe sampling points. ASCAT, downscaling and simulation methods of soil moisture estimation have high correlation values with each other. Even though there were changes in slope gradient along the transect, the seasonal changes at soil moisture sampling points remained uniform for most of the transect. This would suggest that slope had a little influence on seasonal soil moisture variation.



Transect F

All Hydroprobe soil moisture measurement points for Fransect F had high r values between each other, with the exception of point 18, which was poorly correlated to sampling points for the rest of the transect (Table 7.6). ASCAT and simulated soil moisture estimated values had high r with Hydroprobe sampling points 1 and 2 as well as points 8-13 and point 19 along the transect, with moderate to moderately high r with points 3-7 and low to high correlation with points 14-18 along the transect (Table 7.6). This is evidence of a high degree of spatial soil moisture heterogeneity at transect F which is persistent throughout the study period. Downscaled soil moisture is poorly correlated to Hydroprobe soil moisture sampling points for most of transect F. Downscaled soil moisture is also poorly correlated to ASCAT and simulated soil moisture, which are highly correlated with one another. Transect F had homogeneous natural vegetation cover throughout the study period, which indicates that vegetation did not affected seasonal soil moisture variation and soil moisture distribution at this transect.

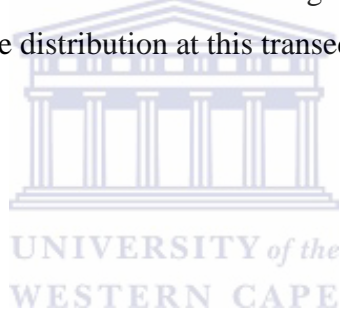


Table 7.6: Pearson's correlation matrix for Hydroprobe soil moisture sampling points (1-19) along the transect and ASCAT 12.5km (*RS 12.5km*), downscaled 1km (*RS 1km*) and simulated (*Sim*) soil moisture estimates for Transect F for all sampling days.

	1	2	3	4	5	6	7	8	9	10	11	12	13	14	15	16	17	18	19	RS 12.5km	RS 1km	Sim	
1	1																						
2	0.99	1																					
3	0.90	0.91	1																				
4	0.90	0.92	0.95	1																			
5	0.88	0.88	0.99	0.94	1																		
6	0.90	0.92	0.91	0.96	0.91	1																	
7	0.91	0.93	0.97	0.94	0.98	0.96	1																
8	1.00	1.00	0.89	0.91	0.86	0.91	0.91	1															
9	0.99	0.97	0.86	0.82	0.84	0.86	0.89	0.98	1														
10	0.95	0.91	0.71	0.75	0.69	0.81	0.77	0.93	0.97	1													
11	0.98	0.95	0.82	0.80	0.80	0.86	0.87	0.96	0.99	0.99	1												
12	0.98	0.95	0.76	0.82	0.72	0.85	0.79	0.97	0.98	0.98	0.99	1											
13	0.96	0.91	0.80	0.83	0.78	0.85	0.83	0.93	0.95	0.96	0.98	0.98	1										
14	0.83	0.86	0.95	0.96	0.93	0.84	0.87	0.84	0.73	0.62	0.68	0.71	0.72	1									
15	0.98	0.99	0.96	0.95	0.95	0.93	0.95	0.98	0.96	0.89	0.93	0.92	0.92	0.90	1								
16	0.90	0.92	0.96	0.90	0.93	0.81	0.90	0.90	0.85	0.76	0.78	0.80	0.76	0.94	0.95	1							
17	0.96	0.97	0.95	0.98	0.94	0.97	0.96	0.96	0.92	0.86	0.92	0.90	0.93	0.92	0.97	0.91	1						
18	-0.12	-0.11	0.09	0.22	0.06	0.01	-0.07	-0.13	-0.29	-0.33	-0.28	-0.19	-0.08	0.36	-0.05	0.05	0.07	1					
19	0.96	0.89	0.97	0.97	0.97	0.90	1.00	0.83	0.94	-0.12	0.88	0.31	0.82	1.00	0.99	0.97	0.98	0.97	0.97	1			
RS 12.5km	0.88	0.81	0.60	0.62	0.57	0.71	0.67	0.84	0.90	0.95	0.94	0.95	0.94	0.46	0.78	0.56	0.77	-0.32	0.64	0.64	1		
RS 1km	0.32	-0.05	0.55	0.04	0.57	-0.13	0.52	-0.08	0.30	-0.25	0.29	-0.25	0.25	0.28	0.40	0.34	0.49	0.22	0.83	0.01	0.01	1	
Sim	0.85	0.80	0.65	0.59	0.64	0.72	0.76	0.82	0.90	0.84	0.90	0.85	0.82	0.41	0.77	0.53	0.76	-0.51	0.85	0.89	0.11	0.11	1

7.5 Summary

When analysing the three methods of soil moisture estimation (ASCAT, downscaling and simulation) to that of the Hydroprobe estimates, the key observations were as follows:

- In Malmesbury, ASCAT and downscaled soil moisture estimates, generally underestimated Hydroprobe soil moisture estimates during the wet periods (July – early September 2013), but are in good agreement during the drying period (late September – November 2013), and underestimated them during the dry period (December 2013- January 2014). Simulated values are similar to Hydroprobe soil moisture, but capture variability better than remote sensing derived soil moisture estimates (coarse and fine resolution) during the dry period.
- Transects D and F at Riebeeck had a good agreement among the three methods during the wet and drying periods. Remote sensing and simulation methods overestimate in situ soil moisture values at Transect E during this period. Downscaled and simulated soil moisture estimates were in good agreement for all three transects during the dry period, but ASCAT soil moisture estimates underestimated Hydroprobe soil moisture at Transects D and E during the dry period while being in reasonable agreement with Hydroprobe soil moisture at Transect F during this time period.
- Downscaled values did not reproduce the peaks which were more prominent in ASCAT values, as attributed to ASCAT soil moisture sensitivity to rainfall. These differences were most evident during the dry period. Thus, the trend of downscale soil moisture estimates was smoother than those of ASCAT, but showed more variation than the simulated values.
- Seasonal trends of the ASCAT, downscaled and simulated soil moisture reproduced Hydroprobe seasonal soil moisture trends well.

From the comparison of remote sensing derived soil moisture (ASCAT and downscaled) to simulated soil moisture estimates the following observations were made:

- At Malmesbury, the ASCAT soil moisture estimates were in good agreement with simulated soil moisture during the wet and beginning of the drying period (July-

September 2013), after which ASCAT soil moisture estimates only compared well to peak simulation soil moisture values and were higher than simulation values otherwise.

- For the transects at Riebeek, the ASCAT soil moisture estimates compared poorly to simulated values during wet-drying periods (July- September 2013), but were in good agreements for the period thereafter (October 2013- January 2014). It was noted at both sites that peak soil coarse resolution remotely sensed soil moisture estimates were consistently higher than simulated ones which was most evident during drier periods.
- Downscaled soil moisture estimates were not in good agreement with simulated values throughout the study period for all three transects at the Mamesbury site. At all three transects, downscaled values were lower than simulated values during the wet to drying period and were higher than simulated values from the drying to dry period.
- At the Riebeek site however, Transects D and F had downscaled soil moisture estimates which were lower than simulated values during the wet to drying period (5-15% soil water content), while the two estimates coincided at Transect E during this period. All three transects had good agreement between downscaled and simulated soil moisture estimates during the drying to dry period of the study.

The correlation matrices showed that there was higher heterogeneity within the sampling transects for the Malmesbury site with only Transect C indicating uniform changes in soil moisture throughout the transect for the duration of the study period. Similarly, at transects A and B, the methods of soil moisture estimation showed marked differences in correlation with the temporal soil moisture stability at various in situ measurement points, correlating poorly in some areas and well within others at the individual transects, while again at Transect C, change in in situ soil moisture measurements at sampling points correlated well with the three methods of soil moisture estimation. Correlation between soil moisture temporal variations at different Hydroprobe sampling points were generally well correlated at the Riebeek study site, with good correlation being observed between in situ measurement temporal variation and temporal variation in the estimated soil moisture values.

It is noted that there was poor agreement between remotely sensed (ASCAT and downscaled) and Hydroprobe soil moisture estimates during the dry periods at locations with sandy and sandy loam soils (Malmesbury and Riebeek). Remotely sensed (ASCAT and downscaling) methods

performed better at the sandy loam sites (Riebeek) when compared to the Hydroprobe soil moisture estimates. Vegetation cover changes along transects did not greatly influence the accuracy of downscaled soil moisture estimates. It was noted that at Transect B which has sandy soil and a steeper slope gradient, slope affected the comparison of Hydroprobe estimates to ASCAT, downscaled and simulated soil moisture estimates. This was in contrast to findings at Transect E, which had sandy loam soils and a steep slope gradient. At this transect it was found that slope did not affect the distribution of Hydroprobe soil moisture, when compared to ASCAT, downscaled and simulated soil moisture.



8. Discussion and Conclusion

8.1 Introduction

In this section, the results obtained during the analyses conducted in Chapters 4, 5, 6 and 7 will be discussed. The accuracy of the various methods for estimating soil moisture will be discussed as well as factors which may have affected their accuracy. Firstly in situ soil moisture measurements will be discussed, followed by coarse resolution soil moisture results, downscaled soil moisture results and simulation soil moisture results. This is then followed by a summary of the performance of the various methods proposed for estimating soil moisture, with challenges which are common and unique.

8.2 In situ soil moisture measurements

Hydroprobe soil moisture estimates were used as the reference for the evaluation of various methods proposed for estimating soil moisture and thus their accuracy directly affects the accuracy of this assessment. The amount of data which the Hydroprobe measurements provides also allowed for a thorough assessment of the drying seasonal trend.

In situ soil moisture measurements made by the Hydrosense probe (Hydroprobe) were calibrated against soil moisture measurements made with the gravimetric method. This calibration used gravimetric soil moisture samples taken during the wet drying and dry periods to cover a wide range of soil moisture conditions. Most transects had reasonable r^2 relationships between gravimetric measurements and Hydroprobe measurements, but the RMSE values were generally high. These findings indicate that the Hydroprobe should ideally be calibrated for each soil type. The amount of days on which in situ soil moisture sampling occurred was very limited in this study because of the in situ sampling design which aimed at getting a good spatial representation of the soil moisture conditions at the selected sites and in transects. Due to this sampling design, the spatial component of soil moisture conditions was well represented, but compromises were made with regard to the frequency of sampling. Satellite data was not always available for the day of sampling, thus the nearest available day with satellite data was used. This factor also

affected the accuracy of remote sensing soil moisture estimation, especially during periods of bigger daily soil moisture variation.

Hydroprobe soil moisture estimation showed that sandy soils experienced higher soil moisture values than loamy soils during wet periods but also lower values during dry periods. Slope also had a bigger effect on soil moisture variation for Transects with sandy soils. The strongest topographic feature which affected soil moisture was the relative elevation, as soils found in valleys (Transects A, C and F) were consistently wetter than other transects, similar to finding by Famiglietti et al. (1998). Vegetation type is linked to land use in this study and it was also noted that land use affected soil water content, with natural land cover having high observed soil moisture content.

8.3 Microwave derived soil moisture estimates

While analysing the ASCAT soil moisture estimates, it was concluded that the microwave derived soil moisture estimates produced results of comparable accuracy at the two sites being investigated. Both sites had one transect at which the ASCAT estimates underestimated, one site which was overestimated and one site which had a good fit with Hydroprobe soil moisture estimates during the wet period. During the dry period, soil moisture was overestimated at two of the transects at Malmesbury, but underestimated at all three transects at Riebeek. The good comparison of averaged Hydroprobe measurements for all transects at each site, would suggest that ASCAT soil moisture estimates may be a good representation of the average soil moisture conditions occurring throughout the study period at both sites. The differences between ASCAT soil moisture estimates and Hydroprobe estimates which was observed at the Riebeek and Malmesbury study sites were partly as a result of the comparison of different depths of soil moisture measured by the soil moisture probe and estimated by ASCAT. (Brocca et al., 2010), similarly concluded that this difference in observed depth of soil moisture may well cause an underestimation of microwave soil moisture estimation accuracy. Seasonal vegetation effects on ASCAT soil moisture estimation accuracy is expected to be minimised by the change detection approach used for soil moisture estimation in combination with the multi-incidence angles used for backscatter registration (Bartalis et al., 2007, Gelsthorpe et al., 2000). However, because of

the overestimation of ASCAT soil moisture observed at 2 of the transects at Malmesbury, ASCAT soil moisture accuracy may be lower during the dry period, possibly as a result of increased topographic effects on backscatter sensitivity during this period. This increased error in soil moisture estimates may also be partly owing to the fact microwave penetration of the soil surface is lower in drier conditions (Chauhan et al., 2003).

From this it was concluded that the use of ASCAT soil moisture estimates are feasible in areas with sandy and loamy soils. The vegetation cover types of the two sites were mostly homogeneous and the differences in mean slope values between the two sites did not appreciably affect accuracy of soil estimate retrievals.

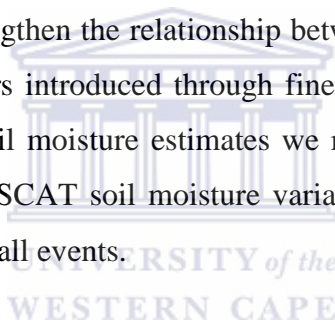
8.4 Downscaled soil moisture estimates

Downscaled soil moisture estimated remotely, using land surface temperature (LST), normalised difference vegetation index (NDVI) and microwave soil moisture (ASCAT) data performed reasonably well at 4 of the 6 transects (A, C, D and E). The downscaling method performed moderately to poorly only for Transects B, C, E and F during the wet season while only performing poorly for Transects B and C during the dry period. Chuan et al. (2003), suggests that there are two possible sources of error attributed to the brightness temperature linear regression model:

1. Regression error- errors based on the coarse resolution soil moisture estimates and transferred to downscaled estimates via the regression coefficients α_{ij}
2. Precision error- attributed to precision inaccuracies of LST and NDVI values

Regression error for these two study sites in terms of coarse resolution soil moisture inputs for calibration of α_{ij} is assumed to be within acceptable accuracy margins as these estimates were found to represent average moisture conditions reasonably well at both sites for the duration of the study. There were however some concerns during the dry period about the accuracy of the ASCAT product, but based on the method of calibration (least difference of two squares method), low values were likely to have small effects on the calibration of the regression coefficients.

Precision error of the LST and NDVI products (at 1km scale) used are assumed to have little effect, as the accuracy of these products are well validated and also scaled values were used to reduce possible errors in this regard. It is however noted that LST values were extremely high at both study areas during the summer period ($>50^{\circ}\text{C}$). The issue of precision error however does arise in the homogeneity or heterogeneity of land cover, as well as with local topography at the various transects and their immediate surrounding areas. The lower the vegetation cover and slope is, the higher the expected accuracy of the estimated LST and NDVI values at high resolution expected to be (Walker et al., 2003). This was evident in that downscaling of soil moisture at transects with low slope gradients with less vegetation cover performed the best during the study while downscaling transects that were more densely vegetated and/or had steeper slopes did more poorly. This factor is also affected by the heterogeneity of NDVI found in the immediate surroundings of pixels in which transects were located in. Chuan et al. (2003) proposes the use of albedo to strengthen the relationship between LST-NDVI and soil moisture, but this may not account for errors introduced through fine scale land surface heterogeneities. Daily variations in downscaled soil moisture estimates were reflective of LST variations, which were not as prominent as daily ASCAT soil moisture variation as they better represented soil moisture variations caused by rainfall events.



8.5 Soil water balance model

The soil water balance model performed reasonably well at the Riebeek site and moderately at the Malmesbury site as compared to Hydroprobe estimates. The Malmesbury site had higher RMSE values between the in situ soil moisture observation and simulated soil moisture as compared to the Riebeek site. Errors in the model performance may be attributed to the use of in situ rainfall and temperature measurements made at weather station WS1 and WS2. Rainfall and near surface air temperature may be highly variable in time and space. The weather station where these input data was collected for the Malmesbury site was 5km away from the site, while the Riebeek weather station was located within the site. This was evident in that Hydroprobe soil moisture peaks were observed during October 2013 at all transects in Malmesbury but not reflected in the relevant simulation results.

Even though the simulations at the Riebeek site compared better to Hydroprobe estimates, which did not compare as well to simulations at the Malmesbury site, it is believed that the assumption that lateral subsurface movement of water is negligible may be inaccurate, due to the low hydraulic conductivity experienced in the soil moisture mid-ranges (10-15%). Thus it is presumed, that owing to this slow infiltration rates and topography of the area, soil water is likely to move downslope, which may well explain the soil moisture values during the dry period at Riebeek being higher than those at Malmesbury. This difference in soil moisture between simulated and observed values at Riebeek experienced during the dry period may also be as a result of lower actual evapotranspiration. This may be attributed to a crusting of the top few cm of the soil column, which may then impede free movement of water vapour into the atmosphere from the subsurface via evaporation. This hardened top layer experienced at transects in Riebeek is attributed to the elevated levels of clay and silt particles in the soils as well as compaction due to tillage and herding practices. This hardening of the upper soil crust may then also significantly affect runoff rates at the relevant transects. The soils at Malmesbury are sandier and better drained, especially at transect A.

At the Malmesbury transects B and C, very high soil moisture values observed with the Hydroprobe measurements, may also be attributed to the presence of contours at the surface where surface runoff may be accumulated. This is a localised phenomenon and would be difficult to incorporate into the simple model structure. The rainfall interception rate is also likely to have varied along each transects depending on the density of vegetation cover. Such variations affect evaporation and transpiration rates. These effects are difficult to quantify and thus the model sought to aggregate these spatially and temporally by providing averaged estimates of the magnitude of relevant processes, namely rainfall interception, runoff evapotranspiration.

8.6 Summary

In this study, the estimation of soil moisture using downscaling of remote sensing data and hydrological modelling using routinely available meteorological data was investigated as alternatives to in situ measurements in the semi-arid regions of the Western Cape Province of South Africa. The following was concluded based on analysis of soil moisture in situ

observations and soil moisture estimations, based on the selected methods, for the time period of July 2013-January 2014.

Remotely sensed soil moisture estimates (ASCAT) with coarse spatial resolution provided soil moisture information with reasonable accuracy throughout the study period, based on the comparisons of Hydroprobe estimates with ASCAT estimates. This suggests that the use of ASCAT data is feasible and these estimates may be used for application at macro-scale hydrology ($>1000\text{km}^2$).

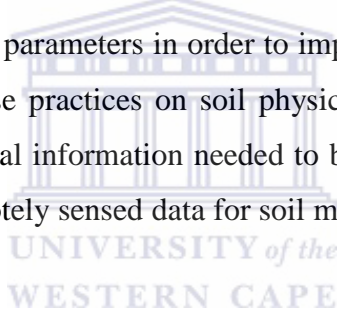
The downscaling of soil moisture estimates also provided reasonable results when examining generally seasonal soil moisture trends. At fine scales (1km^2), there were transects where the downscaling performed well and ones where it performed poorly. The main source of error using this method was identified as the fine scale surface heterogeneities. These heterogeneities were difficult to account for during in situ soil moisture measurement at certain transects and should be considered when employing this method. Soil water balance modelling provided acceptable seasonal variations in soil moisture but failed to capture fine temporal scale (1-2days) variations at the study sites.

Downscaled soil moisture estimates using the brightness temperature linear regression model and those obtained using a soil water balance model are thus feasible options for obtaining general trends in soil moisture (especially where regular in situ measurements are not feasible). Where high precision estimates are needed, such as application in precision agricultural irrigation, these may not be adequate. Downscaled soil moisture may be feasible, however, where there is uniform land surface cover at the fine scale, but not in areas with heterogeneous land surface cover.

The soil water balance model used may also not be feasible due to its inability to capture fine temporal and spatial variation in surface soil moisture. More accurate results can be obtained using a soil water balance model that more accurately describes the temporal variations in land surface conditions and with the input of more accurate rainfall data. The characterisation of accurate spatial rainfall estimates or measurements, however fell outside the scope of the study. High resolution satellite rainfall observations are available but may need to be evaluated before integrating them into a model within the area being investigated.

The use of ASCAT, downscaling and soil water balance modelling was found to be most accurate at Transects A and D, which indicates that these methods performed best in areas of natural vegetation where there was little to no agricultural impacts on the soil physical properties. They however did not work particularly well at Transects B, C, E and F during the wet periods especially where slope gradients were generally higher and the dominant land use was pasturelands with winter wheat crop rotations. The reasons for these performances may differ slightly, most important effects on soil moisture estimation, noted during this study on all three methods of soil moisture estimation, are those caused by land use on soil physical properties.

Due to the fact that many areas still have data availability constraints for in situ measurements downscaling of remotely sensed data may be a feasible approach in at meso- and large scales. Further research however needs to be conducted in order to improve understand spatial aggregation effects of land surface parameters in order to improve downscaling of soil moisture, and the spatial impacts of land use practices on soil physical properties. In situ soil moisture monitoring networks are still crucial information needed to better understand remote sensing of soil moisture, downscaling of remotely sensed data for soil moisture estimation and modelling of soil moisture at various scales.



9. References

- Africa, E. 2011. *Presentation to the Portfolio: Update on the management of recent disaster events*. Cape Town, South Africa: Portfolio Committee on Cooperative Governance and traditional Affairs.
- Albergal, C., Rüdiger, C., Carrer, D., Calvet, J.-C., Fritz, N., Naeimi, V., Bartalis, Z. & Hasenauer, S. 2009. *An Evaluation of ASCAT surface moisture products with in-situ observations in Southwestern France*. *Hydrology and Earth System Sciences*, 13, 115-124.
- Arnold, J. G., Srinivasan, R., Muttiah, R. S. & Williams, J. R. 1998. *Large area hydrologic modeling and assessment part 1: model development* *Journal of the American Water Resources Association*, 34, 73-89.
- Arrett, R. W. & Clark, C. A. *Functional relationship among soil moisture, vegetation cover and surface fluxes*. *Proceedings 21st Conference in Agricultural and Forest Meteorology, March 7-11 1994 San Diego, CA*. American Meteorological Society, J37-J38.
- Asner, G. P. 1998. *Biophysical and biochemical sources of variability in canopy reflectance*. *Remote Sensing of Environment*, 64, 134-153.
- Bartalis, Z., Wagner, W., Naeimi, V., Hasenauer, S., Scipal, K., Bonekamp, H., Figa, J. & Anderson, C. 2007. *Initial soil moisture retrievals from the METOP-A Advanced Scatterometer (ASCAT)*. *Geophysical Research Letters*, 34.
- Bastiaanssen, W. G. M. & Bos, M. G. 1999. *Irrigation performance indicators based on remotely sensed data: a review of literature*. *Irrigation and Drainage Systems*, 13, 291-311.
- Ben-Dor, E., Irons, J. R. & Epema, G. F. 1999. *Soil reflectance*. In: RENCZ, A. N. (ed.) *Remote sensing for earth science: Manual of remote sensing*. New York: Wiley and Sons.
- Bergström, S. 1991. *Principles and confidence in hydrological modelling*. *Nordic Hydrology*, 22, 123-136.
- Bevan, J. K. 2001. *Rainfall-Runoff Modelling- The Primer*, Chichester, John Wiley & Sons Ltd.
- Bevan, K. 1989. *Changing ideas in hydrology -The case of physically-based models*. *Journal of Hydrology*, 105, 157-172.
- Bindlish, R. & Barros, A. P. 2002. *Sub-pixel variability of remotely sensed soil moisture: an inter-comparison study of SAR and ESTAR*. *IEEE Transactions on Geoscience and Remote Sensing*, 40, 326-337.
- Bolten, J. D., Crow, W. T., Zhan, X., Jackson, T. J. & Reynolds, C. A. 2010. *Evaluating the utility of remotely sensed soil moisture retrievals for operational agricultural drought monitoring*. *IEEE Transactions on Geoscience and Remote Sensing*, 30, 57-66.
- Bosch, D. D., Lakshmi, V., Jackson, T. J., Choi, M. & Jacobs, J. M. 2006. *Large scale measurements of soil moisture for validation of remotely sensed data: Georgia soil moisture experiment of 2003*. *Journal of Hydrology*, 323, 120-137.
- Boucher, A. 2007. *Downscaling of satellite remote sensing data: Application to land cover mapping*. Doctor of Philosophy, Stanford University.
- Brocca, L., Hasenauer, S., Lacava, T., Melone, F., Moramarco, T., Wagner, W., Dorigo, W., Matgen, P., Martínez-Fernández, J., Llorens, P., Latron, J., Martin, C. & Bitelli, M. 2011. *Soil moisture estimation through ASCAT and AMSR-E sensors: An intercomparison and validation study across Europe*. *Remote Sensing of Environment*, 115, 3390-3408.

- Brocca, L., Melone, F., Moramarco, T. & Morbidelli, R. 2010. Spatial-temporal variability of soil moisture and its estimation across scales. *Water Resources Research*, 46, W02516.
- Brocca, L., Morbidelli, R., Melone, F. & Moramarco, T. 2007. Soil moisture spatial variability in experimental areas of Central Italy. *Journal of Hydrology*, 333, 356-373.
- Brocca, L., Tullo, T., Malone, F., Moramarco, T. & Morbidelli, R. 2012. Catchment scale soil moisture spatial-temporal variability. *Journal of Hydrology*, 422-423, 63-75.
- Brutsaert, W. 2005. *Hydrology: An Introduction*, New York, Cambridge University Press.
- Bugan, R. D. H., Jovanovic, N. Z. & De Clercq, W. P. 2012. The water balance of a seasonal stream in the semi-arid Western Cape (South Africa). *Water SA*, 38.
- Cantón, Y., Solé-Benet, A. & Domingo, F. 2004. Temporal and spatial patterns of soil moisture in semiarid badlands of SE Spain. *Journal of Hydrology*, 285, 199-214.
- Carlson, T. 2007. An Overview of the "Triangle Method" for Estimating Surface Evapotranspiration and Soil Moisture from Satellite Imagery. *Sensors*, 7, 1612-1629.
- Carlson, T., Gillies, R. & Perry, E. 1994. A method to make use of thermal infrared temperature and NDVI measurements to infer surface soil water content and fractional vegetation cover. *Remote Sensing Reviews*, 9, 161-173.
- Carlson, T. B., Gillies, R. R. & Schmugge, T. J. 1995. An interpretation of methodologies for indirect measurement of soil water content. *Agricultural and Forest Meteorology*, 77, 191-205.
- Caroll, T. R. 1981. Airborne soil moisture measurement using natural terrestrial gamma radiation. *Soil Science Society of America*, 132, 358-366.
- Chauhan, N. S., Miller, S. & Ardanuy, P. 2003. Spaceborne soil moisture estimation at high resolution: a microwave-optical/IR synergistic approach. *International Journal of Remote Sensing*, 24, 4599-4622.
- Chen, Y. 2006. Letter to the editor on "Rank Stability or Temporal Stability". *Soil Science Society of America*.
- Chow, V. T., Maidment, D. R. & Mays, L. W. 1988. *Applied Hydrology*, McGraw-Hill.
- Cosh, M. H., Jackson, T. J., Moran, S. & Bindlish, R. 2008. Temporal persistence and stability of surface soil moisture in a semi-arid watershed. *Remote Sensing of Environment*, 112, 304-313.
- Cosh, M. H., Jackson, T. J., Starks, P. J. & Heathman, G. C. 2006. Temporal stability of surface soil moisture in the Little Washita River Watershed and its applications in satellite soil moisture product validation. *Journal of Hydrology*, 323, 168-177.
- Dai, A., Trenberth, K. E. & Qian, T. 2004. A global dataset of Palmer Severity Index for 1870-2002: Relationship with soil moisture and effects of surface warming. *The American Meteorological Society*, 5, 1117-1130.
- Dalezios, N. R., Loukas, A., Vasiliades, L. & Liakopoulos, H. 2000. Severity-Duration-Frequency analysis of droughts and wet periods in Greece. *Hydrological Society Journal*, 45, 751-770.
- Dalezios, N. R., Papazafiriou, Z. G., Papamichail, D. M. & Karakostas, T. S. 1991. Drought assessment for the potential of precipitation enhancement in northern Greece. *Theoretical applied Climatology*, 44, 75-88.
- Das, N. N., Entekhabi, D. & Njoku, E. G. 2011. An algorithm for merging SMAP radiometer and radar data for high resolution soil moisture retrieval. *IEEE Transactions on Geoscience and Remote Sensing*, 49, 1504-1512.

- De Clerq, W., Jovanovic, N. & Fey, M. 2010. *Land use impacts on salinity in Berg River water*. Pretoria: Water Research Commission.
- Eilers, V. H. M., Carter, R. C. & Rushton, K. R. 2007. A single layer soil water balance model for estimating deep drainage (potential recharge): An application to cropped land in semi-arid North-east Nigeria. *Geoderma*, 140, 119-131.
- Entin, J. K., Robock, A., Vinnikov, K. Y., Hollinger, S. E., Liu, S. & Namkhai, A. 2000. Temporal and spatial scales of observed soil moisture variations in the extratropics. *Journal of Geophysical Research*, 105, 865-877.
- European Meteorological Satellites, E. 2013 *Earth Observation Portal* [Online]. Available: <https://archive.eumetsat.int> [Accessed 23 November 2013].
- Famiglietti, J. S., Rudnicki, J. W. & Rodell, M. 1998. Variability in surface moisture content along a hillslope transect: Rattlesnake Hill, Texas. *Journal of Hydrology*, 210, 259-281.
- Fereres, E., Goldhamer, D. A. & Parsons, L. R. 2003. Irrigation water management of horticultural crops. *Hortscience*, 38, 1036-1042.
- Fernandez, J. M. & Ceballos, A. 2005. Mean soil moisture estimation using temporal stability analysis. *Journal of Hydrology*, 312, 28-38.
- GARMIN. 2014. What is GPS? [Online]. Available: <http://www8.garmin.com/aboutGPS/> [Accessed 1 February 2014].
- Gelsthorpe, R. V., Schied, E. & Wilson, J. J. W. 2000. ASCAT-Metop's Advanced Scatterometer. *European Space Agency Bulletin*, 102, 19-27.
- Gillies, R., Carlson, T., Kustas, W. & Humes, K. 1997. A verification of the 'triangle' method for obtaining surface soil water content and energy fluxes from remote measurements of the Normalized Difference Vegetation Index (NDVI) and surface radiant temperature. *International Journal of Remote Sensing*, 18, 3145-3166.
- Global Climate Observing System 2010. *Implementation plan for the global observing system for climate in support of the UNFCCC (2010 update)*. Geneva, Switzerland: World Meteorological Organization (WMO).
- Gómez-Plaza, A., Martínez-Mena, M., Albaladejo, J. & Castillo, V. M. 2001. Factors regulating spatial distribution of soil water content in small catchments. *Journal of Hydrology*, 253, 211-226.
- Grayson, R. B., Western, A. W. & Chiew, F. H. S. 1997. Preferred states in spatial soil moisture patterns: Local and nonlocal controls. *Water Resources Research*, 33, 2897-2908.
- Gruhler, C., De Rosnay, P., Hasenauer, S., Holmes, T., De Reu, R., Kerr, Y., Mougin, E., Njoku, E., Timouk, F., Wagner, W. & Zribi, M. 2010. Soil moisture active and passive microwave products: intercomparison and evaluation over a Sahelian site. *Hydrology and Earth System Sciences*, 14, 141-156.
- Hardie, A. G. & Botha, A. 2010. *Biochar amendment of infertile Western Cape sandy soil: Implications for food security*. Hope Project. Stellenbosch, SA: Stellenbosch University.
- Hargreaves, G. H. & Samani, Z. A. 1985. Crop evapotranspiration from temperature. *Transactions of ASAE*, 1, 96-99.
- Harsch, E. 1992. Drought devastates Southern Africa. *Drought Network News*, 4, 17-19.
- Hassan, R. M. & Backeberg, G. *Drought management in SA: Potential for economic policy* International Drought Symposium, 2010 University of California, Riverside.
- Hayes, M. J., Svoboda, M. D., Wilhite, D. A. & Vanyarkho, O. V. 1999. Monitoring the 1996 drought using the standardised precipitation index. *Bulletin of the American Meteorological Society*, 80, 429-438.

- Hillel, D. 1989. *Introduction to Soil Physics*, San Diego, Academic Press.
- Idso, S. B., Jackson, R. D., Reginato, R. J., Kimball, B. A. & Nakama, F. S. 1975. The dependence of bare soil albedo on soil water content. *Journal of Applied Meteorology*, 14, 109-113.
- ILWIS. 2013. *Installation guide ILWIS and the GEONETCAST Toolbox [Online]*. Available: http://www.ilwis.org/geonetcast_toolbox_ilwis_installation_instructions.htm [Accessed 15 December 2013].
- Jackson, T. J. 1980. Profile soil moisture from space measurements. *Journal of the Irrigation and Drainage Division- ASCE*, 25, 81-92.
- Jackson, T. J., Cosh, M. H., Bindlish, R., Starks, P. J., Bosch, D. D., Seyfried, M. S., Goodrich, D. C., Moran, M. S. & Du, J. 2010. Validation of advanced microwave scanning radiometer soil moisture products. *IEEE Transactions on Geoscience and Remote Sensing*, 48, 4256-4272.
- Janssen, P. H. M. & Heuberger, P. S. C. 1995. Calibration of process-oriented models. *Ecological Modelling*, 83, 55-66.
- Jones, S. B., Wraith, J. M. & Or, D. 2002. Time domain reflectometry measurement principles and applications. *Hydrological Processes*, 16, 141-153.
- Jongens-Roberts, S. M. & Mitchell, D. T. 1986. The distribution of dry mass and phosphorus in a evergreen fynbos shrub species, *Leucospermum parile* (Salisb. Ex J. Knight) sweet (proteaceae) at different stages of development. *New Phytologist*, 103, 669-683.
- Jovanovic, N., Bugan, R. & Israel, S. 2013. Quantifying the Evapotranspiration Component of the Water Balance of Atlantis Sand Plain Fynbos (South Africa). In: ALEXANDRIS, S. G. (ed.) *Evapotranspiration - An Overview*.
- Kendy, E., Gérard-Merchant, P., Walter, M. T., Zhang, Y., Lui, C. & Steenhuis, T. S. 2003. A soil-water-balance approach to quantify groundwater recharge from irrigated cropland in the North China Plain. *Hydrological Processes*, 17, 2011-2031.
- Kidd, C. 2001. Satellite rainfall climatology: A review. *International Journal of Climatology*, 21, 1041-1066.
- Kim, G. & Barros, A. P. 2002. Downscaling of remotely sensed soil moisture with a modified fractal interpolation method using contraction mapping and ancillary data. *Remote Sensing of Environment*, 83, 400-413.
- Koster, R. D., Mahanama, S. P. P., Livneh, B., Lettenamaier, D. P. & Reichle, R. H. 2010. Skill in streamflow forecasts derived from large-scale estimates of soil moisture and snow. *Nature Geoscience*, 3, 613-616.
- Krause, P., Boyle, D. P. & Bäse, F. 2005. Comparison of different efficiency criteria for hydrological model assessment. *Advances in Geosciences*, 5, 89-97.
- Kuo, W.-L., Steenhuis, T. S., McCulloch, C. E., Mohler, C. L., Weinstein, D. A., DeGloria, S. D. & Swamy, D. P. 1999. Effect of grid size on runoff and soil moisture for a variable-source-area hydrology model. *Water Resources Research*, 35, 3419-3428.
- Lacava, T., Brocca, L., Calice, G., Melone, F., Moramarco, T., Pergola, N. & Tramutoli, V. 2010. Soil moisture variations monitoring by AMSU-based soil wetness indices: A long-term inter-comparison with ground measurements. *Remote Sensing of Environment*, 114, 2317-2325.
- Legates, D. R. & McCabe Jr., G. J. 1999. Evaluating the use of "goodness-of-fit" measures in hydrologic and hydroclimatic model validation. *Water Resources Research*, 35, 233-241.

- Lipiec, L. & Hatano 2003. *Quantification of compaction effects on soil physical properties and crop growth. Geoderma*, 116, 107-136.
- Lobell, D. B. & Asner, G. P. 2002. *Moisture effects on soil reflectance. Soil Science Society of America Journal*, 66, 722-727.
- Loijens, H. S. 1980. *Determination of soil water content from terrestrial gamma radiation measurements. Water Resources Research*, 16, 565-573.
- Martinez, C., Hancock, G. R., Kalma, J. D., Wells, T. 2008. *Spatio-temporal distribution of near-surface and root zone soil moisture at the catchment scale. Hydrological Processes*, 22(14), 2699-2714.
- Meigh, J. R., Mckenzie, A. A. & Sene, K. J. 1999. *Spatial and temporal comparisons of droughts over Korea with East Asia. International Journal of Climatology*, 23, 223-233.
- Mekonnen, D. F. 2009. *Satellite remote sensing for soil moisture estimation: Gumara Catchment, Ethiopia. Master of Science, University of Twente.*
- Merlin, O., Chehbouni, A., Kerr, Y. H. & Goodrich, D. C. 2006. *A downscaling method for distributing surface soil moisture within a microwave pixel: Application to the Monsoon '90 data. Remote Sensing of Environment*, 101, 379-389.
- Merlin, O., Walker, J. P., Chehbouni, A. & Kerr, Y. 2008. *Towards deterministic downscaling of SMOS soil moisture using MODIS derived soil evaporative efficiency. Remote Sensing of Environment*, 112, 3935-3946.
- Moriassi, D. N., Arnold, J. G., Van Liew, M. W., Bingner, R. L., Harmel, R. D. & Veith, T. L. 2007. *Model Evaluation Guidelines for Systematic Quantification of Accuracy in Watershed Simulations. Transactions of ASAE* 50, 885-900.
- Naeimi, V., Scipal, K., Bartalis, Z., Hasenauer, S. & Wagner, W. 2009. *An improved soil moisture retrieval algorithm for ERS and METOP scatterometer observation. IEEE Transactions on Geoscience and Remote Sensing*, 47, 1999-2013.
- Narasimhan, B. & Srinivasan, R. 2005. *Development and evaluation of Soil Moisture Deficit Index (SMDI) and Evapotranspiration Deficit Index (ETDI) for agricultural drought monitoring. Agricultural and Forest Meteorology*, 133, 69-88.
- National Aeronautics and Space Administration (NASA). 2014. *SRTM 90m Digital Elevation Data from the CHIAR Consortium for Spatial Information [Online]. Available: <http://gcmd.nasa.gov/records/GCMD CGIAR SRTM 90.html> [Accessed 30 November 2013].*
- Norbiato, D., Borga, M., Esposti, S. D., Gaume, E. & Anquetin, S. 2008. *Flash flood warning based on rainfall thresholds and soil moisture conditions: An assessment for gauged and ungauged basins. Journal of Hydrology*, 362, 274-290.
- O'Connor, J. E. & Costa, J. E. 2004. *The world's largest floods, past and present- Their causes and magnitudes. U.S. Geological Survey Circular*, 1254, 13.
- Oregon Department of Transportation 2005. *Hydrology. ODOT Hydraulics manual. Oregon.*
- Pahl-Wostl, C. 2007. *Transition towards adaptive management of water facing climate and global change. Water Resources Management*, 21, 49-62.
- Palmer, W. C. 1965. *Meteorological drought. U.S. Department of Commerce.*
- Panigrahi, B. & Panda, S. N. 2003. *Field test of a soil water balance simulation model. Agricultural Water Management*, 58, 223-240.
- Pellenq, J., Kalma, J., Boulet, G., Saulnier, G.-M., Woodridge, S., Kerr, Y. & Chehbouni, A. 2003. *A disaggregation scheme for soil moisture based on topography and soil depth. Journal of Hydrology*, 276, 112-127.

- Penna, D., Borga, M., Norbiato, D. & Dalla Fontana, G. 2009. Hillslope scale soil moisture variability in a steep alpine terrain. *Journal of Hydrology*, 364, 311-327.
- Rebello, A. G., Boucher, C., Helme, N., Mucina, L. & Rutherford, M. C. 2006. Fynbos biome. In: MUCINA, L. & RUTHERFORD, M. C. (eds.) *Sterlitzia 19: The Vegetation of South Africa, Lesotho and Swaziland*. Pretoria: South African National Biodiversity Institute.
- Refsgaard, J. C. 1997. Parameterisation, calibration and validation of distributed hydrological models. *Journal of Hydrology*, 198, 69-97.
- Richard, Y. & Pocard, I. 1998. Statistical study of NDVI sensitivity to seasonal and interannual rainfall variations in Southern Africa. *International Journal of Remote Sensing*, 19, 2907-2920.
- Richter, B. D., Mathews, R., Harrison, D. L. & Wigington, R. 2003. Ecologically sustainable water management: Managing river flows for ecological integrity. *Ecological Society of America*, 13, 206-224.
- Riha, S. J., Rossiter, D. G. & Simoens, P. 1994. *GAPS General-Purpose Atmosphere-Plant-Soil Simulator Version 3-0 User's Manual*. Ithaca, New York: Cornell University.
- Rinaldi, V. A. & Francisca, F. M. 1999. Impedance analysis of soil dielectric dispersion (1 MHz-1 GHz). *Journal of Geotechnical and Geoenvironmental Engineering*, 125, 111-121.
- Robock, A., Vinnikov, K. Y., Srinivasan, G., Entin, J. K., Hollinger, S. E., Sperankaya, N. A., Lui, S. & Namkhai, A. 2000. The global soil moisture data bank. *The American Meteorological Society*, 81, 1281-1299.
- Rouault, M. & Richard, Y. 2003. Intensity and spatial extension of drought in South Africa at different time scales. *Water SA*, 29.
- Santhi, C., Arnold, J. G., Williams, J. R., Dugas, W. A., Srinivasan, R. & Hauck, L. M. 2001. Validation of the SWAT model on a large river basin with point and nonpoint sources. *Journal of America Water Resources Association*, 37, 1169-1188.
- Schmugge, T. J. 1983. Remote sensing of soil moisture: Recent advances. *IEEE Transactions on Geoscience and Remote Sensing*, 21, 336-344.
- Schmugge, T. J., Jackson, T. J. & McKim, H. L. 1980. Survey of methods for soil moisture determination. *Water Resources Research*, 16, 961-979.
- Schultz, G. A. 1994. Meso-scale modelling of runoff and water balances using remote sensing and other GIS data. *Hydrological Sciences Journal*, 39, 121-142.
- Silva, J. S. & Rego, F. C. 2003. Root distribution of a Mediterranean shrubland in Portugal. *Plant and Soil*, 255, 529-540.
- Šimůnek, J., Šejna, M. & van Genuchten, M. T. 1998. *The HYDRUS-1D software package for simulating water flow and solute transport in two-dimensional variably saturated media Version 2.0*. IGWMC-TPS-70. Golden, CO: International Ground Water Modeling Centre.
- Soares, J. V. & Almeida, A. C. 2001. Modeling the water balance and soil water fluxes in a fast growing Eucalyptus plantation in Brazil. *Journal of Hydrology*, 253, 130-147.
- South African Weather Bureau 1972. *District rainfall for South Africa and the annual march of rainfall over southern Africa*. Pretoria: South African Weather Bureau.
- Steenhuis, T. S., Jackson, C., Kung, K.-J. S. & Brutsaert, W. H. 1985. Measurement of groundwater recharge on eastern Long Island. *Journal of Hydrology*, 79, 145-169.
- Su, Z., Yacob, A., Wen, J., Roerink, G., He, Y., Gao, B., Boogaard, H. & van Diepen, C. 2003. Assessing relative soil moisture with remote sensing data: theory, experimental

- validation, and application to drought monitoring over the North China Plain. *Physics and Chemistry of the Earth, Parts A/B/C*, 28, 89-101.
- Tansey, K. J., Millington, A. C., Battikhi, A. M. & White, K. H. 1999. Monitoring soil moisture dynamics using satellite imaging radar in northeastern Jordan. *Applied Geography*, 19, 325-344.
- Thompson, R. B., Gallardo, M., Valdez, L. C. & Fernández, M. D. 2007. Using plant water status to define threshold values for irrigation management of vegetable crops using soil moisture sensors. *Agricultural Water Management*, 88, 147-158.
- Thorup-Kristensen, K., Cortasa, M. S. & Loges, R. 2009. Winter wheat roots grow twice as deep as spring wheat roots, is this important for N uptake and N leaching losses? *Plant Soil*, 322, 101-114.
- Thurow, T. L., Blackburn, W. H., Warren, S. D. & Taylor, J. C. A. 1987. Rainfall interception by midgrass, shortgrass, and live oak mottes. *Journal of Range Management*, 40, 455-460.
- Tilman, D., Cassman, K. G., Matson, P. A., Naylor, R. & Polasky, S. 2002. Agricultural sustainability and intensive production practices. *International Weekly Journal of Science*, 418, 671-677.
- Topp, G. C. 2003. State of the art measuring soil water. *Hydrological Processes*, 17, 2993-2996.
- Topp, G. C., Davis, J. L. & Annan, A. P. 1980. Electromagnetic determination of soil water content: measurements in coaxial transmission lines. *Water Resources Research*, 16, 574-582.
- U.S Geological Survey, U. S. G. S. 2014. Data Access [Online]. Land Process Distributed Active Archive Center. Available: https://lpdaac.usgs.gov/data_access [Accessed 25 January 2014].
- Van Genuchten, M. T. 1980. A closed-form equation for predicting the hydraulic conductivity of unsaturated soils *Soil Science Society of America Journal*, 44, 892-898.
- Van Liew, M. J., Arnold, J. G. & Garbrecht, J. D. 2003. Hydrologic simulation on agricultural watersheds: Choosing between two models. *Transactions of ASAE*, 46, 1539-1551.
- Verspeek, J., Stoffelen, A., Portabella, M., Bonekamp, H., Anderson, C. & Saldana, J. F. 2010. Validation and Calibration of ASCAT using CMOD5.n. *IEEE Transactions on Geoscience and Remote Sensing*, 48, 386-395.
- Vinnikov, K. Y., Robock, A., Sperankaya, N. A. & Schlosser, C. A. 1996. Scales of temporal and spatial variability of midlatitude soil moisture. *Journal of Geophysical Research*, 101, 7163-7174.
- Wagner, W., Lemoine, G. & Rott, H. 1999. A method for estimating soil moisture from ERS scatterometer and soil data *Remote Sensing of Environment*, 70, 191-207.
- Wagner, W., Naeimi, V., Scipal, K., De Reu, R. A. M. & Martinez-Fernandez, J. 2007. Soil moisture from operational meteorological satellites. *Hydrogeology Journal*, 15, 121-131.
- Walker, J. P., Houser, P. R. & Willgoose, G. R. 2003. Active microwave remote sensing for soil moisture measurement: a field evaluation using ERS-2. *Hydrological Processes*, 17, 0-0.
- Walker, J. P., Willgoose, G. R. & Kalma, J. D. 2004. In situ measurement of soil moisture: a comparison of techniques. *Journal of Hydrology*, 293, 85-99.
- Wallace, J. S., Gash, J. H. C. & Sivakumar, M. V. K. 1990. Preliminary Measurements of Net Radiation and Evaporation over Bare Soil and Fallow Bushland in the Sahel. *International Journal of Climatology* 10, 203-210.

- Wang, K. C. & Liang, S.L. 2009. *Evaluation of ASTER and MODIS land surface temperature and emissivity products using long-term surface longwave radiation observations at SURFRAD sites. Remote Sensing of Environment, 113(7), 1556-1565.*
- Wang, X., Xie, H., Guan, H. & Xiaobing, Z. 2007. *Different responses of MODIS-derived NDVI to root-zone soil moisture in semi-arid and humid regions. Journal of Hydrology, 340, 12-24.*
- Ward, A. D. & Trible, S. W. 2003. *Environmental Hydrology, Second Edition, United States of America, Lewis Publishers.*
- Wei, M.-Y. 1995. *Soil Moisture. In: WEI, M.-Y. (ed.). NASA Headquarters: NASA.*
- White, R. E. 2006. *Principles and Practice of Soil Science: The Soil as a Natural Resource, 4th Edition, Blackwell Publishing.*
- Wilson, R. G. 1971. *Methods of Measuring Soil Moisture. Technical Manual Series. Ottawa, Canada: The Secretariat, Canadian National Commission for the International Hydrological Decade.*
- Zeglin, S. 1996. *Soil Moisture Measurement. Filed Measurement Techniques in Hydrology-Workshop Notes. Clayton: Corpus Christi College.*
- Zollweg, J. A., Gburek, W. J. & Steenhuis, T. S. 1996. *SMoRMod- a GIS-integrated rainfall-runoff model applied to a small northeast U.S. watershed. Transaction American Society of Agricultural Engineers, 39, 1299-1307.*



Appendices



UNIVERSITY *of the*
WESTERN CAPE

Appendix A: Transect A – Riverlands Nature Reserve



Appendix B: Transect B - Rondevlei Farm



Appendix C: Transect C- Niewepost



Appendix D: Transect D- Goedetrou Farm



Appendix E: Transect E- De Gift



Appendix F: Transect F- De la Gift

